NBSIR

RF ATTENUATION MEASUREMENT SYSTEM USING A SQUID

Robert T. Adair
Nolan V. Frederick
Donald B. Sullivan

Electromagnetics Division
and Cryogenics Division
Institute for Basic Standards
National Bureau of Standards
Boulder, Colorado 80302

September 1977

D D C
RECEIVED
NOV 22 1977
A

(14) NBSIR-77-863

(6) RF ATTENUATION MEASUREMENT SYSTEM USING A SQUID

(10) Robert T. /Adair,
Nolan V. /Frederick
Donald B. /Sullivan

Electromagnetics Division
and Cryogenics Division
Institute for Basic Standards
National Bureau of Standards
Boulder, Colorado 80302

(11) September 1977   (12) 157 p.
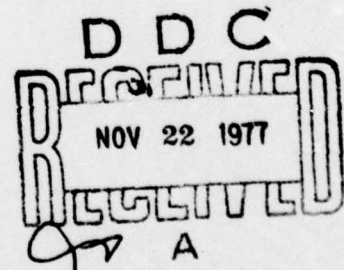
Prepared for :

Army /Navy /Air Force
Calibration Coordination Group

390891   LB

IMPORTANT NOTICE

Certain commercial equipment is identified in this report. This identification does not imply endorsement by the National Bureau of Standards nor does it imply that the equipment identified is necessarily the best available for the purpose.

CONTENTS

CONTENTS (Continued)

LIST OF FIGURES

.

LIST OF FIGURES (Continued)

LIST OF TABLES

RF ATTENUATION MEASUREMENT SYSTEM USING A SQUID*

Robert T. Adair, Nolan V. Frederick, and Donald B. Sullivan

This report describes a unique portable system for measuring attenuation at 30 MHz over a range of 50 dB to an accuracy of 0.005 dB per 20 dB. This system does not require any reference standard. A SQUID (Superconducting QUantum Interference Device) with its associated instrumentation is used to determine attenuation in terms of Bessel Function Zeros. A SQUID is a loop of superconducting metal closed by a weak point contact called a Josephson junction, operating in liquid helium.

The system specifications, description, and theory of operation are presented. A complete system operating procedure including data reduction techniques is given along with a discussion of sources of errors.

Considerable additional information and diagrams are presented as an aid to the user in understanding and operating the system.

Key words: Josephson junction; quantum interference; rf attenuation; superconductivity.

1. GENERAL INFORMATION

1.1 Introduction

This document contains a description, specifications, operating procedures, theory of operation, and parts list for the RF Attenuation Measurement System based on the SQUID. This system, designed and constructed by the National Bureau of Standards (NBS), Boulder, Colorado, is a compact portable system designed as a very precise standard for calibrating various types of laboratory attenuators. This system does not require any reference standard. It is relatively inexpensive and easy to set up and operate. This attenuator calibration system has several unique features:

a. The relative ease of construction of the system, e.g., the accuracy of the measurements, does not depend on high precision machining of mechanical parts such as in waveguide below cutoff attenuators.

b. The system does not require a standard of attenuation. It requires only a table of Bessel functions to determine the exact change in attenuation between any two given flux quanta nulls.

c. This technique provides a broad frequency range of operation without tuning.

d. The readout technique makes it relatively easy to automate measurements.

A superconducting quantum interference device (SQUID) can be thought of as a transducer that converts variations in magnetic flux into nearly perfect periodic variations in microwave impedance which are sensed as the change in the microwave reflection coefficient. Most of the applications of SQUIDs, e.g., magnetometers, gradiometers, etc., have capitalized on their high sensitivity and their unique periodic response to magnetic flux. However, the rf attenuation application is the first which attempts to capitalize on the particular characteristics of the waveform of the rf biased SQUID. In this respect, the success of the continuing efforts on the attenuation application is a measure of the utility of the SQUID waveform.

The period of a SQUID corresponds to one magnetic flux quantum (ϕ_o = 2e/h = 2.067854 x 10^{-15} Wb). This provides a convenient natural means of measuring attenuation.

*Superconducting Quantum Interference Device.

These devices are very accurate over a wide dynamic range. Electrical quantities are measured by counting periods (flux quanta) in the response of a SQUID in the same manner that length can be measured by counting wavelengths of light emitted by a laser.

Under ideal conditions, if the SQUID input current I is an rf current, then the SQUID output response is the zero-order Bessel function of the magnitude of the rf input current.

Thus the output of the microwave readout circuit is proportional to $J_0(2\pi I/I_0)$ where I is the rf input current amplitude and I_0 is the current necessary to drive one quantum of magnetic flux into the SQUID. I_0 need not be known to make attenuation measurements. The values of the argument $2\pi I/I_0$ at the flux quanta nulls or zeros can be found in a table of Bessel functions. A properly constructed single measurement system can be used to measure attenuation from dc to 1 GHz with accuracies comparable to existing conventional techniques. Several successful prototype measurement systems have been constructed at the National Bureau of Standards based on the SQUID [1,2].* The system described here operates only at 30 MHz primarily to calibrate 30-MHz variable waveguide below-cutoff attenuators.

This SQUID system for rf attenuation measurement has been improved over earlier systems by a number of significant changes. A redesign of the L-band SQUID has resulted in a significantly simpler geometry which provides an adjustable coupling for precise matching to the electronics. The redesigned SQUID contains a permanently adjusted point contact in a replaceable cartridge.

Attenuation measurements with this system rely heavily on proper signal processing in the room temperature components, and a careful study of these conditions indicates a series of areas where errors can be generated. These signal handling problems and appropriate solutions are discussed in detail. This system is engineered for routine measurements in a real standards laboratory environment.

1.2 Specifications

Electrical

Frequency of Operation (can be altered with appropriate rf source plug-in modules)	30 MHz
Input and Output Impedances (VSWR 1.05 at insertion point)	50 + j0 ohms
Attenuation Measurement Range	50 dB
Resettability	± 0.001 dB
Repeatability	± 0.001 dB
Calibration Accuracy	± (0.005 dB/20 dB)
RF Input Power to Device Under Test	250 mW maximum
AC Power Requirement	115 VAC, 60 Hz 1.0 Ampere (nominal)

---

*Figures in brackets indicate the literature references at the end of this paper.

<div align="center">

Mechanical

</div>

Connectors at Insertion Point   Precision Type N

<u>SQUID Control Chassis</u>   <u>SQUID Readout Chassis</u>

Dimension:

Width	5.9 cm	52.0 cm
Depth (including knobs)	17.2 cm	50.0 cm
Height	21.2 cm	40.3 cm
Mass	2.4 kg	21.9 kg

<div align="center">

Cryogenic

</div>

<u>Dewar</u>   <u>SQUID</u>

Gross Capacity	33.3 liters	Material Babbitt (with Niobium Point contact)		
Evaporation	2.0%/day max.			
Height (with casters)	111.4 cm	Height (including connectors)		3.7 cm
Outside Diameter	53.3 cm	Diameter		3.4 cm
Mass Empty (with casters)	33.1 kg	Mass	$\simeq$ 305 gm	
Mass Full (with casters)	$\simeq$ 37.3 kg			
Neck Inner Diameter	38.1 mm			

1.3 Description

The system shown in figures 1.1 and 1.2 is a precise attenuation measurement system having an accurate dynamic range of 50 to 60 dB nominally. This means an actual measurement range of 50 to 60 dB when calibrating an NBS Model VII attenuation standard which has an initial insertion loss of 30 dB. Basically the system consists of an rf biased SQUID; an electronics package (the SQUID Readout Unit) figure 1.3, consisting of an rf signal source (30 MHz in the original system), amplifier, rf level control circuit, digital counter with trigger circuit, oscilloscope, and associated controls and power supplies; and the null indicator for the NBS designed phase-sensitive detector which serves as the (Bessel Function) null detector. A second electronics package (the SQUID Control Unit), figure 1.4, mounts on top of the Dewar. This unit contains the L-Band pump frequency components on one side and the signal processing electronics on the other side. This measurement system is complete when the device under test (DUT) is connected in the measurement channel at the insertion point.

The system, exclusive of the DUT and the associated interconnecting cables and hardware, will be elaborated on here.

<div align="center">

1-3

</div>
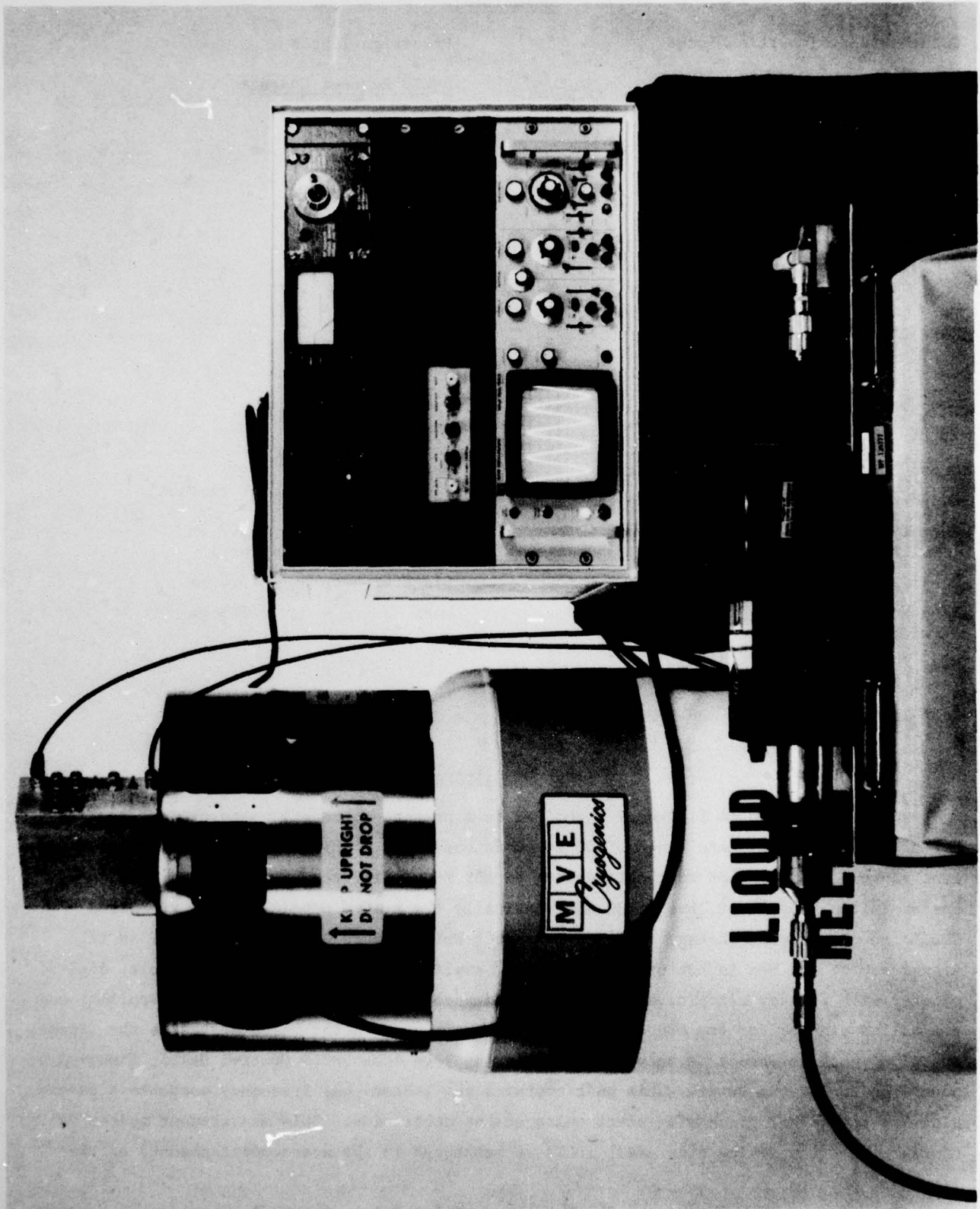
Figure 1.1.   The SQUID attenuation measurement system.
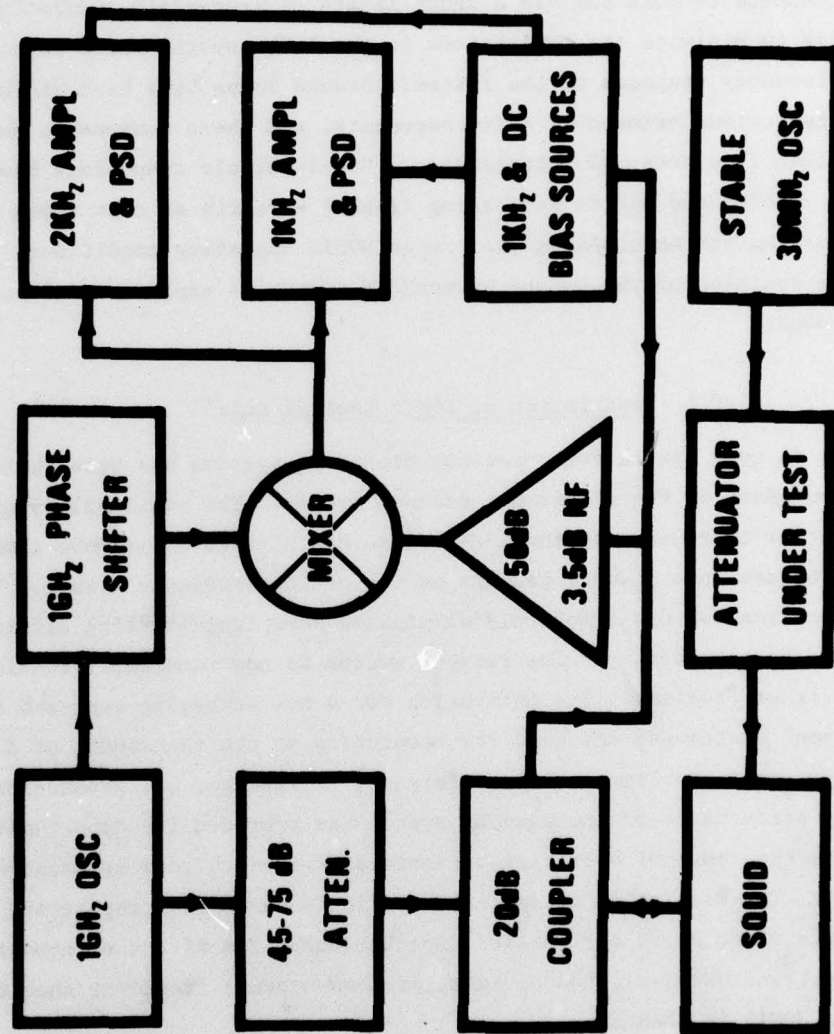
Figure 1.2. Block diagram of attenuation measurement system.

Figure 1.2 illustrates the interconnections of the system components. The major changes from earlier systems [3] have been (a) to replace the simple diode detector with a double-balanced mixer to linearize the 1-GHz detection process and (b) to add a second harmonic phase sensitive (coherent) detector in parallel with the main signal channel. The 1-GHz components and the main signal processing electronics are housed in an aluminum box which is attached directly to the top of the 30-liter liquid helium dewar containing the SQUID. The SQUID connects to this box via a short length of semi-rigid coaxial cable. Every effort was made to minimize the reflections in the 1-GHz system since these reflections distort the frequency response of the system. Ground loops have been minimized to prevent unwanted interactions between circuit components, and these components have been very carefully shielded from external interference. Highly stable components have been used throughout the dc bias and signal processing (1-kHz) circuits so that there are no difficulties in adjusting and maintaining the proper SQUID operating conditions. The rationale behind the addition of the second harmonic detector is explained in the theory section of this document.

1.3.1 Description of SQUID Control Unit

A major advance in this system over previous prototype systems has been the complete repackaging and improvement of the electronic readout system. The availability of smaller and substantially better components in the 1-GHz range has allowed us to move a major portion of the readout system into a small package on top of the cryogenic vessel. The close proximity of SQUID and readout has completely eliminated some long-standing difficulties with interference and bias stability. The readout system is now remarkably stable and should present no further problems. The motivation for a new packaging approach for this attenuation measurement system was the need for resolution at the thousandth of a dB level, as well as the ever-present problems with interference, rf leakage, and ground-loop currents.

The outstanding performance of the readout system has provided the opportunity to systematically define the range of operating parameters over which good attenuation calibrations can be made. The results of these tests are included in this report and clearly indicate a performance which meets our earlier expectations. The effect of nonoptimum settings is not great, and once set, the optimum (microwave pump) frequency should not need resetting unless the SQUID is CHANGED.

The Control Unit contains the dc, 1-kHz, and 1-GHz bias circuits and is mounted on the Dewar head as shown in figure 1.1. The 1-GHz bias components (i.e., the oscillator, attenuator, directional coupler, amplifier, and double-balanced mixer) are mounted as near as possible to the SQUID to reduce the frequency-dependent variations in signal level which are associated with line resonances generated by slightly imperfect impedance matching. These elements are mounted in a thermally-stable, rf tight, machined-aluminum box. Every effort has been made to design and construct the bias circuits for maximum stability. There is no discernible pickup or interaction between the different circuits. Typically, the fractional variations of 1-kHz and dc bias signals are of the order of a few parts in 10^5 with 10% variations in line voltage and 1°C variations in temperature.

The bias and setup controls shown in figure 1.3 are mounted on the aluminum enclosure to eliminate pickup and thermal effects. The dc and 1-kHz circuits are illustrated in figures 1.4, 1.5, and 1.6. The 1-GHz components are on the reverse side as shown in figures 1.7, 1.8, and 1.9. The manually-tuned phase shifter in the lower left quadrant of figure 1.7 serves to deliver the reference signal to the double-balanced mixer. The phase of the reference signal is matched to the primary signal phase to assure a proper phase relationship at the mixer over a wide tuning range. The use of a double-balanced mixer ensures linear detection of only the signal component which varies as the zeroth order Bessel function. All the 1-GHz elements are state-of-the-art commercial components. The mechanical attenuator used in previous units has been replaced with a voltage variable attenuator which is housed in the oscillator enclosure.

1.3.2 Description of SQUID Readout Unit

The Readout Unit (shown in figure 1.10) consists of the RF Source and Null Indicating Unit, a digital counter for counting the Bessel function zeros, and an oscilloscope to monitor the SQUID interference pattern during the setup procedure.

The RF Source and Null Indicating Unit mounts in the Readout Unit cabinet and contains the system power supplies, the 2-kHz phase sensitive detector, the 30-MHz crystal controlled source, the circuit for 30-MHz level control, the readout null meter, and the count generating circuits. This unit is illustrated in figures 1.11, 1.12, 1.13, and 1.14. The components are mounted in modular units, and one need only replace the rf source (30-MHz) module in order to change to another calibration frequency.

The level control circuit shown in figure 1.15 is a precisely-controlled, manually-operated rf output level-set attenuator. The variable capacitor (TMC_2) acts as a variable termination on one port of the hybrid junction contained in the RF Signal Source plug-in module which supplies the Device Under Test with the calibrating frequency signal.

The combination of the variable termination (TMC_2) and the 180° hybrid junction serves as a variable attenuator on the output of the 30-MHz source.

The rf signal source module (shown in figures 1.15, 1.16, and 1.17) consists of a 30-MHz crystal-controlled oscillator, a 30-MHz amplifier, and a signal level controller which operates like a variable attenuator as shown in figure 1.19. This 30-MHz signal appears at the "RF OUTPUT" jack (J4) on the rear panel of the SQUID Readout Unit. The Setup/Run switch on the front panel of the plug-in controls a coaxial relay which switches the rf signal into a 50-ohm load when the switch is placed in the "SETUP" position. This allows the SQUID control parameters to be set up for optimum operation of the system without the 30-MHz measurement signal interfering.

The rf signal level controller consists of a 180° hybrid junction with 65 dB of isolation between the E and H arms. The rf output from the 30-MHz amplifier is fed into the H arm, and the rf output from the E arm is connected via J4 to the input port on the Device Under Test. Colinear arm No. 1 is terminated in a variable piston capacitor with a range from 0.7 to 30 picofarad. Colinear arm No. 2 is also terminated with a variable piston capacitor which serves as a variable termination. See figures 1.15, 1.16, 1.17, and 1.18.
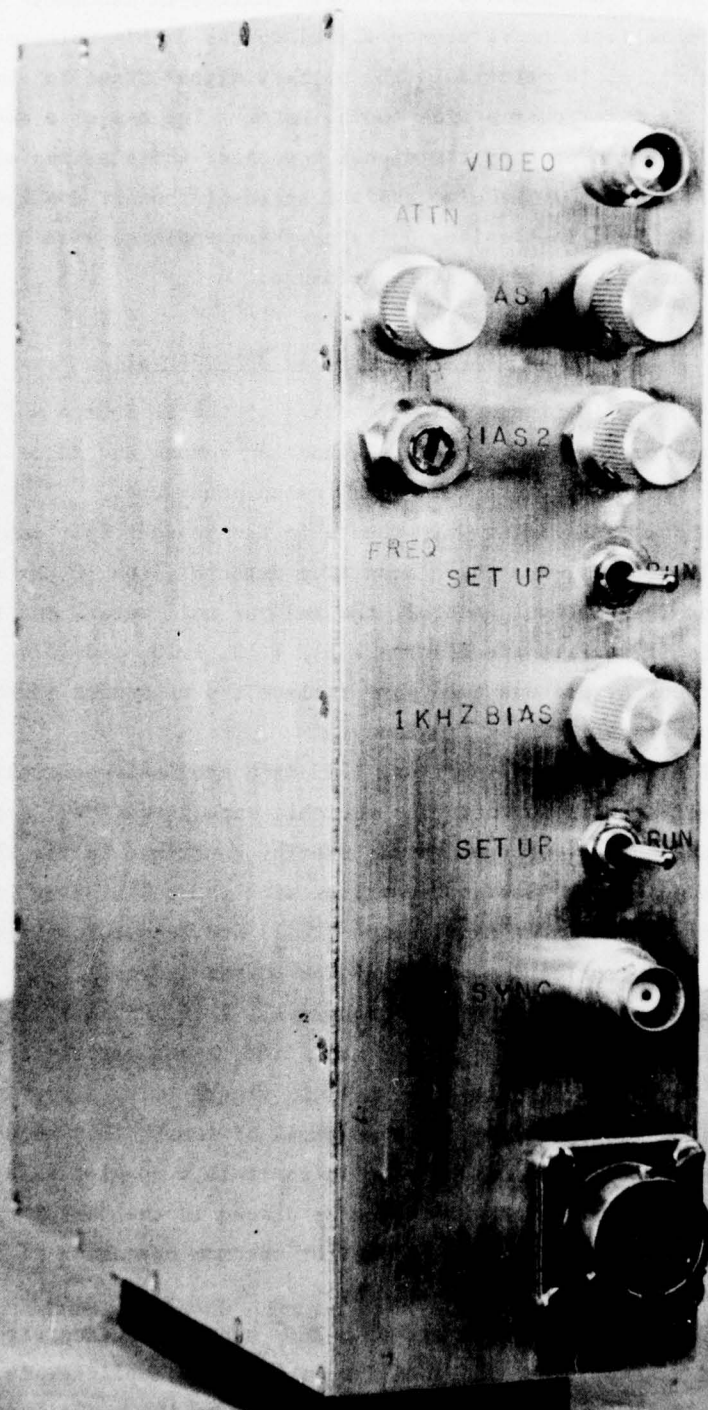
Figure 1.3.   SQUID control unit.
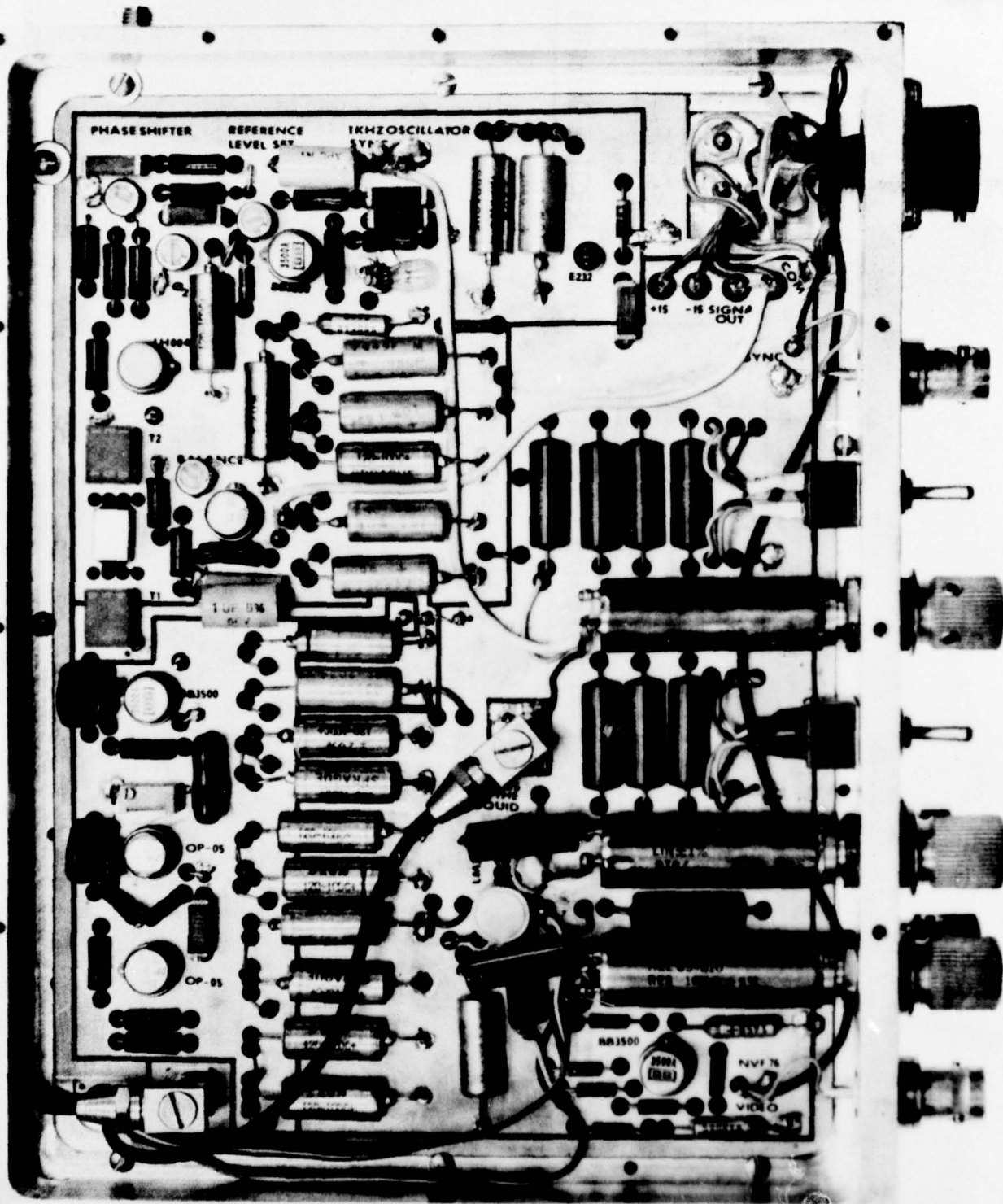
Figure 1.4.   DC and 1-kHz circuits (for bias and detection) contained
in the SQUID control unit.
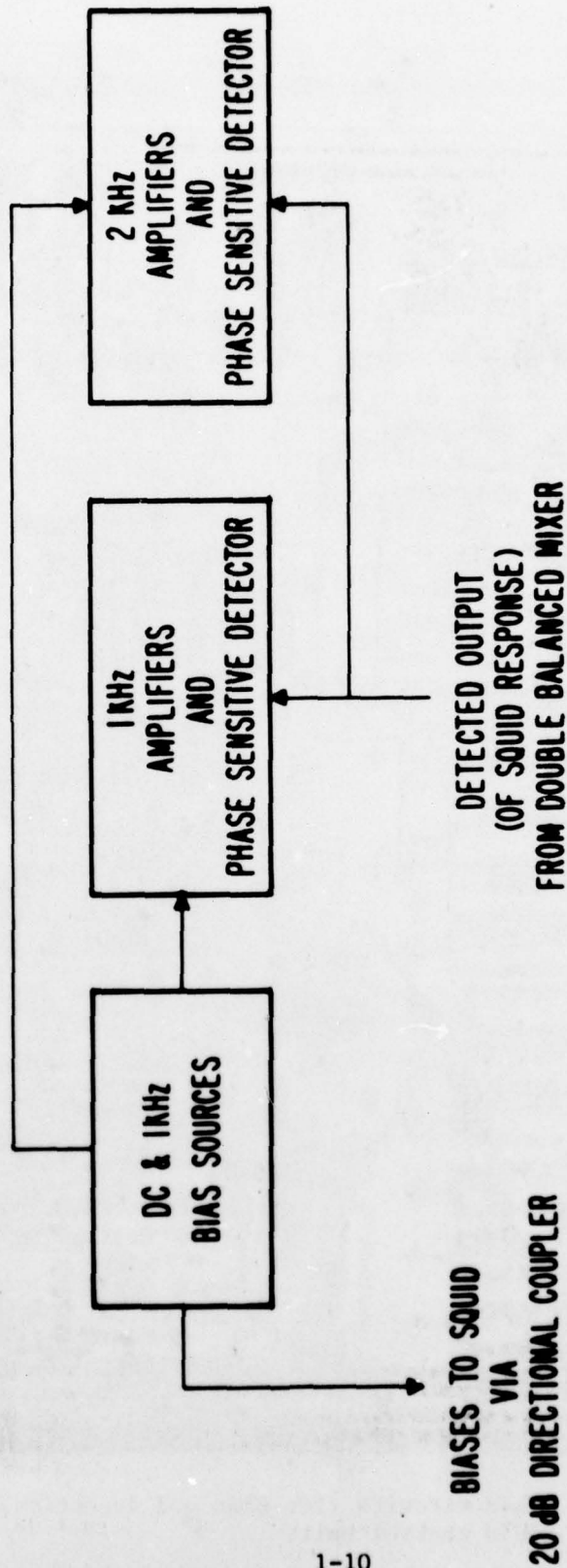
Figure 1.5.   Block diagram of the dc and 1-kHz bias circuits and 1-kHz and 2-kHz phase sensitive detectors.
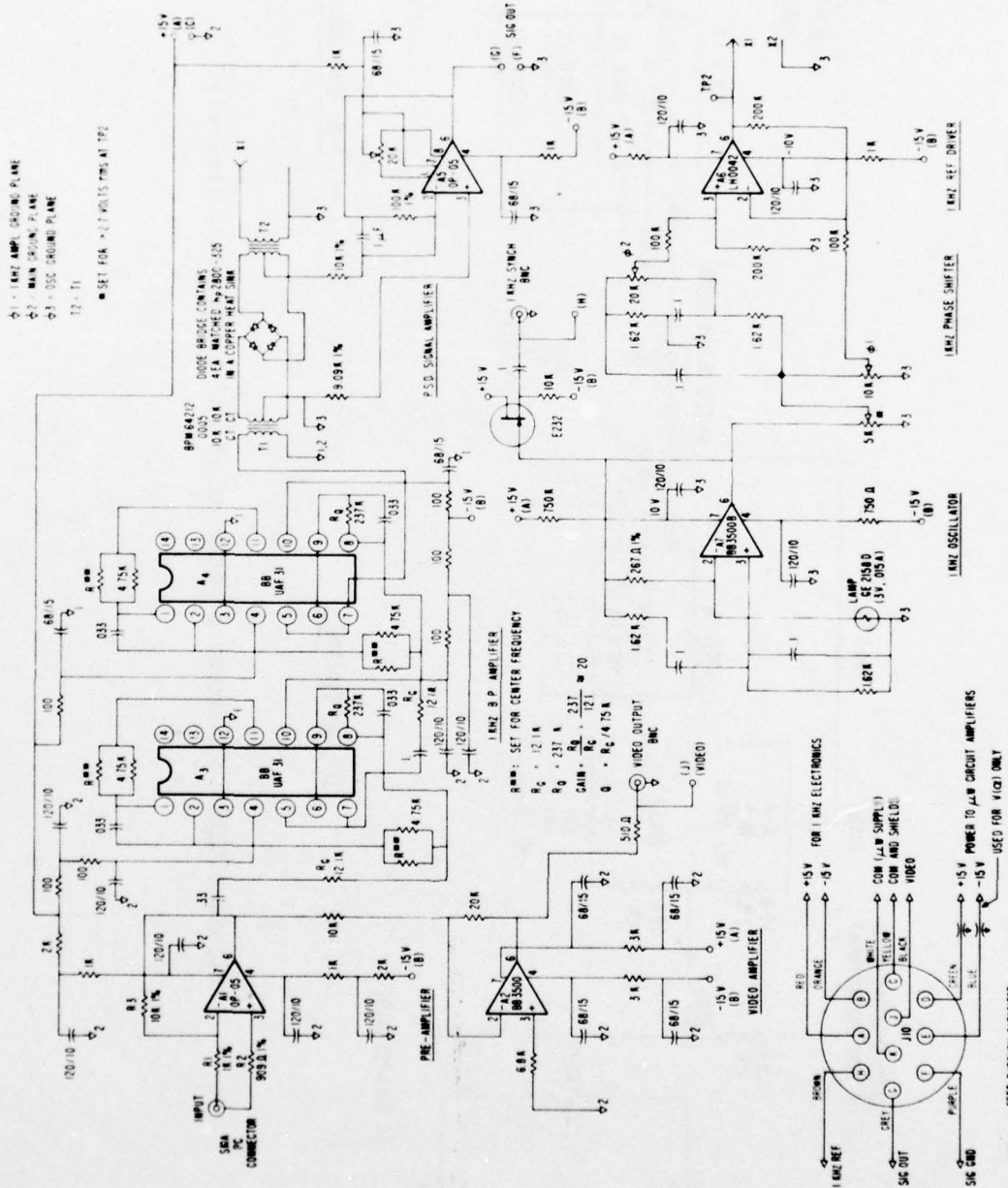
Figure 1.6(a). Schematic diagram of dc and 1-kHz bias circuits and 1-kHz phase sensitive detectors.
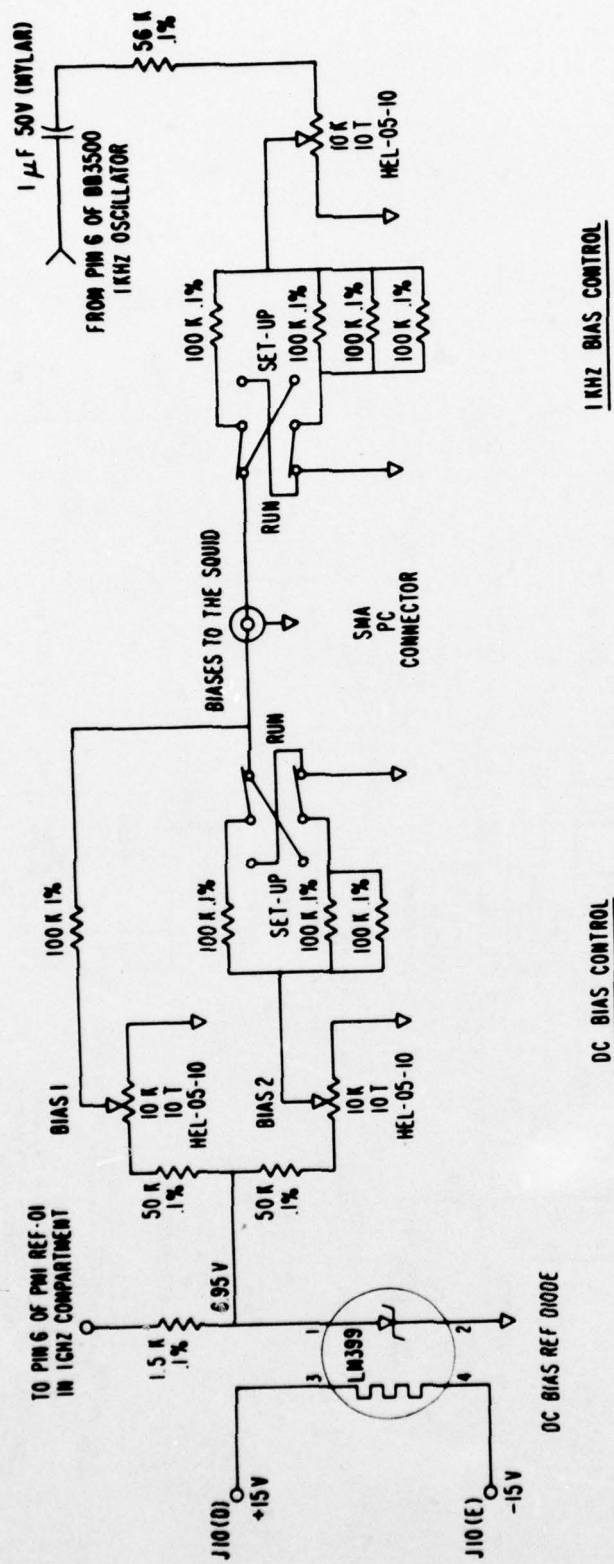
Figure 1.6(b). Schematic diagram of dc and 1-kHz setup controls.
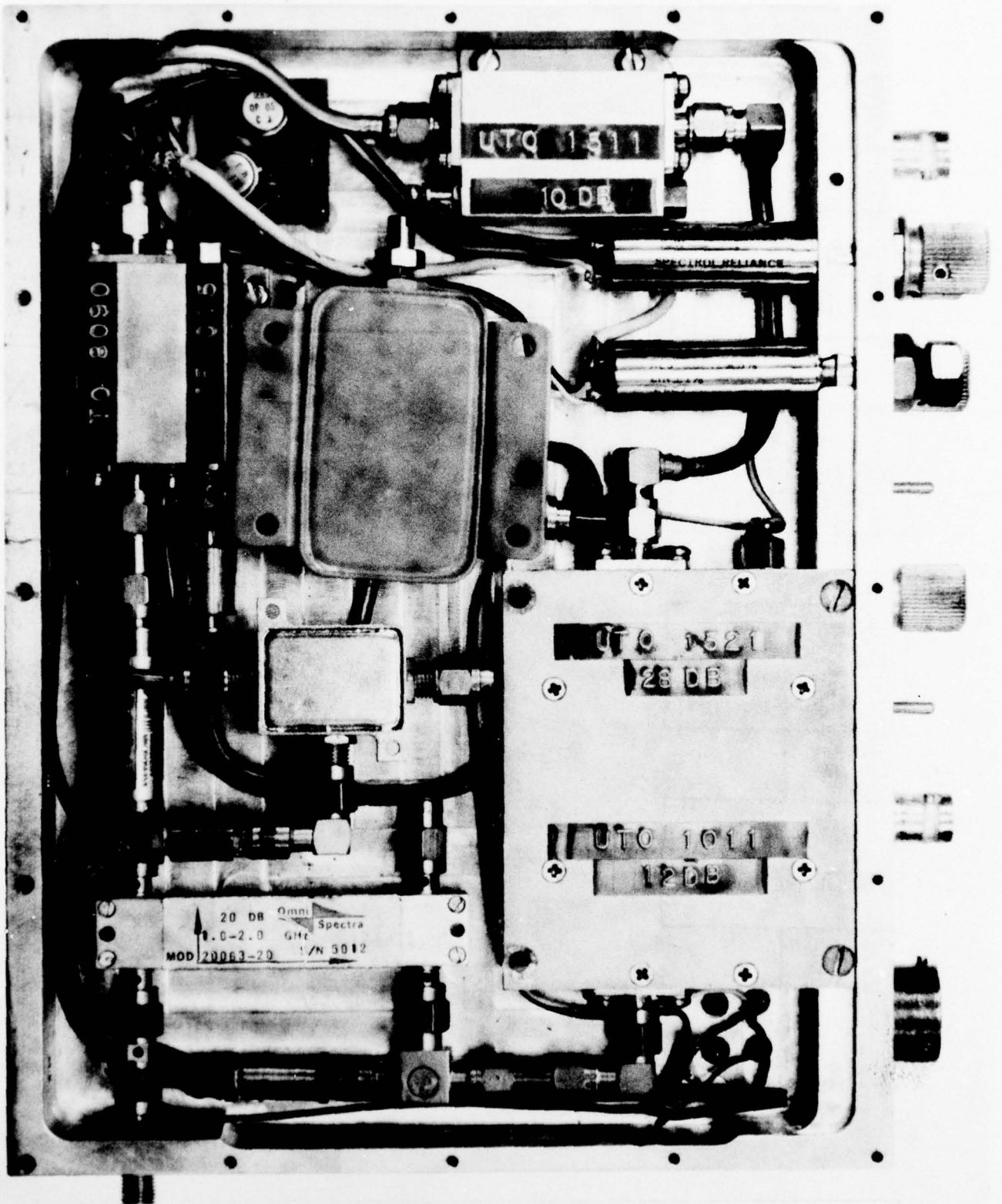
Figure 1.7. Microwave bias components contained in the SQUID control unit.

1-13
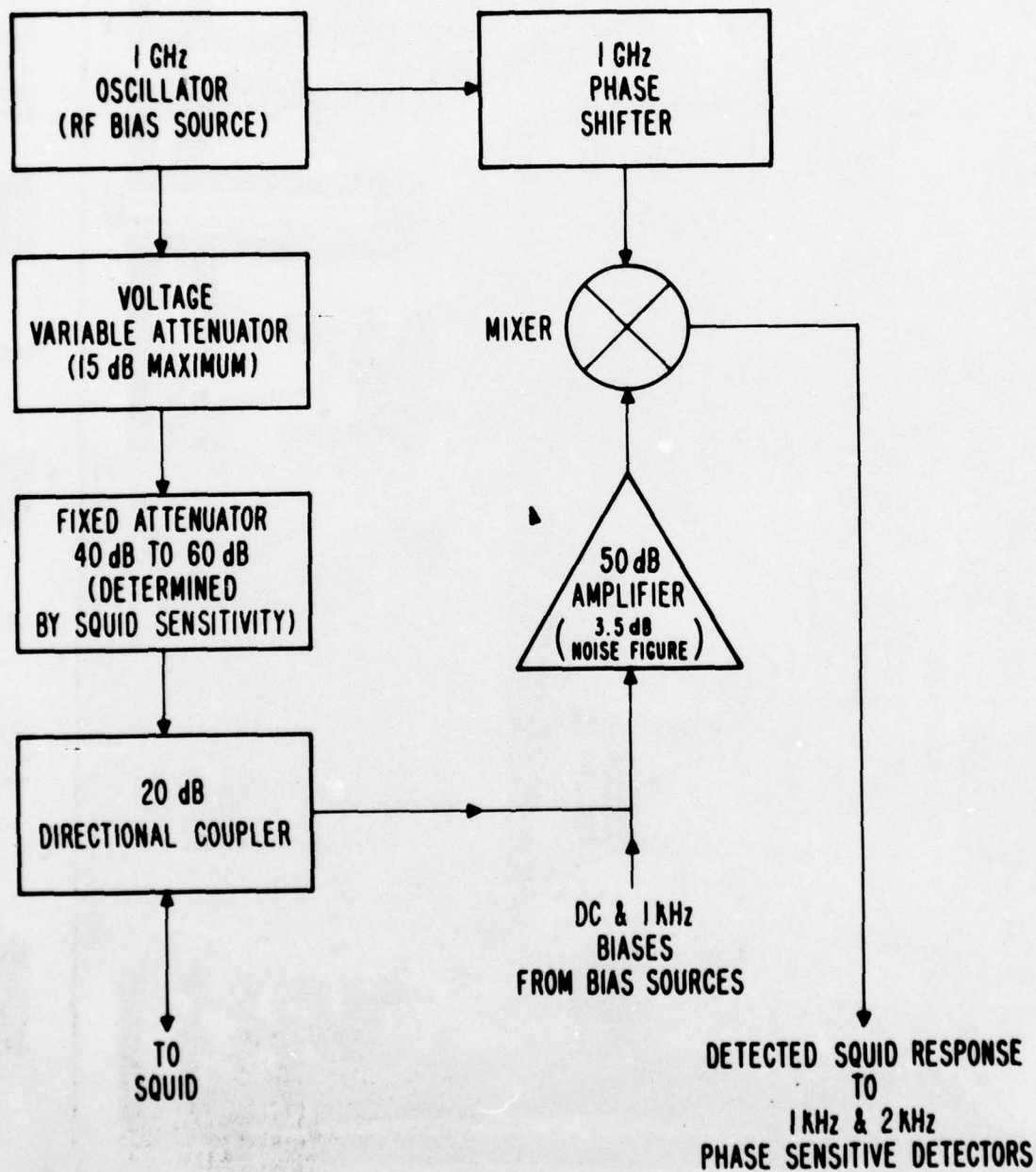
Figure 1.8. Block diagram of microwave bias (1 GHz) circuits.

77 4094
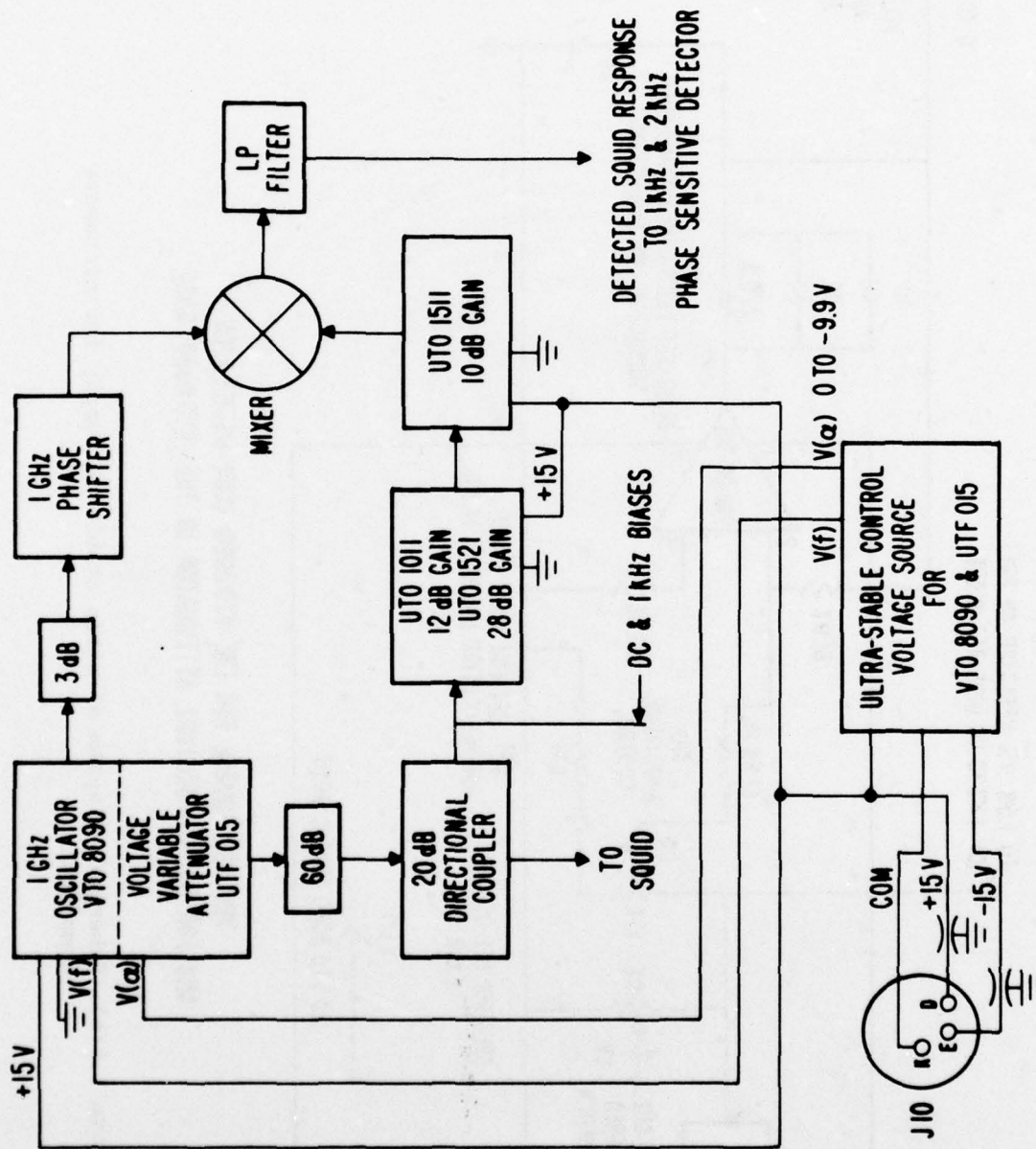
Figure 1.9(a). Schematic block diagram showing power supply connections for SQUID bias (1 GHz) components.
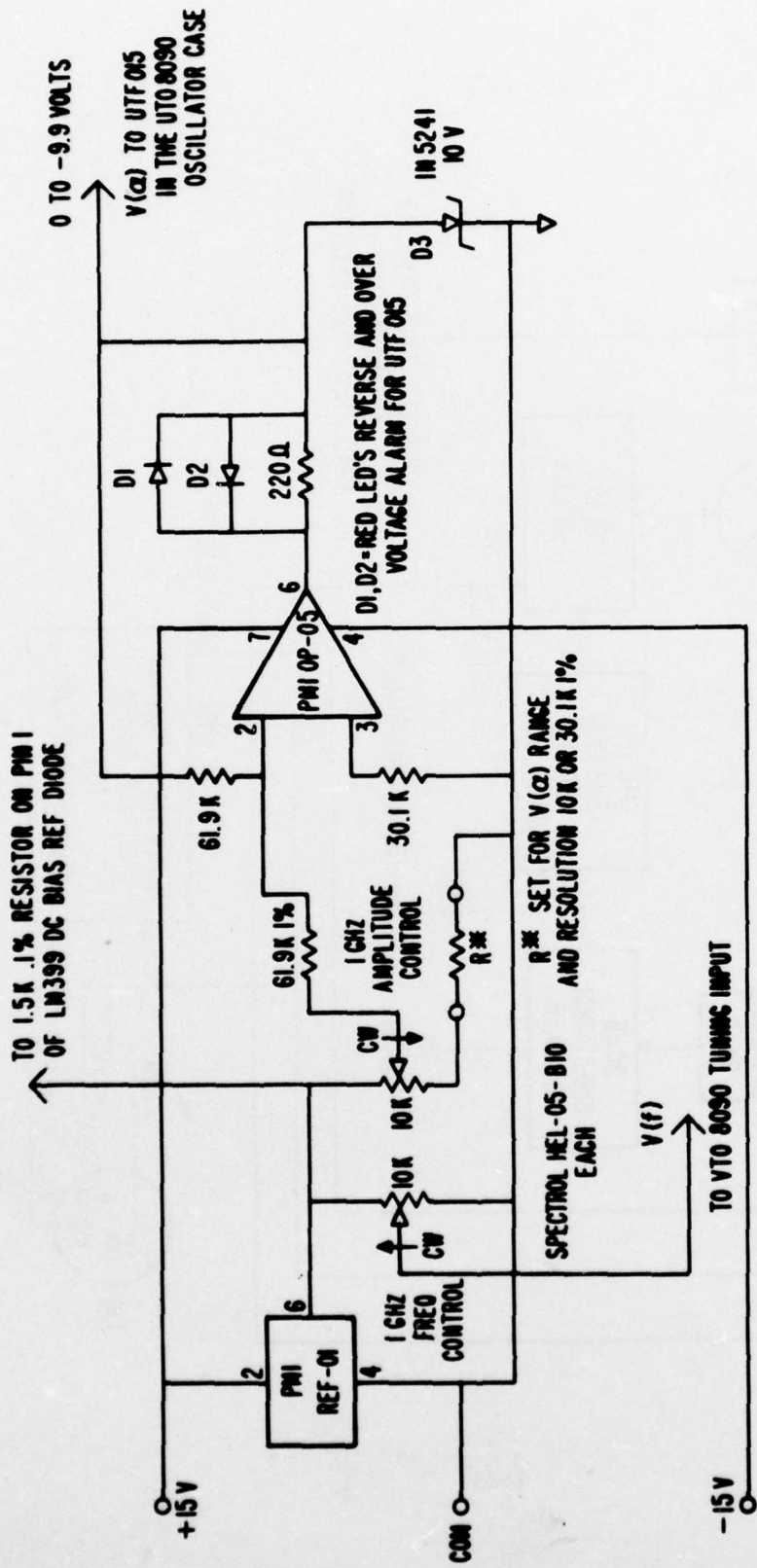
Figure 1.9(b). Schematic diagram of ultra stable dc supply for microwave components.
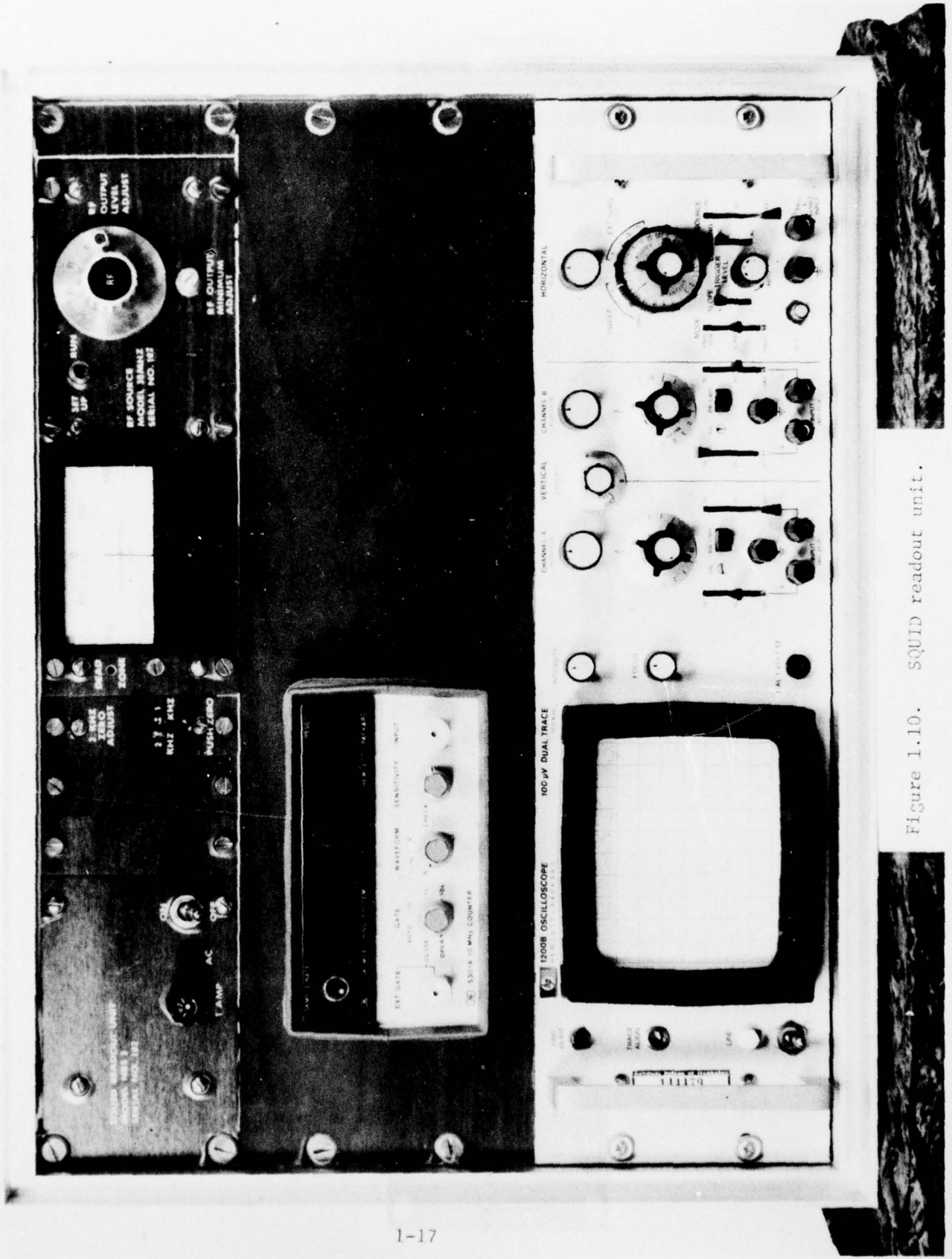
Figure 1.10. SQUID readout unit.
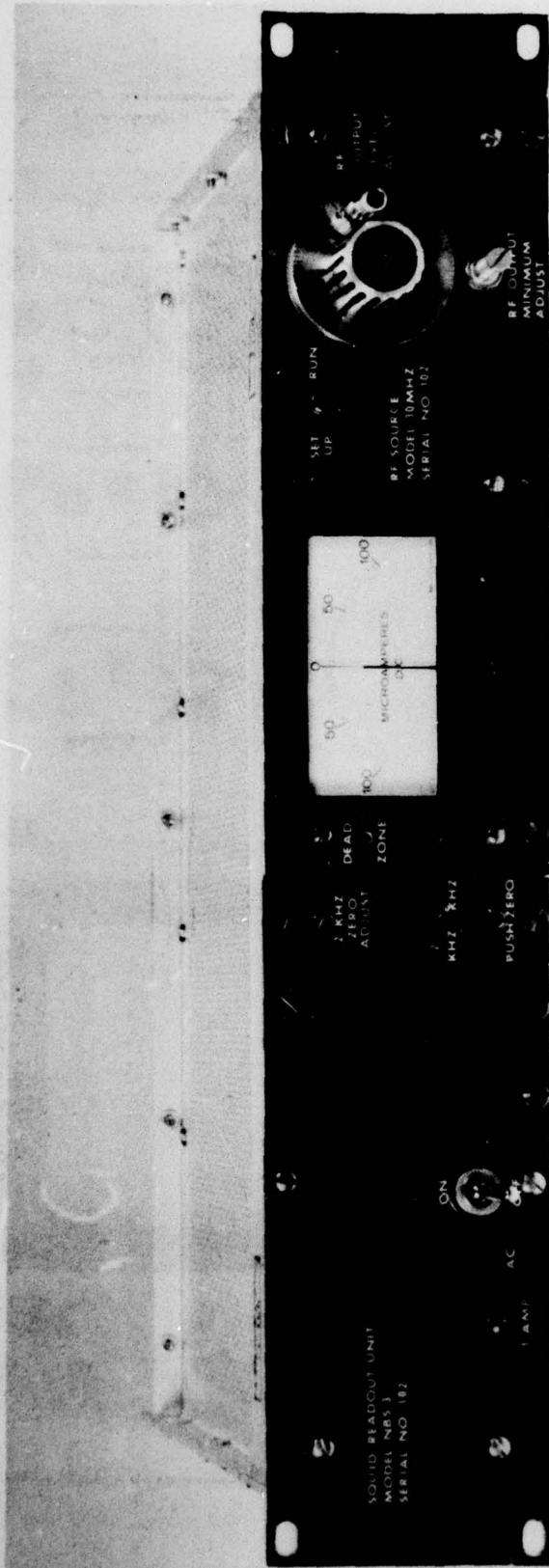
Figure 1.11. Front view of rf signal source and null indicator portion of the SQUID readout unit.
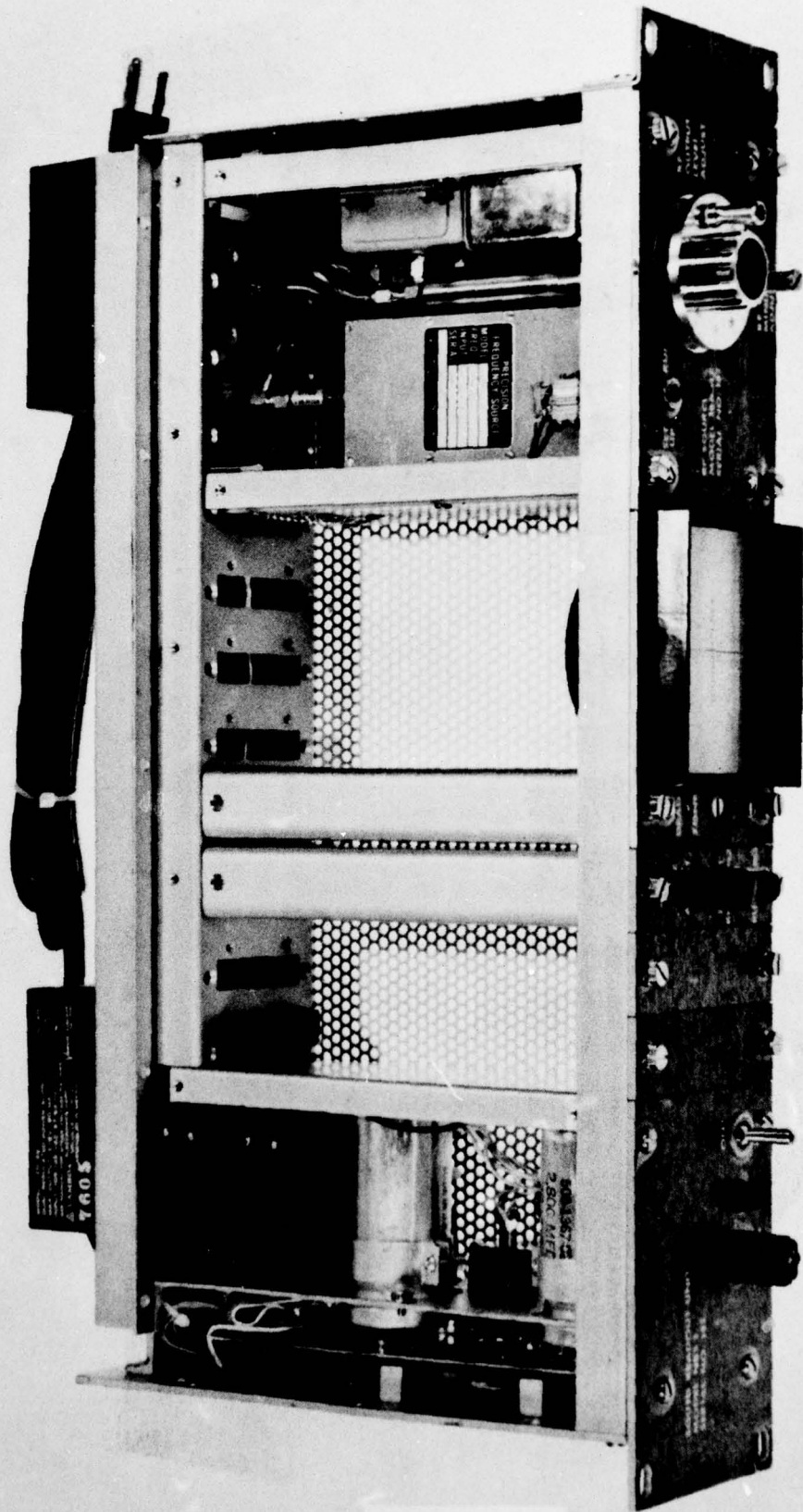
Figure 1.12. Top view of rf signal source and null indicator unit containing (left to right) the power supplies, the 2-kHz phase sensitive detector, the count generating circuits, the 1-kHz phase sensitive detector, and the rf signal source.
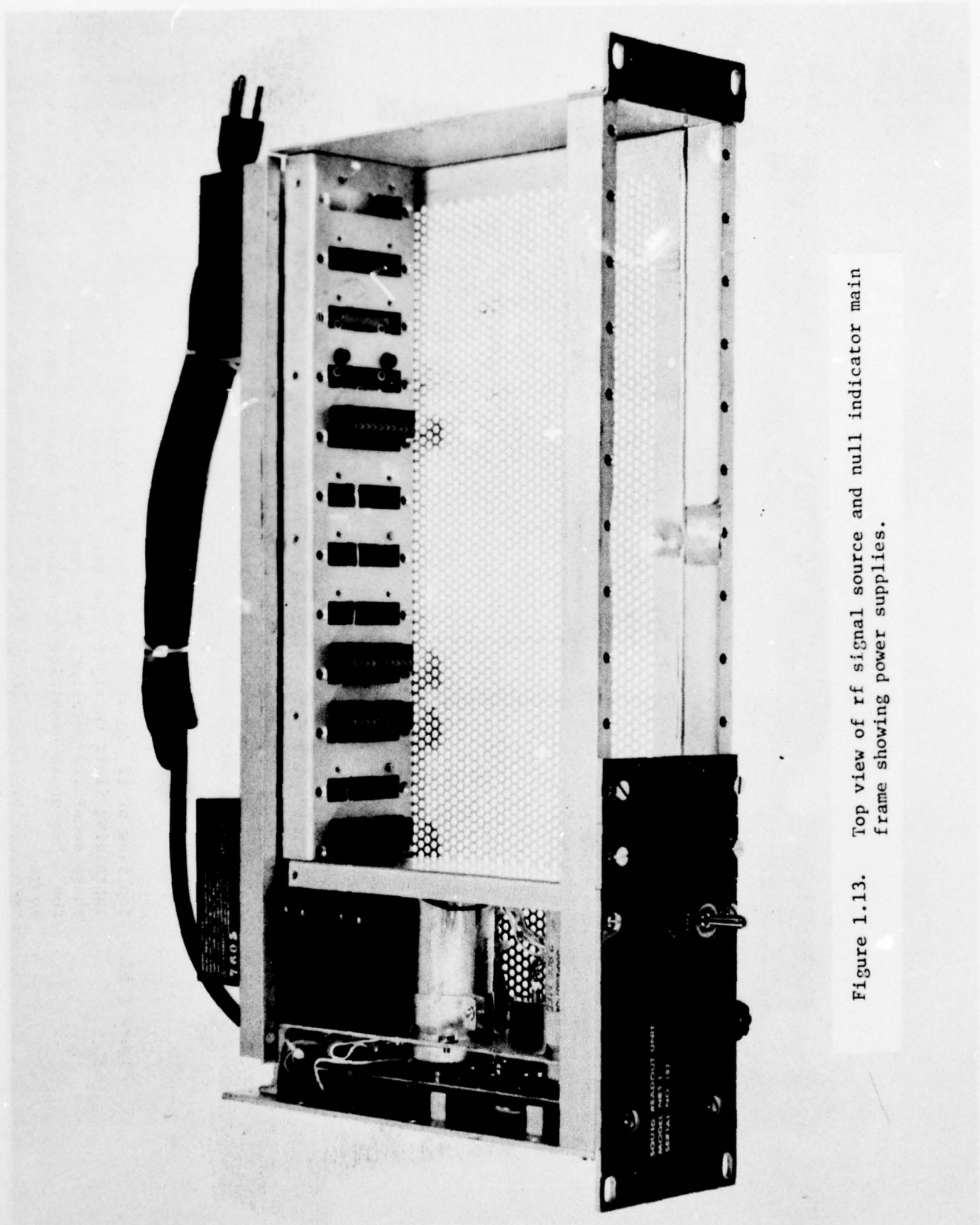
Figure 1.13. Top view of rf signal source and null indicator main frame showing power supplies.
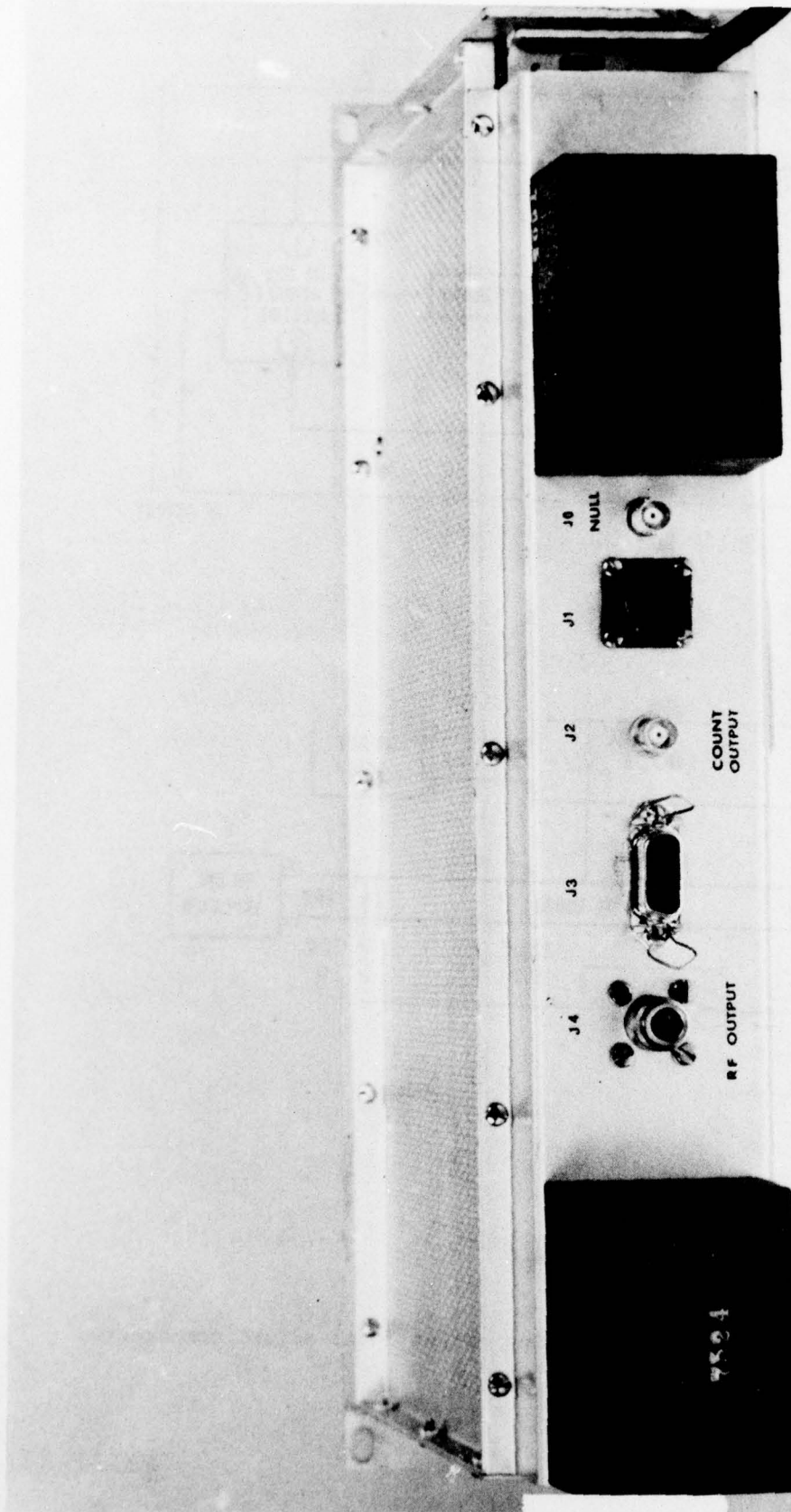
Figure 1.14. Rear view of rf signal source and null indicating unit showing rear panel connectors.

BLOCK DIAGRAM

SCHEMATIC DIAGRAM
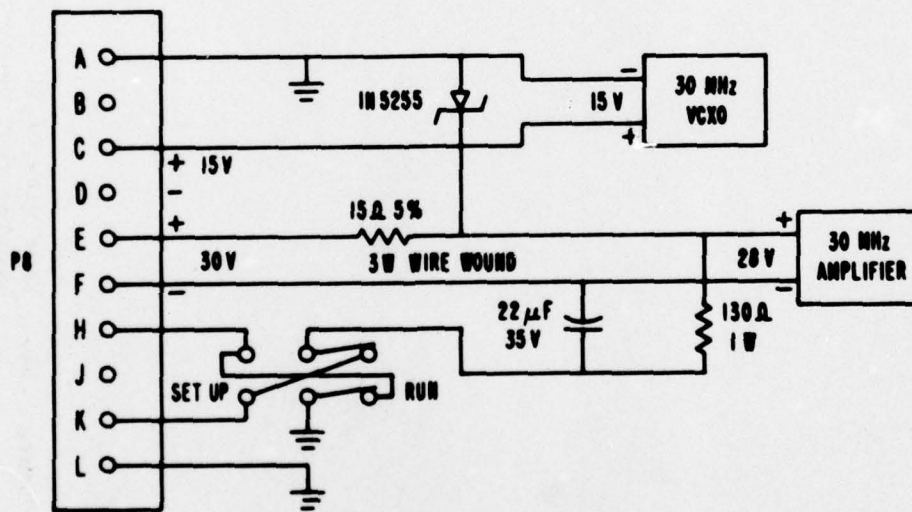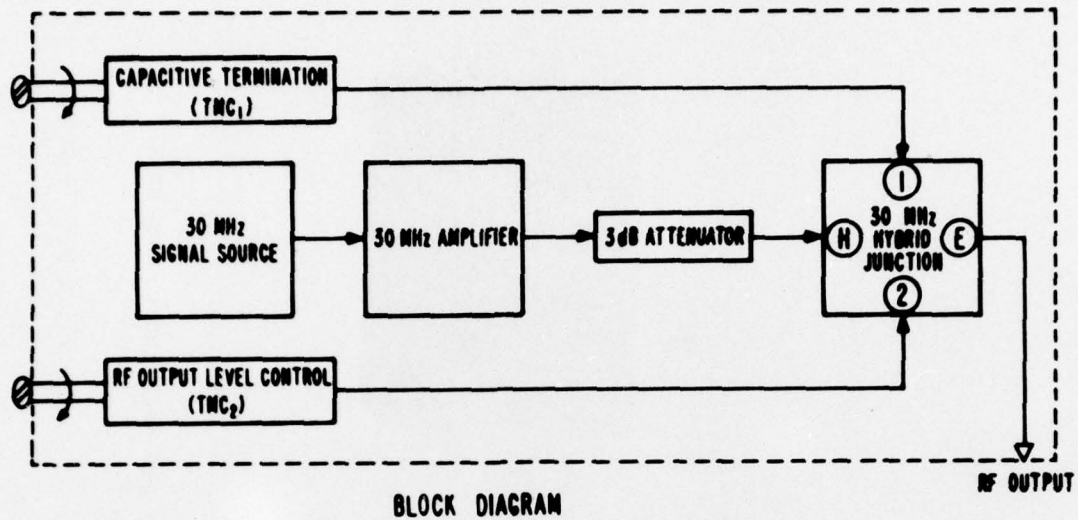
RF SOURCE PLUG-IN

Figure 1.15.   30-MHz plug-in module showing output level adjust components.

Figure 1.16. Front view of rf source module.
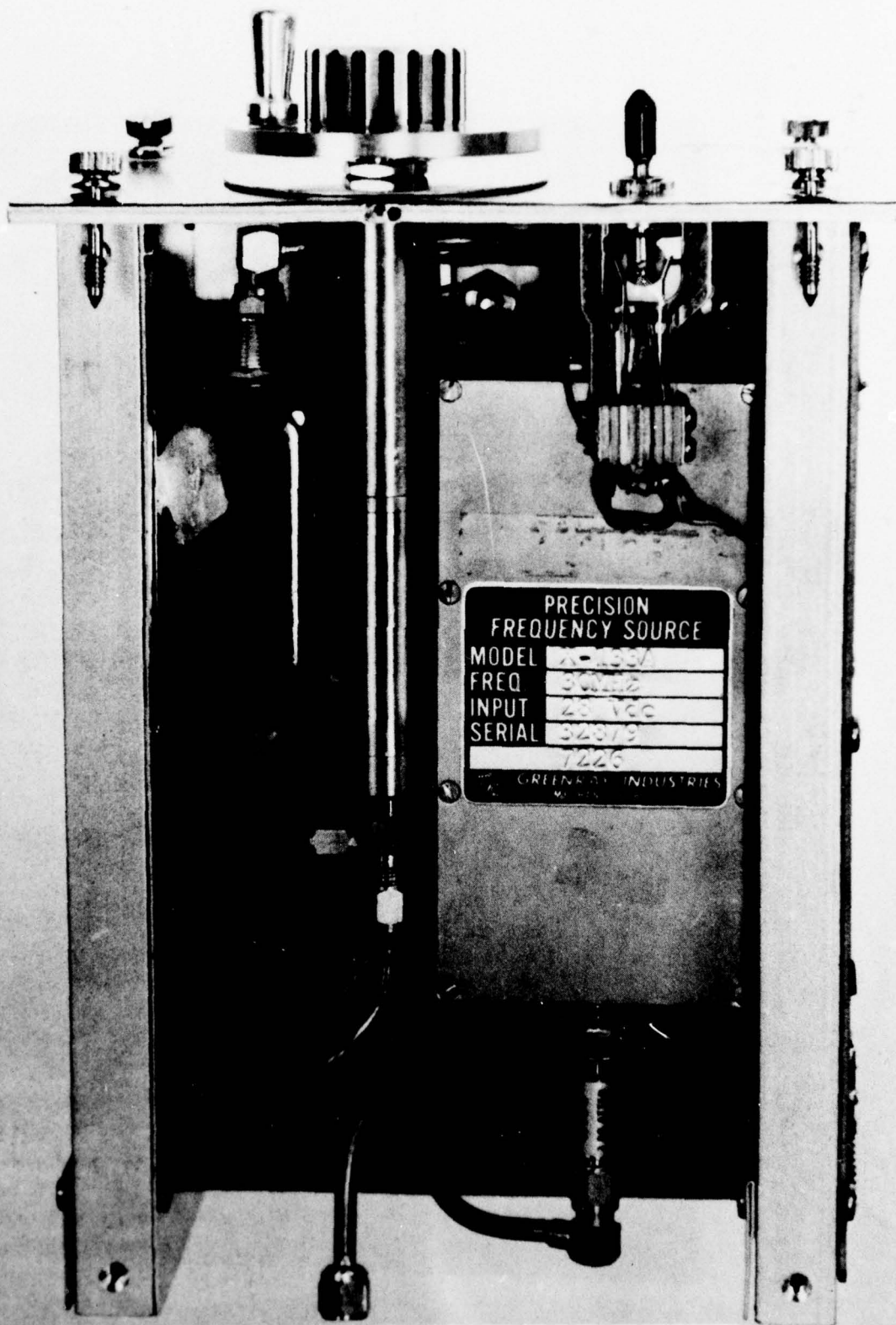
Figure 1.17.   Top view of rf source module.
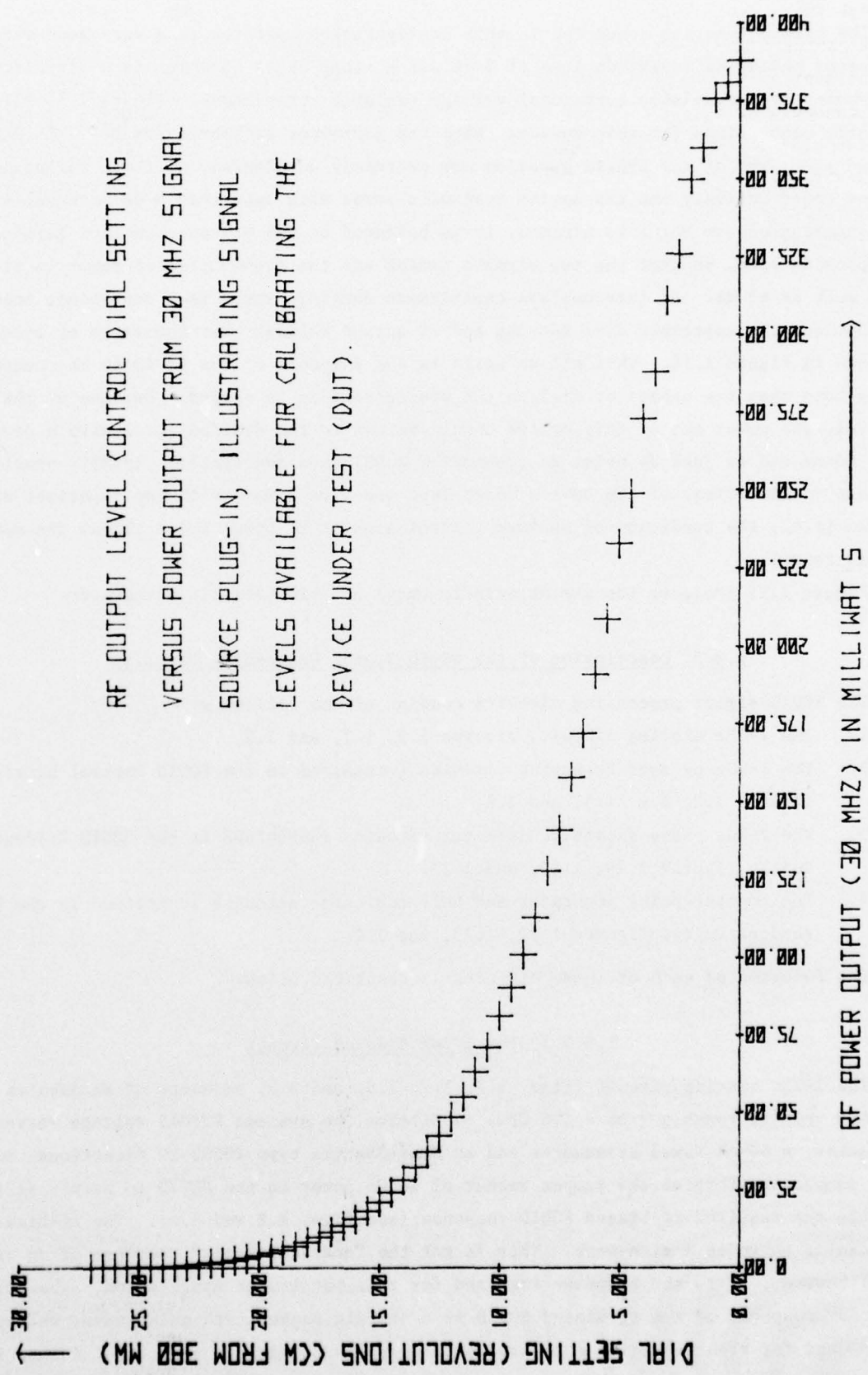
Figure 1.15. RF output level control characteristic curve.

The hybrid junction connected in this configuration operates as a very good variable rf attenuator having an insertion loss of 3 dB and a range of 65 dB which is a significant improvement over available commercial voltage variable attenuators. Figure 1.15 illustrates the basic connections for this device. When the capacitor on hybrid arm No. 1 is maximum, the two side arms of the hybrid junction are extremely unbalanced, so their reflections combine constructively and the device transmits power with less than 3-dB attenuation. When the capacitor on arm No. 1 is minimum, it is balanced by the piston capacitor terminating the opposite port, so that the two signals cancel and the transmitted rf power is attenuated by as much as 65 dB. At intermediate capacitance settings there is a convenient relationship between the capacitor dial setting and rf output voltage over the range of attenuation as shown in figure 1.18. This allows nulls in the response of the SQUID to be counted at a steady rate when the capacitor dial on the source plug-in is varied. Because of the high rf level, the power out of this source should be set to the desired level with a power meter connected to jack J4 prior to connecting a DUT into the system. Usually precise settings (calibration) of the Device Under Test are always made with the capacitor near its maximum (i.e., the condition of maximum transmission of rf power which allows the maximum dynamic range).

Figure 1.18 presents the characteristic curve of this variable attenuator.

1.3.3 Description of the SQUID Signal Processing Circuits

The SQUID signal processing circuits consist of the following:

1. The 1-GHz biasing circuit, figures 1.2, 1.7, and 1.8.
2. The 1-kHz or zero detecting circuits (contained in the SQUID Control Unit), figures 1.2, 1.4, 1.5, and 1.6.
3. The 2-kHz phase sensitive detector circuits (contained in the SQUID Readout Unit), figures 1.19, 1.20, and 1.21.
4. The counter-pulse generator and null indicator circuits (contained in the SQUID Readout Unit), figures 1.22, 1.23, and 1.24.

The function of each of these circuits is described below.

1.3.3.1 The 1-GHz Biasing Circuit

The 1-GHz biasing circuit (figs. 1.2, 1.7, 1.8, and 3.6) consists of an Avantek type VTO 8090 voltage tunable (.96 - 1.6 GHz) oscillator, an Avantek UTF015 voltage variable attenuator, a 60-dB fixed attenuator and an Omni-Spectra type 20063-20 directional coupler. These components furnish the proper amount of 1-GHz power to the SQUID to permit it to generate the required rf-biased SQUID response (see figs. 2.2 and 2.4). The rf-biased SQUID response is shown as a sine-wave. This is not the "characteristic" response of an rf-biased SQUID; however, it is the response required for this particular application. The "characteristic" response of the rf-biased SQUID is a sharply peaked triangular wave, whereas the SQUIDS used for rf-attenuation work are modified so as to yield a sinusoidal rather than a triangular response. The signal emerging from the SQUID passes up through the directional coupler into the 1-GHz amplifiers (Avantek types UTO 1011, UTO 1521, and UTO 1511). The
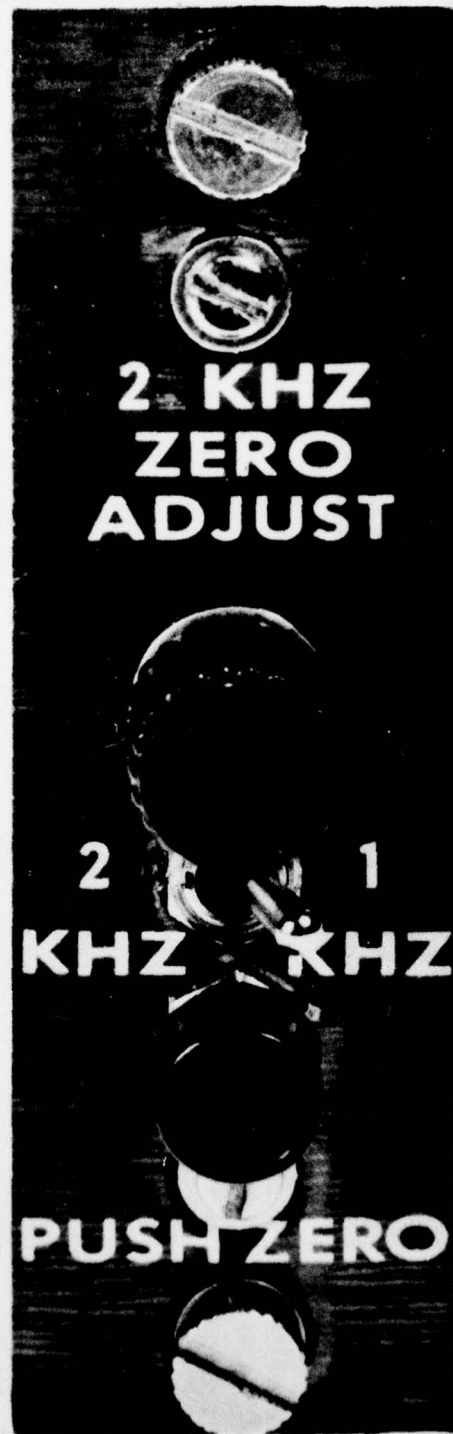
Figure 1.19.   Front view of the 2-kHz phase sensitive detector plug-in.
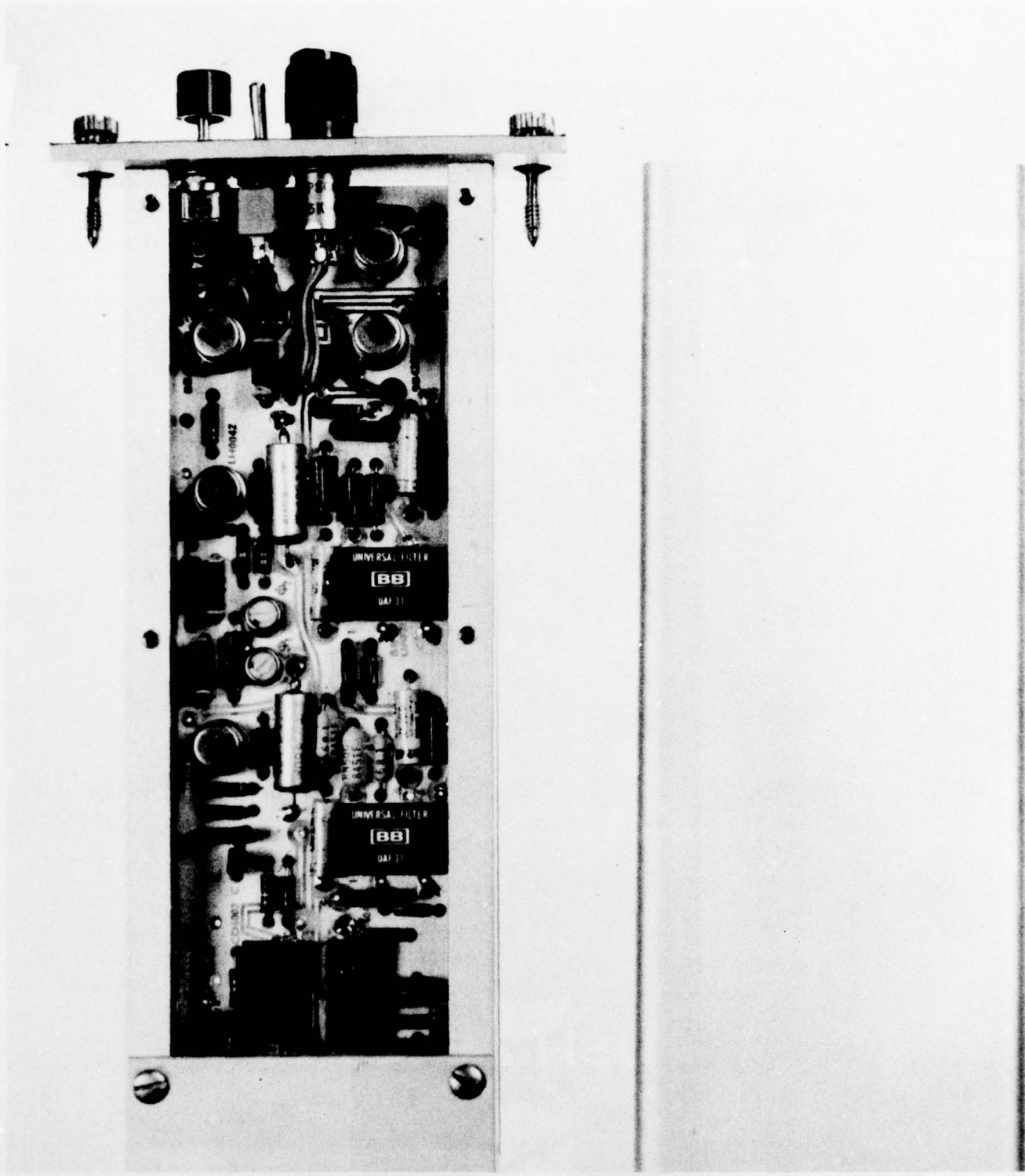
Figure 1.20.   Side view of 2-kHz PSD plug-in.
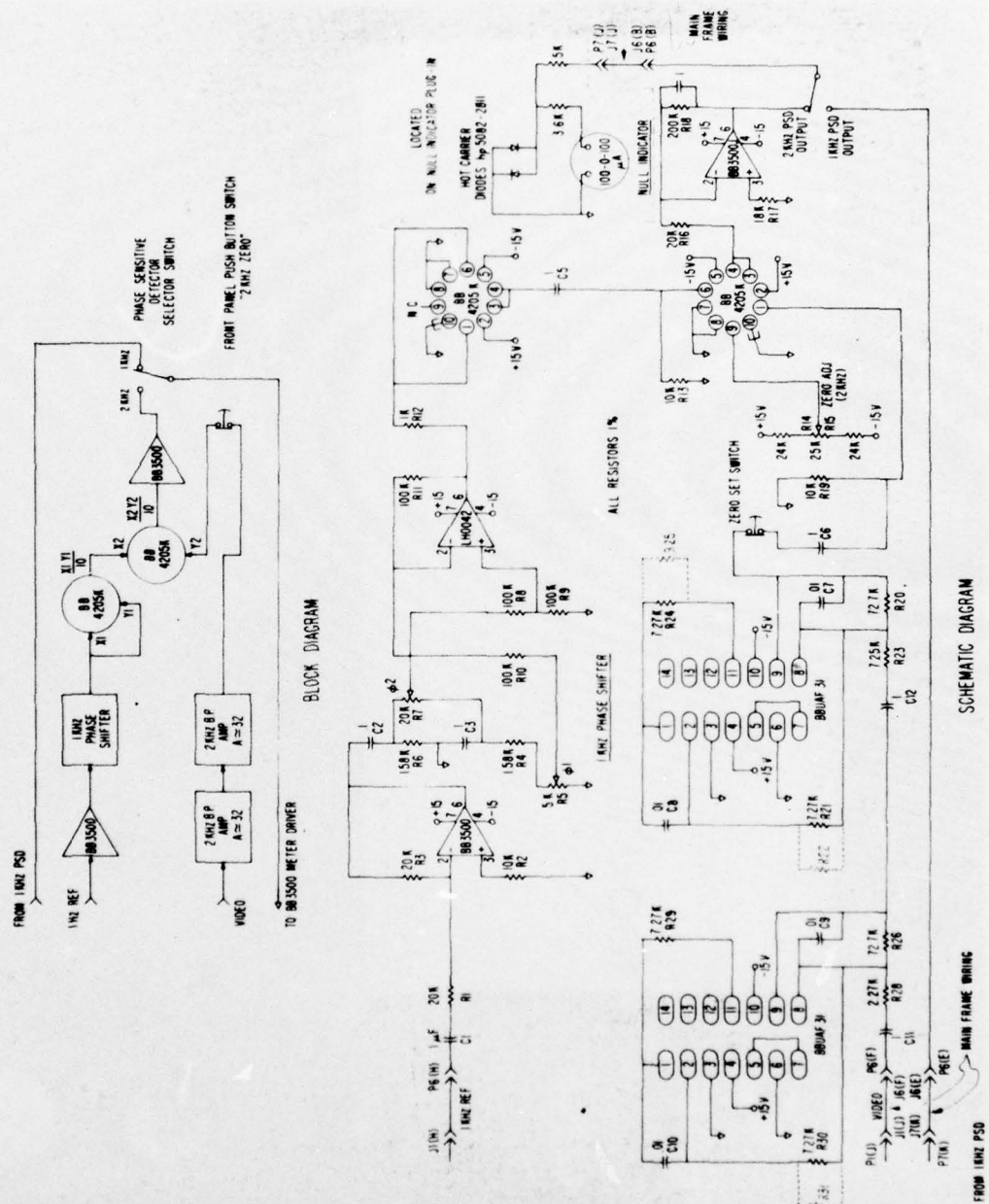
Figure 1.21. Schematic diagram of 2-kHz bandpass amplifier and phase sensitive detector.
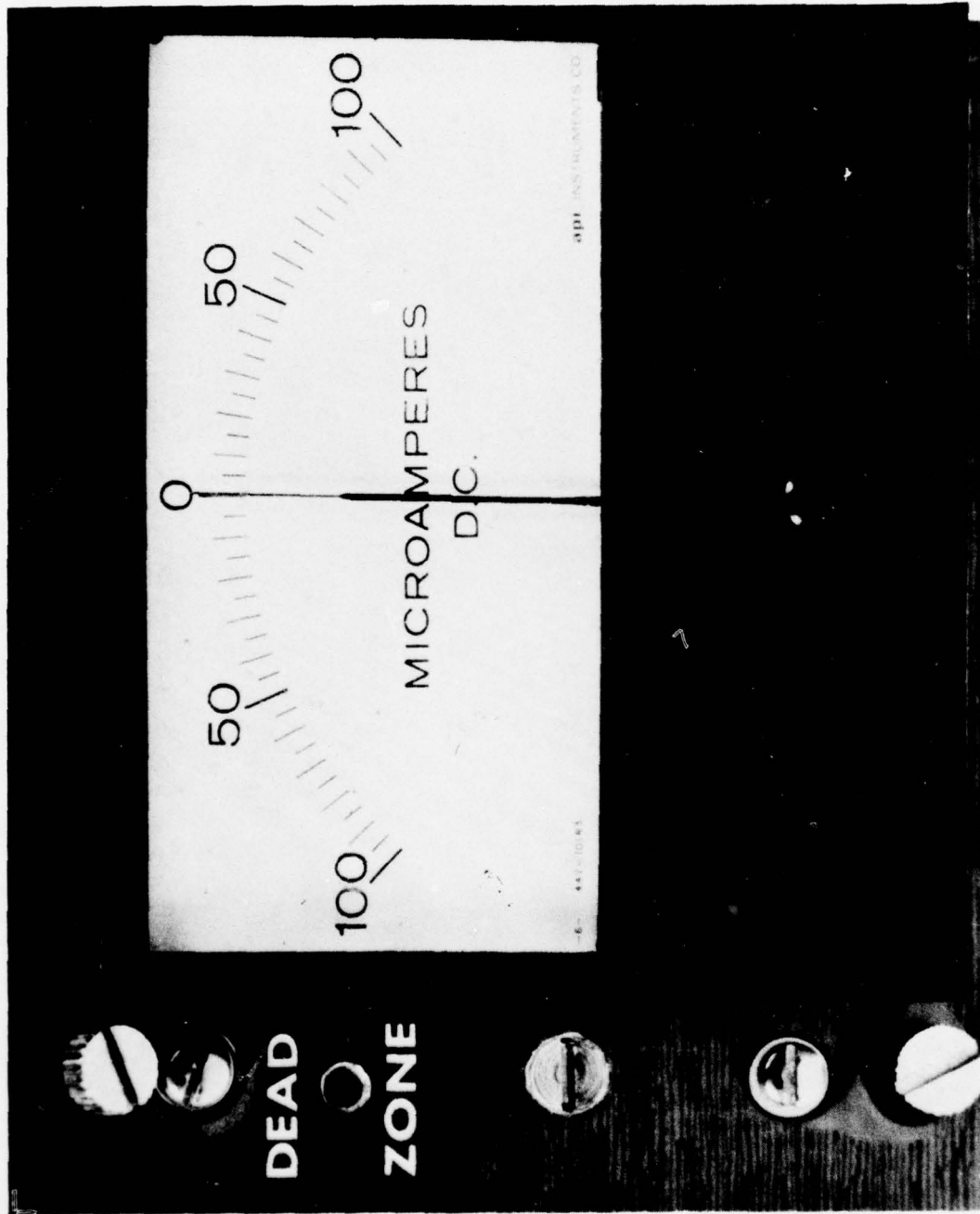
Figure 1.22.   Front view of null indicator plug-in.
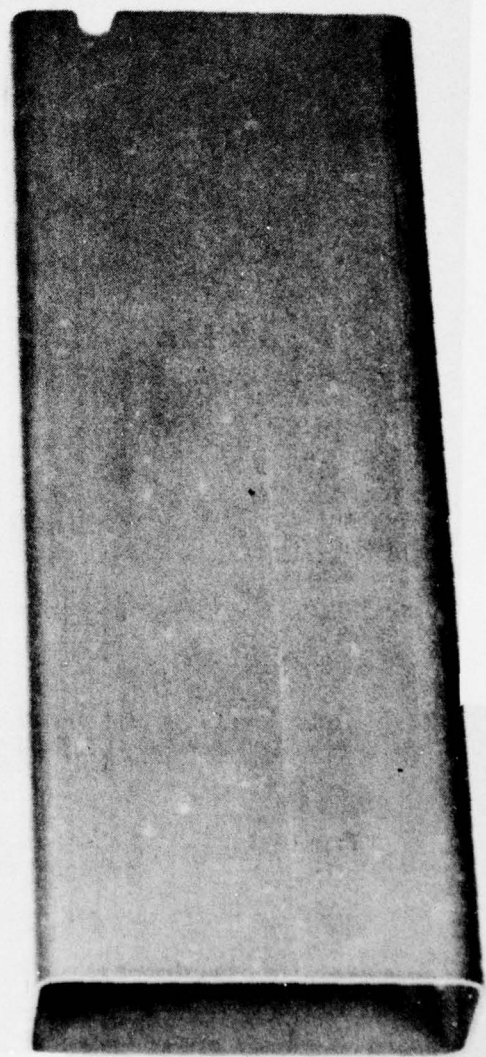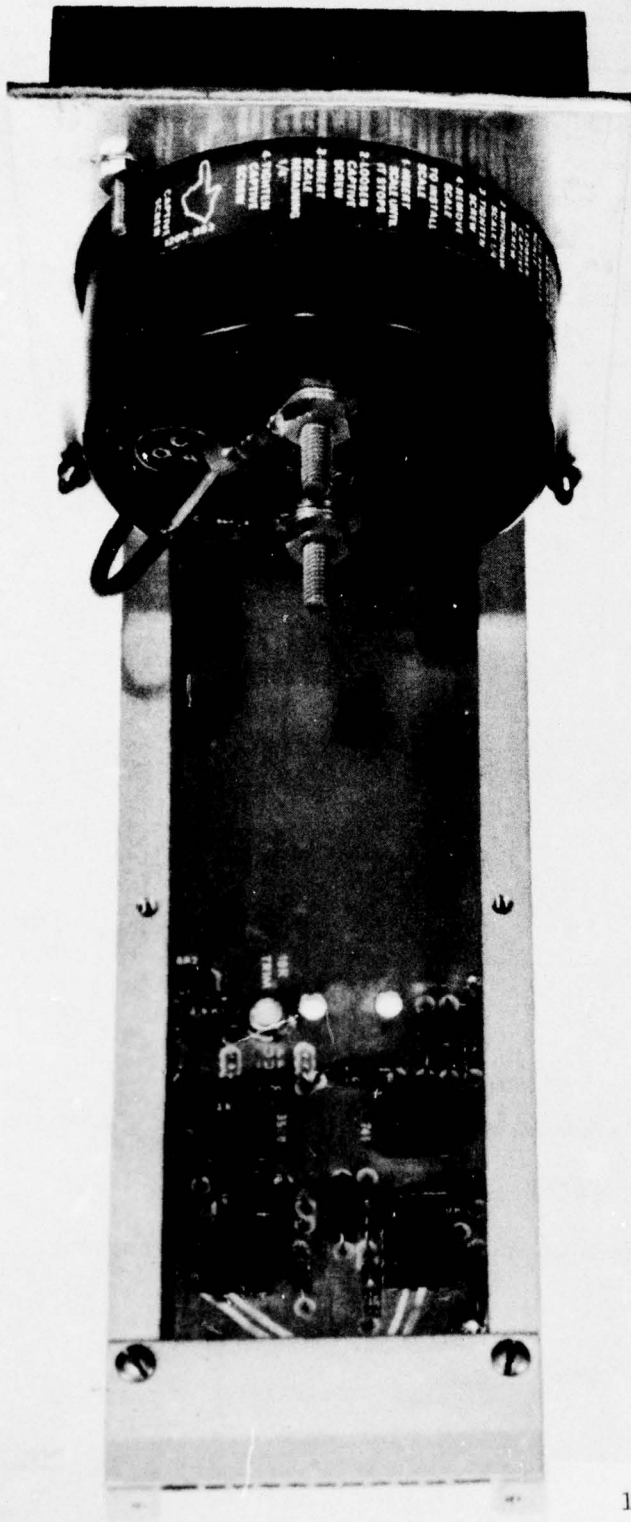
Figure 1.23. Side view of null indicator plug-in.

1-31
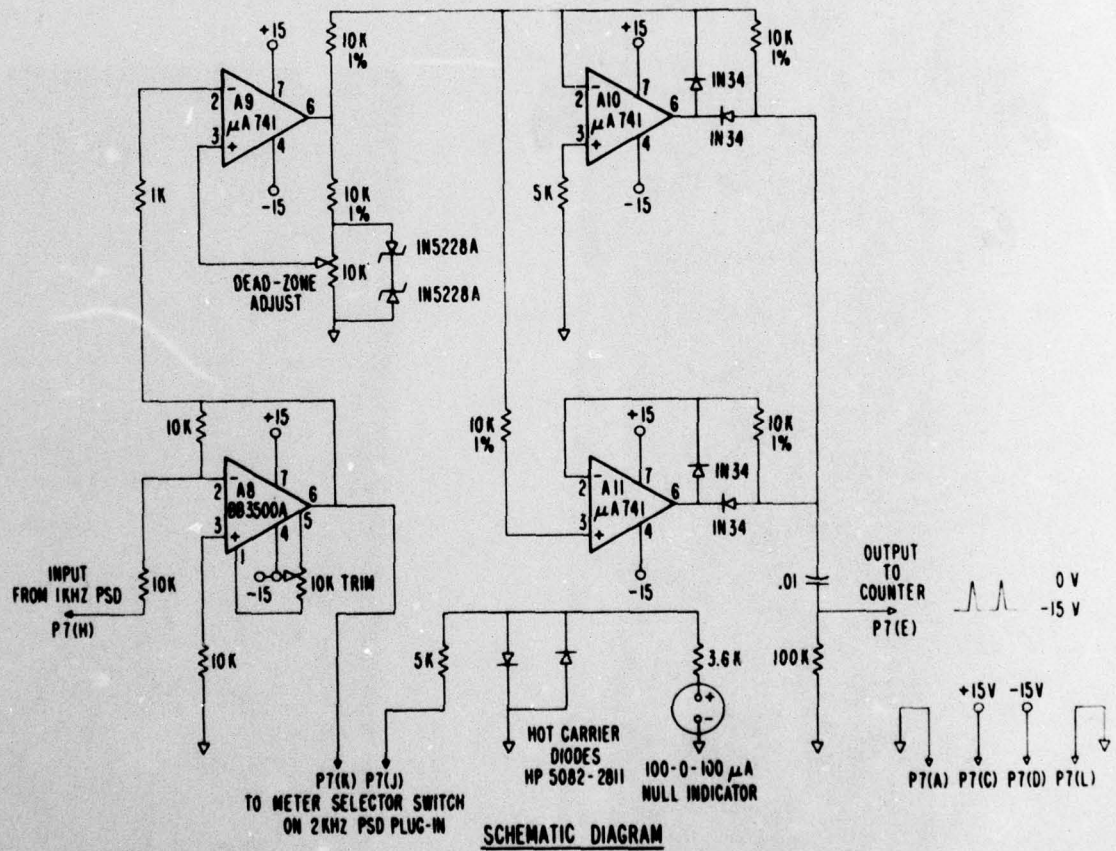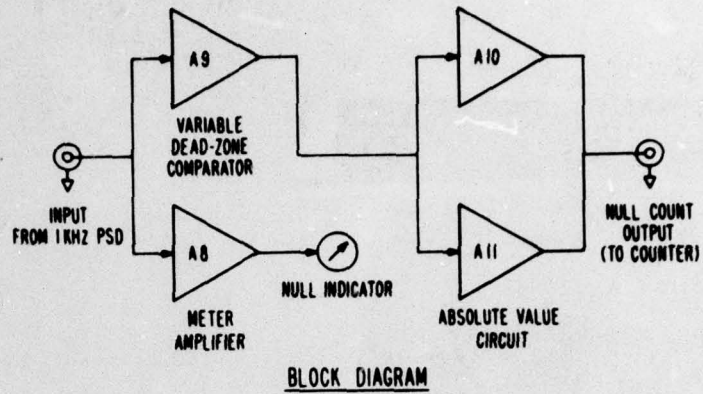
Figure 1.24. Schematic diagram of null indicator and null counting trigger circuits.

1-32

last of these amplifiers (UTO 1511) drives the "R" port of a Merrimac-type DMM 2-500 double-balanced mixer. The "L" port of this mixer is driven by the 1-GHz phase shifter (Merrimac Model psm 2/22401) which receives its signal through a 3-dB fixed pad from the VTO 8090 oscillator.

1.3.3.2 The 1-kHz Zero Detecting Circuits

The output from the double-balanced mixer goes to the 1-kHz preamplifier A_1 (see figs. 1.4, 1.6, 1.8, and 3.7).

The output of this preamp (A_1) is sent two ways; it goes to the 1-kHz amplifier (A_3, A_4, and A_5) and to the video amplifier A_2.

The signal from A_2 goes to the VIDEO output BNC connector on the control unit (which goes to the oscilloscope's vertical input) and to the main cable and thence to the 2-kHz amplifier and synchronous detector (PSD)* in the 2-kHz PSD plug-in in the Readout Unit (see figs. 1.19, 1.20, and 1.21). The signal from the preamp which is sent to the 1-kHz amplifier is amplified and sent to the 1-kHz PSD. The reference for this PSD is generated by the 1-kHz oscillator A_7. This oscillator also provides the 1-kHz bias signal. The 1-kHz PSD output goes to A_5, is amplified, and is sent to the meter amplifier A_8 (fig. 1.24) in the null indicator plug-in in the Readout Unit chassis via the interconnecting cable.

1.3.3.3 The 2-kHz Phase Sensitive Detector Circuits

The output from the video amplifier A_2 goes to the 2-kHz bandpass amplifiers (see fig. 1.21) and into the y_2 input of the BB 4205K multiplier. The 1-kHz reference signal goes through the 1-kHz phase shifter after which its amplitude is squared by the BB 4205K multiplier. The output of this multiplier ($\frac{x_1y_1}{10}$) becomes the x_2 input to the second BB 4205K multiplier. Recall that the y_2 signal into this multiplier comes from the 2-kHz bandpass amplifiers. The product of these two signals ($\frac{x_2y_2}{10}$) is proportional to the 2-kHz component of the detected SQUID rf signal and is proportional to the asymmetry of the rf bias (1-GHz) operating point of the SQUID. This resulting signal is presented to the null indicator (via the 1-kHz – 2-kHz selector switch) when the system is in the setup mode.

1.3.3.4 The Counter-Pulse Generating Circuits

The output from the 1-kHz PSD also goes to a variable dead-zone dual comparator A_9, which drives an absolute value circuit A_{10} and A_{11} (see figs. 1.22, 1.23, and 1.24). These circuits generate a trigger which goes to the counter via a BNC connector (J2) at the rear of the Control Unit chassis. The width of the dead zone is adjusted to prevent false counting due to noise. The action of these circuits is illustrated in figure 1.25.

---

*PSD: Phase Sensitive Detector.

1.3.4 Description of the SQUID

Figures 1.26 and 1.27 show the SQUID, and figure 1.28 shows the complete probe assembly containing the SQUID for attenuation measurements. The adjacent tube is plated with a Pb-Sn alloy upon which a thin sheet of mu-metal is wrapped. This serves to further shield the SQUID from low frequency fields. The bracket at the top is a mechanical support for the Control Unit electronics.

We have long been aware of two different approaches to the achievement of a sinusoidal interference pattern from a SQUID. We have concentrated on the operation of the SQUID in a highly damped mode, a method which calls for the addition of shunt conductance. While this helps, we now find that a low value of critical current provides the most significant improvement in measurement results. The mathematical description of the system operation is more difficult in this regime; however, it is a mode of operation which generates much lower levels of harmonics. A high critical current reflects hysteretic losses into the tank circuit while a low critical current results in a predominantly reactive effect.

The major source of difficulty encountered with earlier systems was the adjustable point contact. Calibrations generated by these systems were occasionally quite good, but dramatic changes often accompanied the readjustment of the contact; a situation which is intolerable for routine calibrations [4]. Recently, Petley et al. [5] have used a network analyzer to study the junction response and have generated an empirical method for contact adjustment.

Our solution to the problem is to completely eliminate routine junction adjustment with the use of permanently adjusted contacts of prescribed characteristics. These contacts are made within a small cartridge which is inserted into a specially-designed, toroidal SQUID. This approach permits the replacement of the cartridge should the contact fail. This arrangement also permits us to make a four-terminal I-V measurement and to thus set the contact for a desired characteristic.

Figure 1.29 shows the SQUID and a cross section of the cartridge with its permanently adjusted contact. The glass approximately matches the total expansion of Nb between 4 K and 300 K.

The two halves of the niobium cartridge are fused to a thin layer of a borosilicate glass which electrically isolates them. The glass we have chosen has a total thermal expansion (between 4 K and 300 K) which closely matches that of niobium thus reducing axial motion of the contact members during temperature cycling.

The point and anvil which form the junction are finished with a fine (#500 grit) emery paper, and are then surface oxidized by a hydrogen-oxygen torch in a manner similar to that described by Strait [6]. Aging effects are reduced by placing a microscopic drop of epoxy on the point of the junction. This is allowed to set after a suitable contact adjustment is completed. We have subjected three separate junctions to more than 100 cycles between 300 K and 78 K in a 14-hour period with no discernible changes observed in the I-V characteristics at 4 K. Figure 1.30 illustrates the I-V characteristics of a SQUID point contact cartridge having a critical current of 10 microampere. A gradual aging over the last 15 months has resulted in ∿ 10 to 20% increases in the shunt resistance. While lesser changes
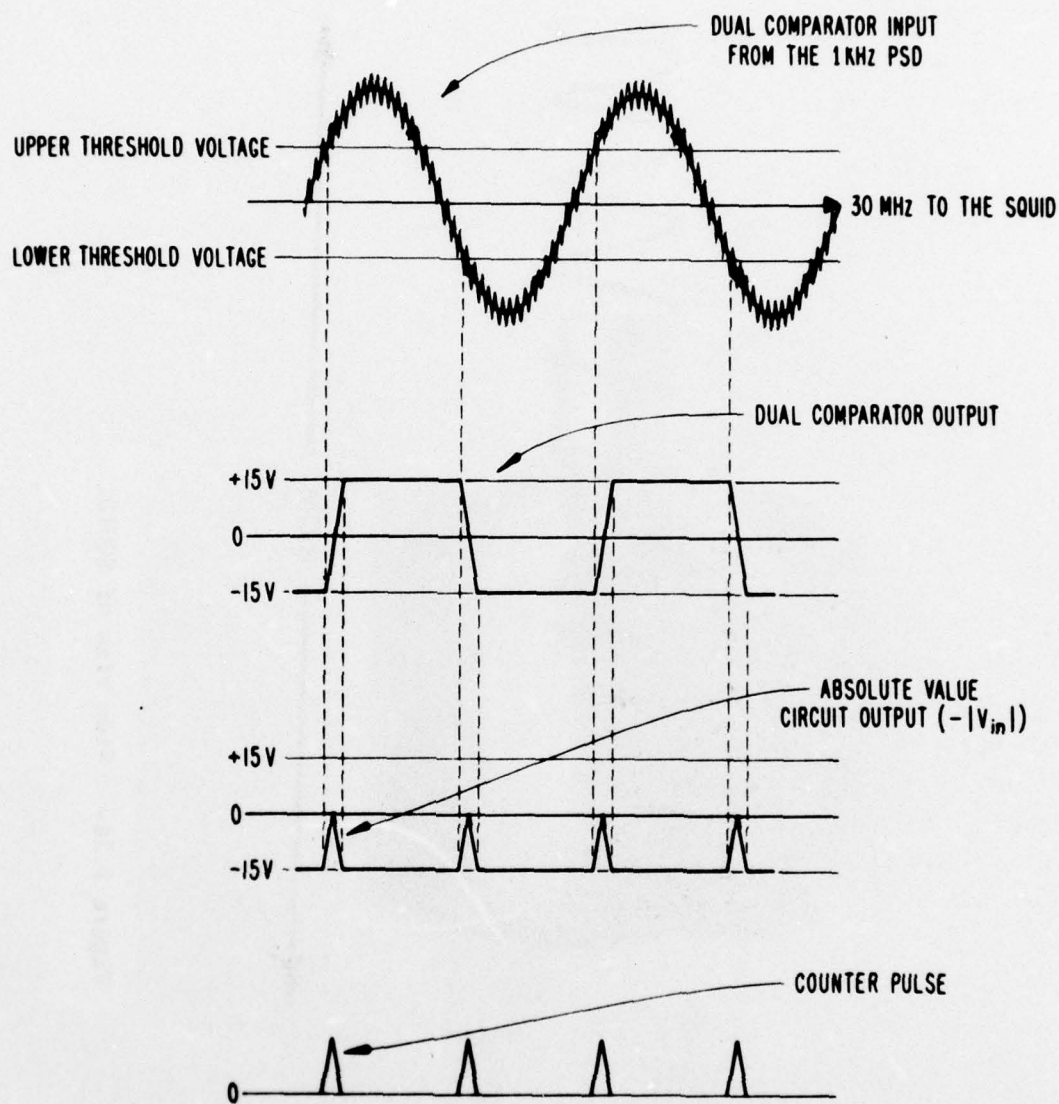
Figure 1.25. Illustration showing the operation of the pulse generating circuit which activates the digital counter to indicate the Bessel function zero number.

1-35

8 CM
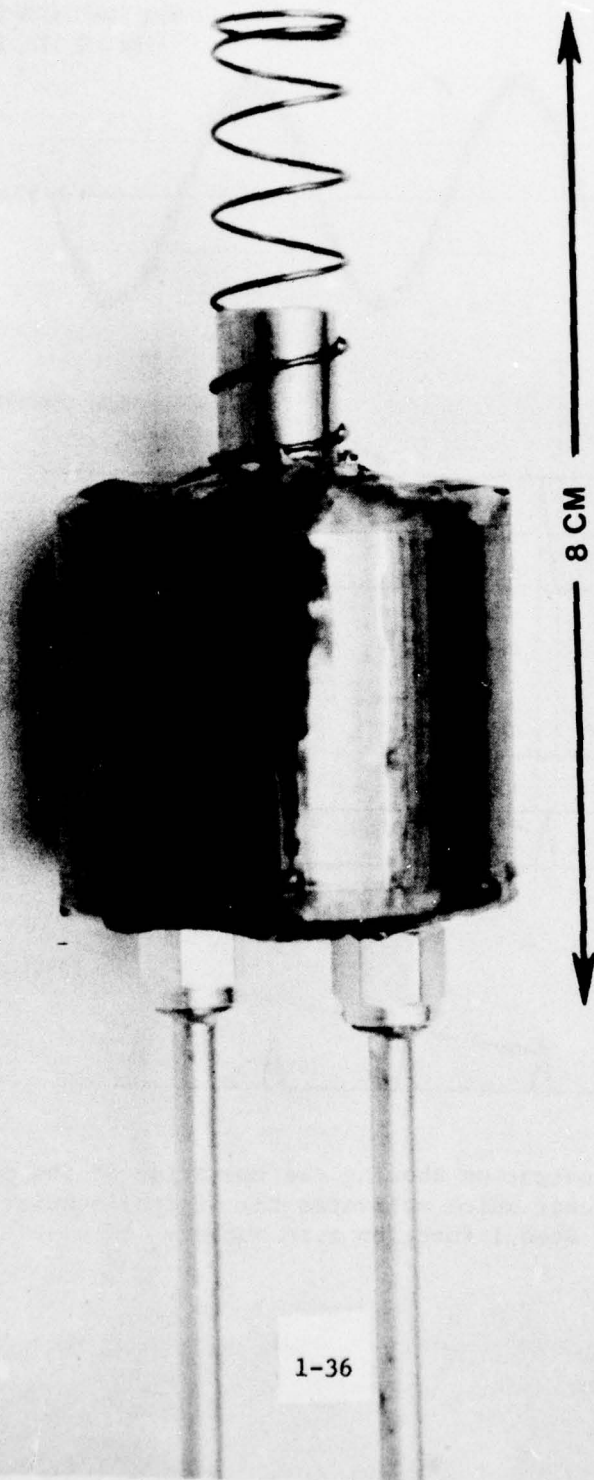
Figure 1.26. Side view of SQUID.
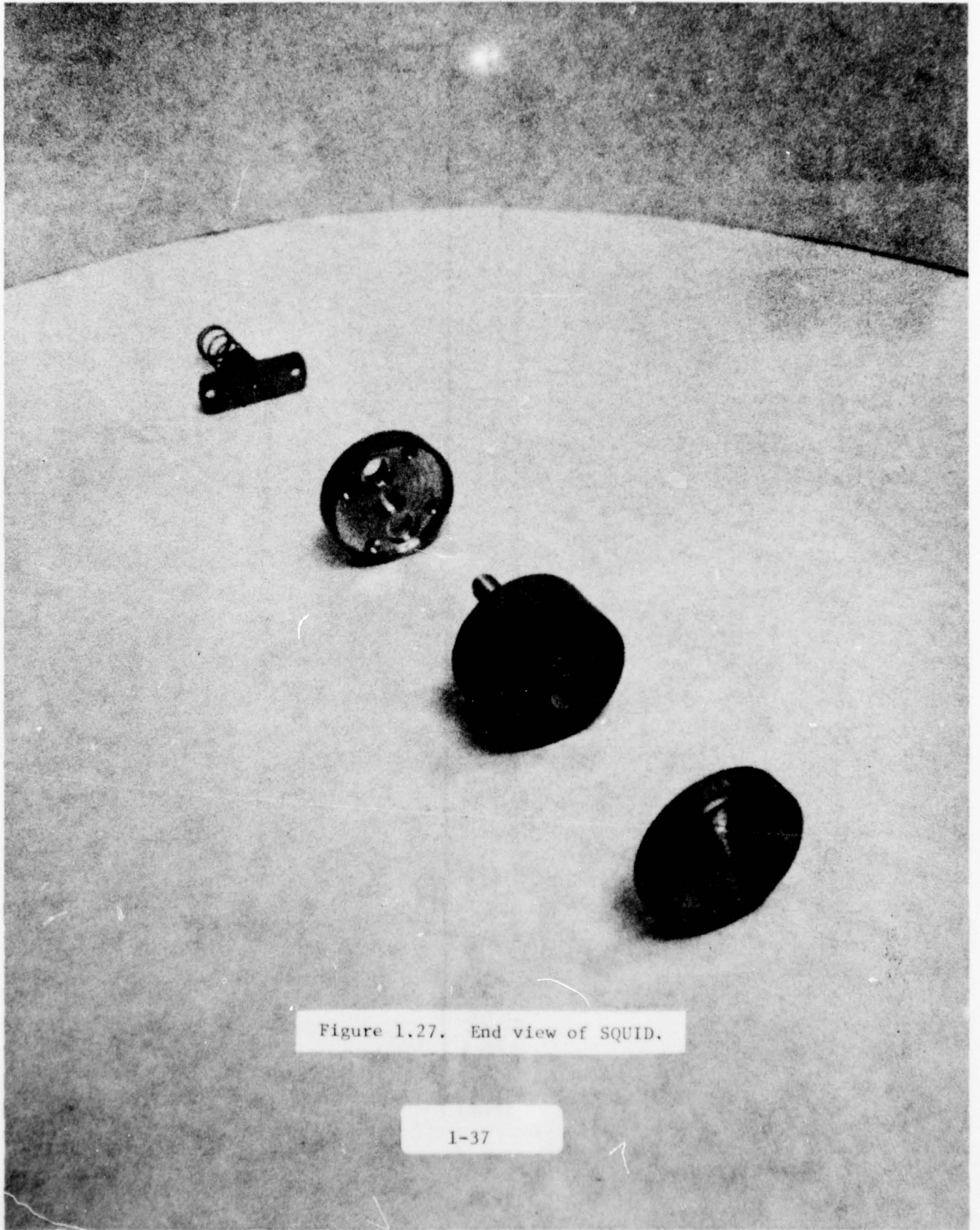
Figure 1.27. End view of SQUID.

1-37

99 CM
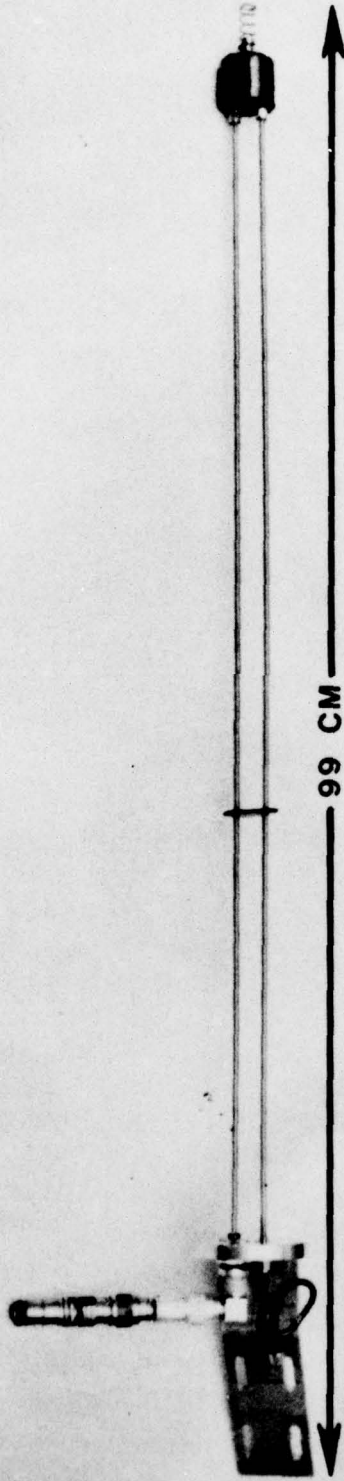
Figure 1.28   View of SQUID probe assembly.
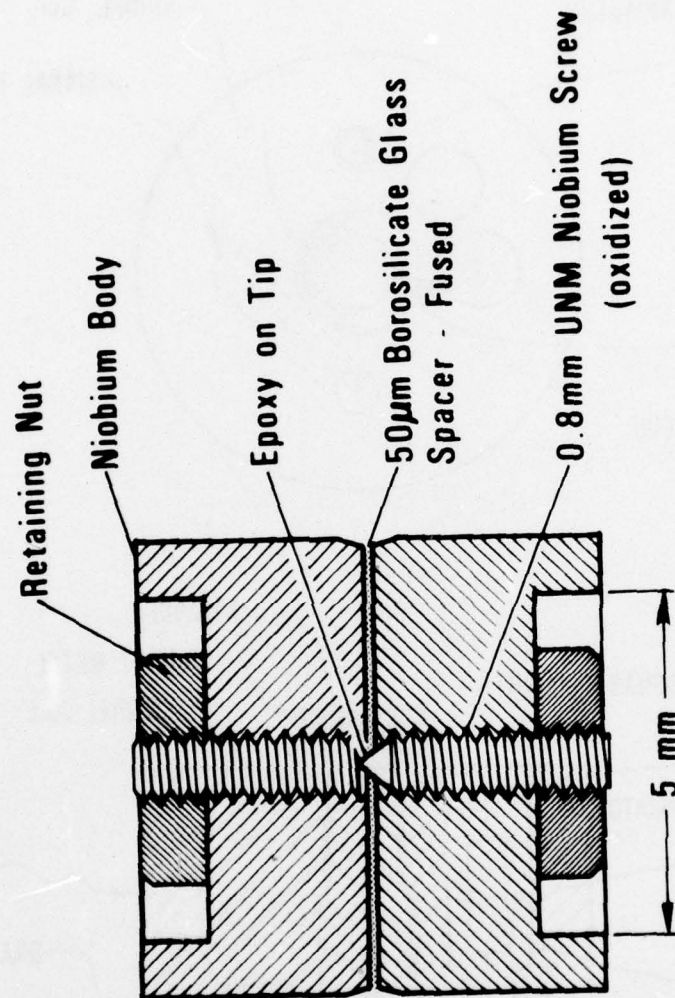
Figure 1.29(a). Diagram of SQUID cartridge with permanent point contact.

Retaining Nut

Niobium Body

Epoxy on Tip

50μm Borosilicate Glass
Spacer - Fused

0.8mm UNM Niobium Screw
(oxidized)

5 mm
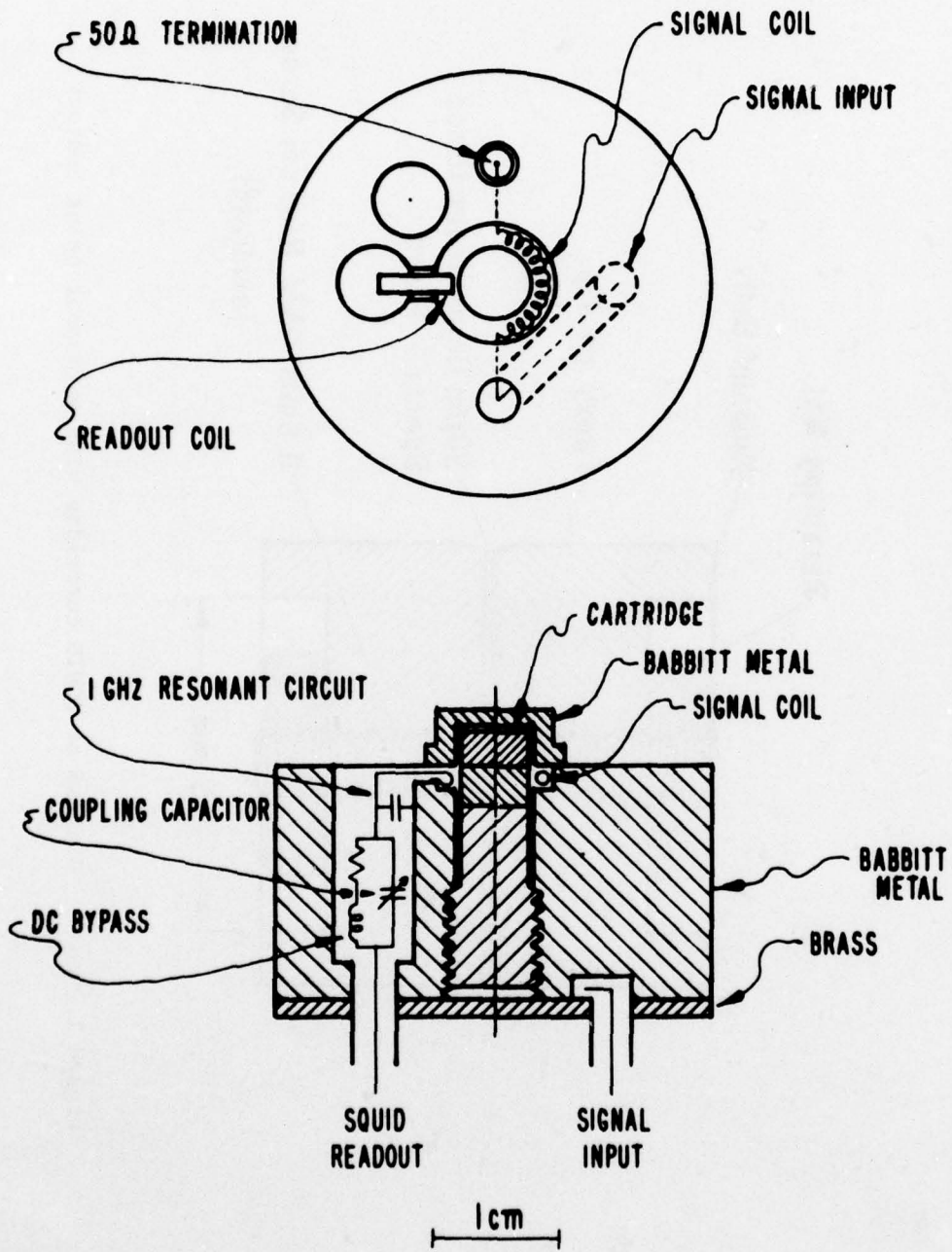
Figure 1.29(b).   Diagram of SQUID body containing cartridge.

1-40
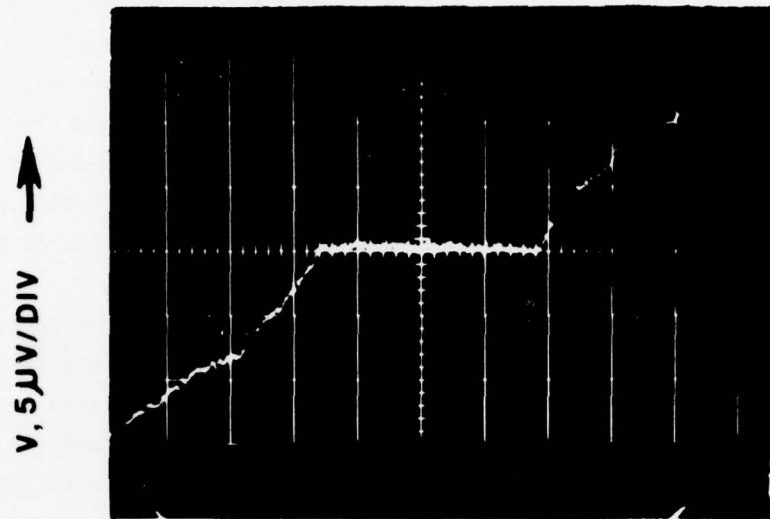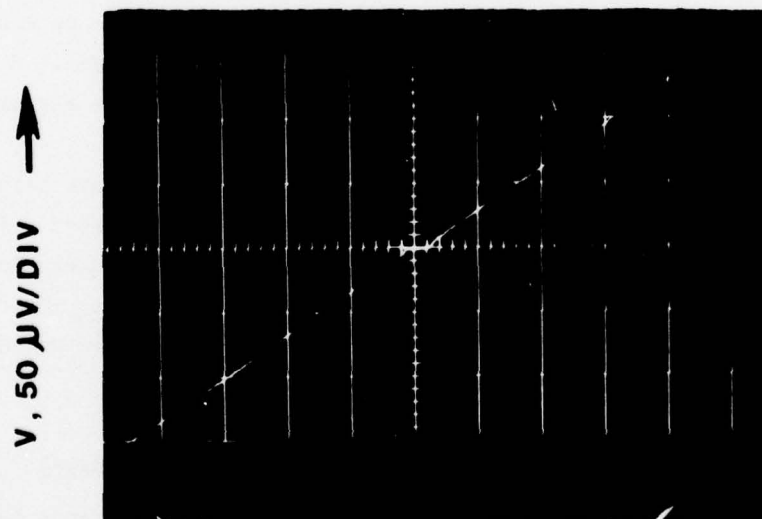
Figure 1.30   Voltage versus current characteristics of a SQUID point
contact cartridge with a 10 microampere critical current.

in critical current have occurred, there is no well established trend toward higher or lower values. We find that contacts with a shunt resistance of one ohm and critical current of $\sim$ 5 μA generate a rather pure sinusoidal interference pattern (in a SQUID with $L \approx 5 \times 10^{-10}$ H) and quite consistent measurements of attenuation result, if all other operating conditions are properly set. At a SQUID inductance of $\sim 10^{-9}$ H, the L/R time constant is 10^{-9} seconds, and thus the transition time for flux entry into the ring is of the same order as the period of the pump oscillation. From electronic analog simulation [7], we note that this results in a rounding of the normal triangular interference pattern [8] into a nearly sinusoidal response. The harmonic purity of the desired sinusoidal interference pattern is further enhanced by operation in the nonhysteretic mode (i.e., $Li_c/\phi_o < 1$) [8].

The SQUID into which this cartridge is inserted is shown in the bottom half of figure 1.29. The inductor for the 1-GHz resonant circuit is a one-turn copper strip in the toroidal cavity. The dc bypass of the coupling capacitor is simply a 1-cm length of 0.025-mm diameter resistance wire. Coupling between the SQUID and resonant circuit is readily adjusted by physically moving the inductor, and an ideal match of the resonant circuit to the line is achieved with the variable coupling capacitor. A schematic diagram of the SQUID circuit appears in figure 1.31.

Figure 1.32 illustrates a calibration run performed with improper circuit parameters. Two separate problems are indicated here. The strong deviation at the upper end is generated by the use of a rather large critical current, about 10 μA for cartridge #3. The plus-minus error alternation of odd and even zeros results from operation on a nonlinear portion of the double-balanced mixer (insufficient mixer bias which is easily corrected). Figure 1.33 is a repeat run with a low critical current ($\sim$ 2 μA) cartridge and emphasizes the splitting of zeros.

As described in previous reports, a number of programs have been developed for the HP 9830 desk calculator and plotter which is used with the system. Figures 1.32 and 1.33 show the utility of these peripherals. Figure 1.34 is a computer plot of a recent run with a curve giving a third polynomial fit to the data. This fit to the data allows interpolation as illustrated in figure 1.35. Thus, one could easily generate a table showing attenuator deviations at regular attenuation intervals.

1.3.5 Description of the Cryogenic Vessel

The liquid helium storage vessel which provides the cryogenic bath for the SQUID is shown in figure 1.36.

This Dewar has a gross capacity of 33.4 liters of liquid helium. It does not require an outer shield containing liquid nitrogen for cooling as in earlier dewars. This vessel uses superinsulation and recovers sensible heat by an ultra shielding system in a high vacuum to obtain the excellent thermal performance it enjoys. The inner portion of this Dewar along with the neck and mounting flange on top are constructed of stainless steel. The inner diameter of the neck is nominally 2.2 cm. The operating pressure inside the vessel is 3.45 kilopascals (0.5 PSI) as determined by the 0.64-cm diameter relief valve.

50 Ω COAXIAL LINE
30 MHz SIGNAL

50 Ω LOAD

TOROIDAL
SQUID

50 Ω COAXIAL LINE
L BAND BIAS

DC
BYPASS

COUPLING
CAPACITOR

$f_o \approx 1.2$ GHz
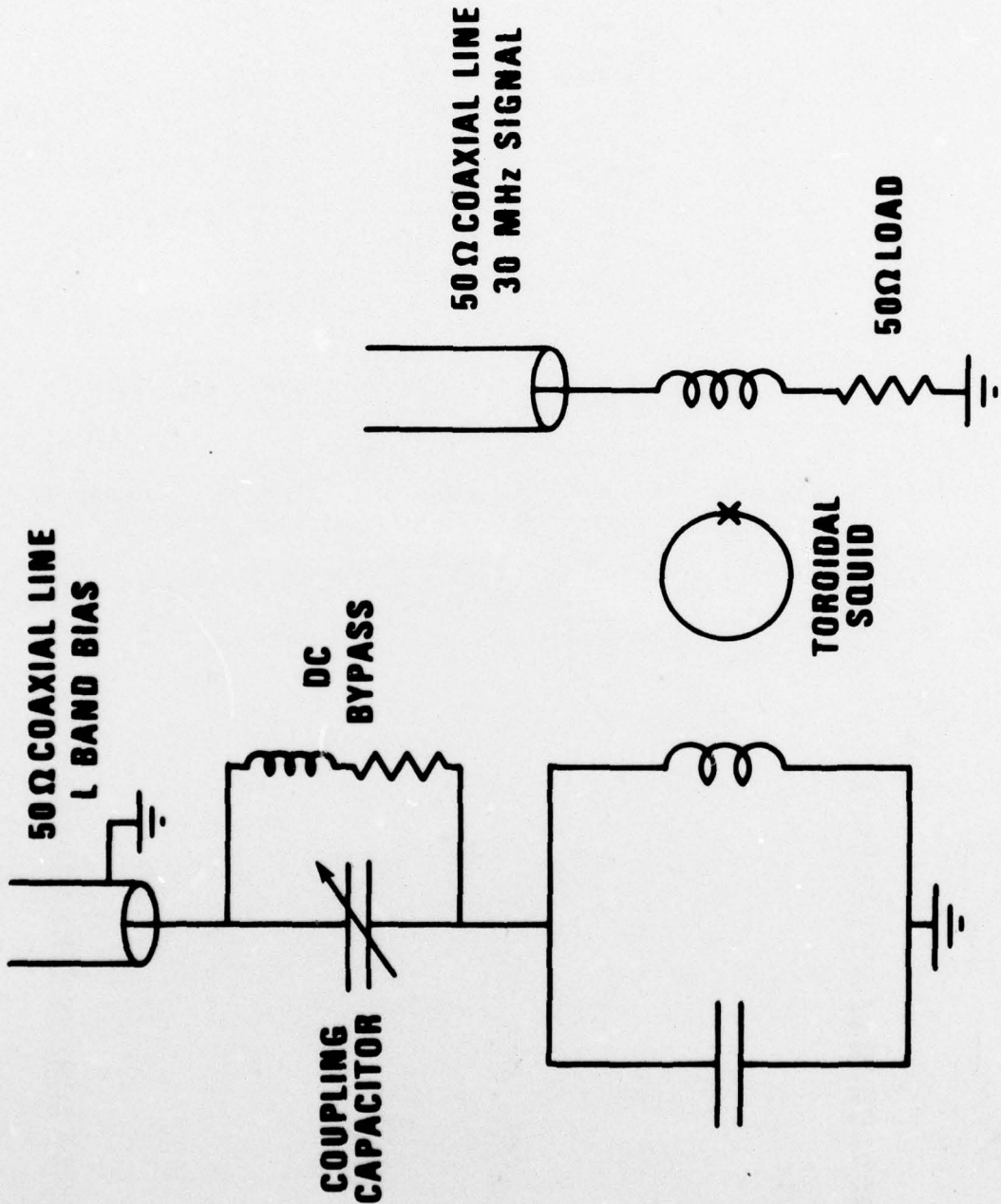
Figure 1.31.   Schematic diagram of SQUID circuit.

THE NUMBER OF DATA POINTS TAKEN IS 15

THE MEAN VALUE OF (T-M) IS 5.28545E-03

THE STANDARD DEVIATION IS 0.014724877

I	THEORY	MEASURED	T-M	(T-M)-MEAN
1	63.8680	63.905	-0.0370	-0.0422
2	56.6503	56.630	0.0208	0.0155
3	52.7456	52.757	-0.0114	-0.0167
4	50.0582	50.067	-0.0088	-0.0140
5	48.0079	48.008	-0.0001	-0.0054
6	46.3500	46.350	0.0000	-0.0053
7	44.9582	44.950	0.0082	0.0029
8	43.7588	43.753	0.0058	0.0005
9	42.7051	42.691	0.0141	0.0088
10	41.7654	41.757	0.0084	0.0032
11	40.9176	40.905	0.0126	0.0073
12	40.1451	40.132	0.0131	0.0079
14	38.7801	38.762	0.0181	0.0128
17	37.0650	37.051	0.0150	0.0097
22	34.7973	34.777	0.0203	0.0150

DEVIATION FROM THE MEAN IN DECIBELS
VERSUS ATTENUATOR SETTING IN DECIBELS

```
       -0.025 DB              0.000              +0.025 DB
       +----+----+----+----+----0----+----+----+----+----+
   34                           .                            34
   35                           .              *             35
   36                           .                            36
   37                           .        *                   37
   38                           .                            38
   39                           .       *                    39
   40                           .     *                      40
   41                           .     *                      41
   42                           .   *                        42
   43                           .      *                     43
   44                         * .                            44
   45                         * .                            45
   46                      *    .                            46
   47                           .                            47
   48                    *      .                            48
   49                           .                            49
   50            *              .                            50
   51                           .                            51
   52                           .                            52
   53        *                  .                            53
   54                           .                            54
   55                           .                            55
   56                           .                            56
   57                           .            *               57
   58                           .                            58
   59                           .                            59
   60                           .                            60
   61                           .                            61
   62                           .                            62
   63                           .                            63
   64    *                      .                            64
       +----+----+----+----+----0----+----+----+----+----+
       -0.025 DB              0.000              +0.025 DB
```
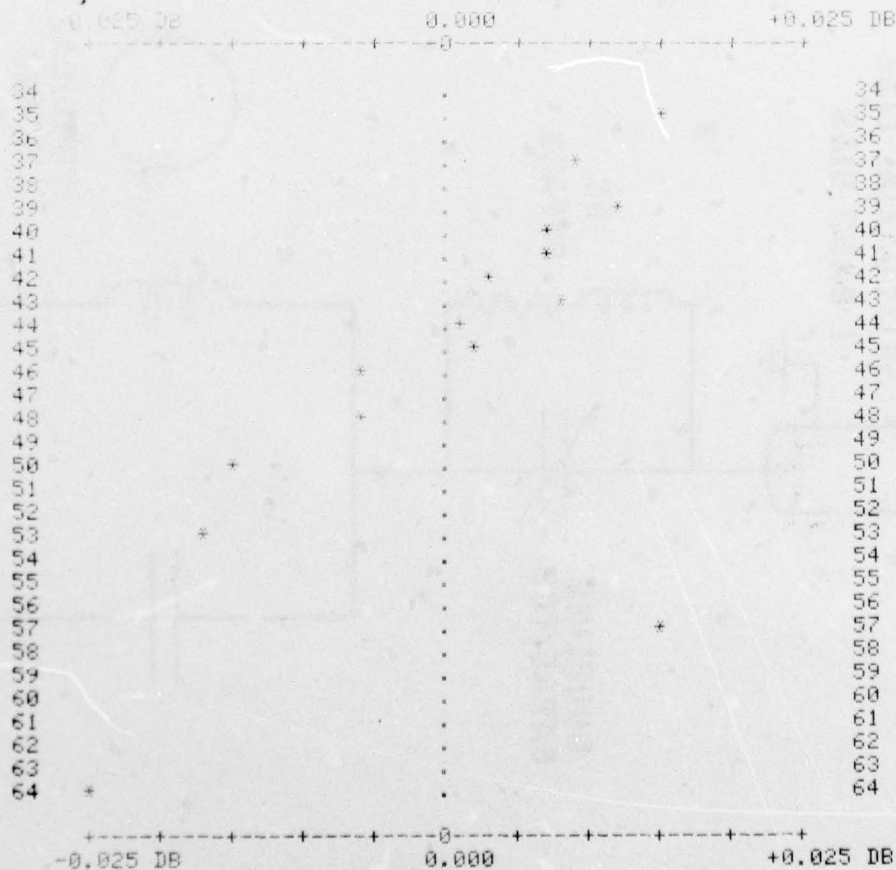
Figure 1.32.   Plot of measurement results using high critical current
               cartridge and insufficient reference level on double-
               balanced mixer.

1-44

```
THE NUMBER OF DATA POINTS TAKEN IS 30

THE MEAN VALUE OF (T-M) IS  -3.02593E-03

THE STANDARD DEVIATION IS 5.73731E-03
```

I	THEORY	MEASURED	T-M	(T-M)-MEAN
1	73.0010	73.027	-0.0260	-0.0229
2	65.7838	65.787	-0.0032	-0.0002
3	61.8786	61.888	-0.0094	-0.0064
4	59.1912	59.190	0.0012	0.0043
5	57.1409	57.152	-0.0111	-0.0080
6	55.4830	55.483	0.0000	0.0030
7	54.0912	54.098	-0.0068	-0.0038
8	52.8918	52.892	-0.0002	0.0029
9	51.8381	51.847	-0.0089	-0.0059
10	50.8984	50.900	-0.0016	0.0015
11	50.0506	50.057	-0.0064	-0.0034
12	49.2781	49.275	0.0031	0.0062
13	48.5688	48.573	-0.0042	-0.0012
14	47.9131	47.911	0.0021	0.0051
15	47.3034	47.307	-0.0036	-0.0006
16	46.7337	46.733	0.0007	0.0037
17	46.1990	46.206	-0.0070	-0.0040
18	45.6954	45.695	0.0004	0.0034
19	45.2194	45.222	-0.0026	0.0004
20	44.7681	44.766	0.0021	0.0051
21	44.3391	44.345	-0.0059	-0.0029
22	43.9303	43.928	0.0023	0.005
23	43.5399	43.544	-0.0041	-0.0011
24	43.1662	43.164	0.0022	0.0053
25	42.8080	42.810	-0.0020	0.0011
26	42.4640	42.463	0.0010	0.0040
27	42.1331	42.136	-0.0029	0.0001
28	41.9143	41.813	0.0013	0.0043
29	41.5063	41.510	-0.0032	-0.0002
30	41.2096	41.208	0.0018	0.0049

```
                    DEVIATION FROM THE MEAN IN DECIBELS
                    VERSUS ATTENUATOR SETTING IN DECIBELS


         -0.025 DB                    0.000                    +0.025 DB
         +----+----+----+----+----+----0----+----+----+----+----+----+
        41                                   .      *                41
        42                                   .   *                   42
        43                                   .      *                43
        44                                   .    *                  44
        45                                   .   *                   45
        46                                   . *                     46
        47                                   .       *               47
        48                              *    .                       48
        49                                   .       *               49
        50                              *    .                       50
        51                                   .        *              51
        52                                   .                       52
        53                                   .  *                    53
        54                              *    .                       54
        55                                .  .                       55
        56                                 *..                       56
        57                                   .      *                57
        58                              *    .                       58
        59                                   .      *                59
        60                                *  .                       60
        61                                   .*                      61
        62                            *      .                       62
        63                                   .   *                   63
        64                                   . *                     64
        65                                   .   *                   65
        66                          *        .                       66
        67                                   .     *                 67
        68                          *        .                       68
        69                                   .*                      69
        70                                   .                       70
        71                                   .                       71
        72                                   .                       72
        73         *                         .                       73

         +----+----+----+----+----+----0----+----+----+----+----+----+
         -0.025 DB                    0.000                    +0.025 DB
```
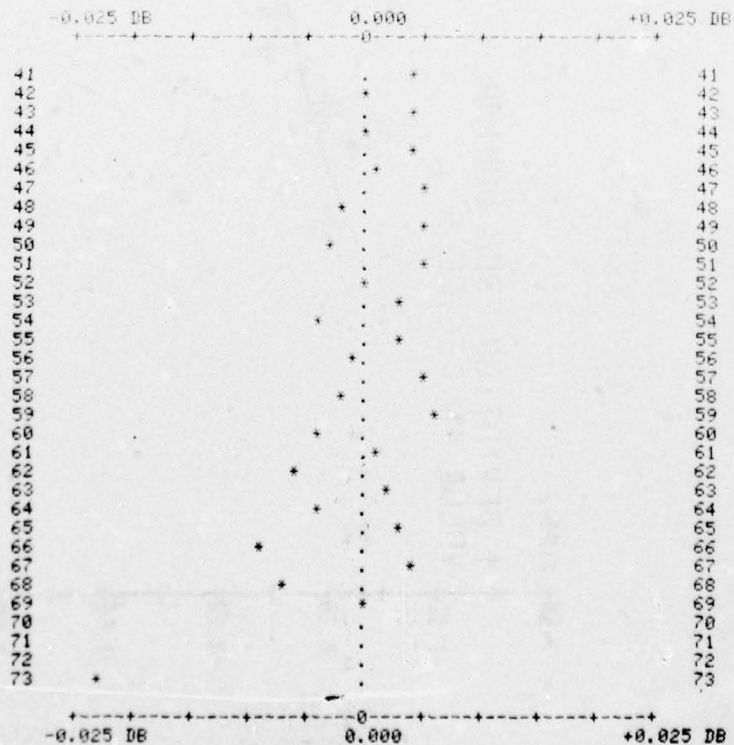
Figure 1.33.   Plot of measurement results with insufficient reference
level on double-balanced mixer.

ATTENUATOR CALIBRATION
USING SQUID SYSTEM
ATTENUATOR MODEL NO. VII
ATTENUATOR SERIAL NO. 3
DATE OF CALIBRATION: 5-17-76
DEGREE OF POLYNOMIAL FIT: 3
SYSTEM OPERATOR: RTA

ATTENUATOR SETTING IN DECIBELS --->
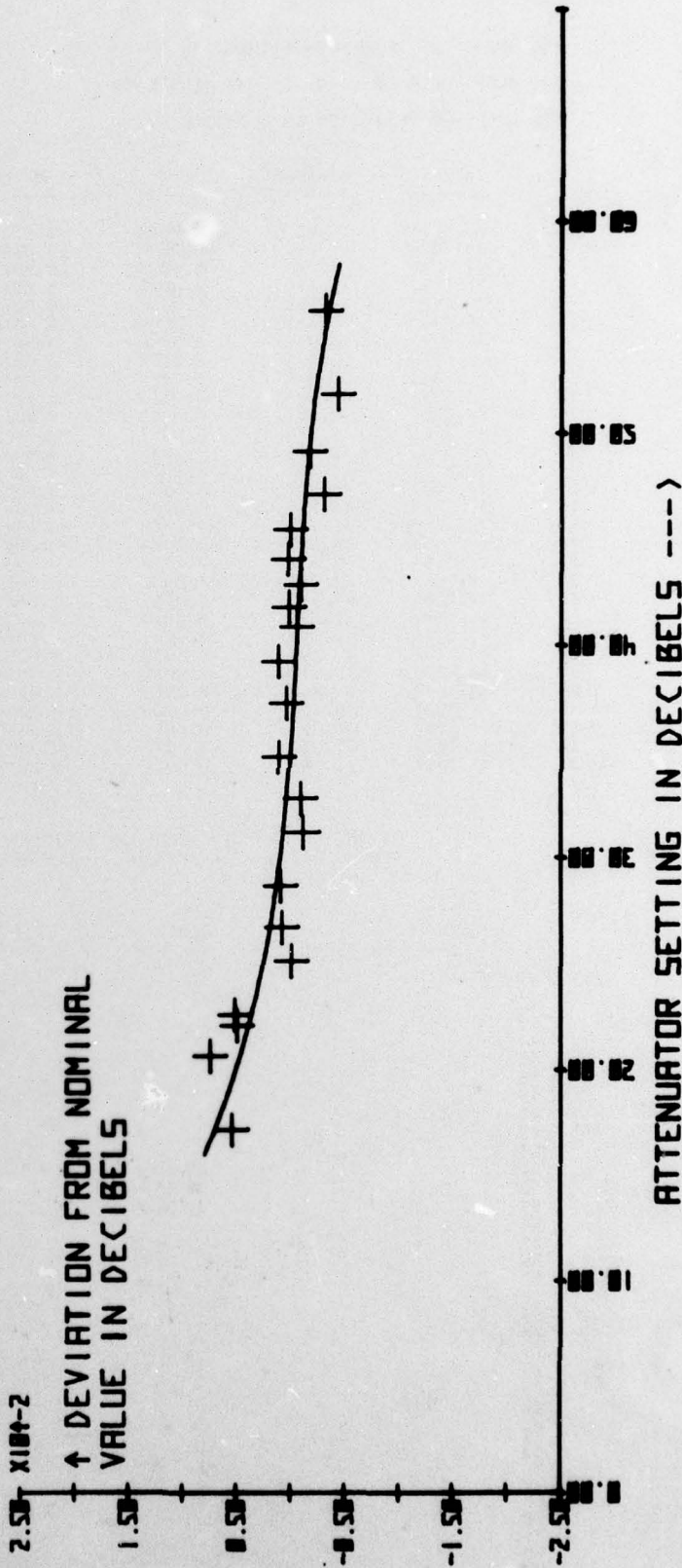
Figure 1.34. Calibration curve fit to data taken on variable attenuator
and plotted with computer.

```
PT.NO.          X            Y

    1       17.1540      0.0054
    2       20.6810      0.0074
    3       22.0990      0.0049
    4       22.6270      0.0051
    5       25.1400     -0.0001
    6       26.7300      0.0008
    7       28.6790      0.0069
    8       31.1980     -0.0012
    9       32.7960     -0.0010
   10       34.7540      0.0011
   11       37.2900      0.0004
   12       39.2640      0.0011
   13       40.8860     -0.0006
   14       41.8250      0.0001
   15       42.8800     -0.0010
   16       44.0780      0.0002
   17       45.4700      0.0000
   18       47.1310     -0.0001
   19       49.1800     -0.0018
   20       51.8700     -0.0044
   21       55.7740     -0.0032
   22       63.0010     -0.0130

NO. POINTS = 22

X:  MEAN= 37.29577273    ST.DEV.= 12.26541990
Y:  MEAN=-9.09091E-05    ST.DEV.= 4.10051E-03

CORR.COEFF.=-0.852154823


COEFFICIENTS

B( 0)=       0.0414
B( 1)=      -0.0032
B( 2)=       0.0001
B( 3)=      -0.0000

R SQUARE =   0.880765120

X=?20
Y(CALC)= 5.10487E-03
X=?25
Y(CALC)= 2.19426E-03
X=?30
Y(CALC)= 6.83008E-04
X=?32
Y(CALC)= 3.50684E-04
X=?34
Y(CALC)= 1.22610E-04
X=?36
Y(CALC)=-3.53973E-05
X=?38
Y(CALC)=-1.57523E-04
X=?40
Y(CALC)=-2.77953E-04
X=?42
Y(CALC)=-4.30872E-04
X=?44
Y(CALC)=-6.50464E-04
X=?46
Y(CALC)=-9.70915E-04
X=?48
Y(CALC)=-1.42641E-03
X=?50
Y(CALC)=-2.05113E-03
X=?55
Y(CALC)=-4.57765E-03
```

Figure 1.35.

Interpolation between calibration points using computer curve fit shown in figure 1.34.

Figure 1.36   Liquid helium storage vessel.

There is also a 1.27-cm diameter relief valve rated at 68.95 kilopascals (10 PSI) on the inner neck and a 1.27-cm diameter relief valve rated at 55.2 kilopascals (8 PSI) on the outer neck. The evaporation rate is specified at 2.5% per day maximum. The incorporation of this storage vessel into the SQUID system has extended the continuous operating time for the system to nearly one month.

This vessel is designed to withstand the rigors of commercial surface transportation. Before transporting, however, the relief shut-off valve must be open and all other vent valves must be closed so that the boil-off gas is circulated between the neck tubes and vented out the relief valve. Aircraft transportation of this container is allowable provided an absolute pressure relief valve set at 104.8 kilopascals (15.2 PSIA) is installed. This valve is available as an option from the manufacturer.

2. THEORY OF OPERATION

2.1 General Information

This section contains the basic theory of operation for the RF Attenuation Measurement System, using the Superconducting Quantum Interference Device as the standard and heart of the system.

2.2 Principle of SQUID Operation

The basic SQUID system configuration is shown in figure 2.1 where I_s represents the Josephson current and I represents the input current.
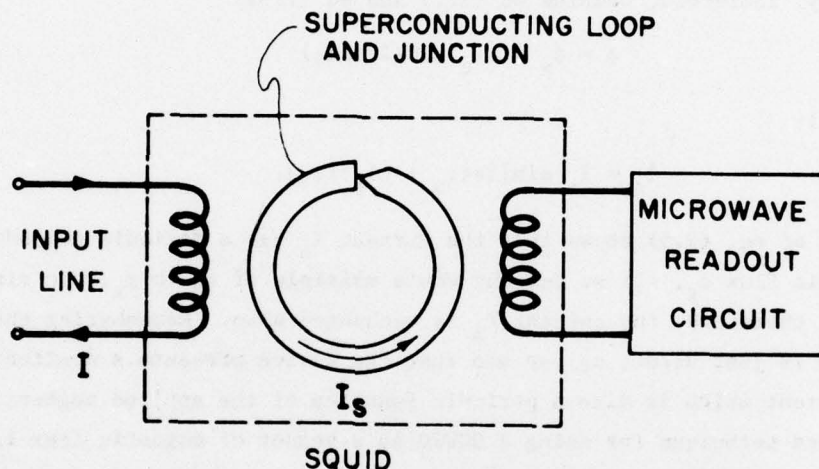
Figure 2.1. Basic SQUID system configuration.

In addition to the usual leakage and displacement currents that flow through any metallic contact, a Josephson junction passes a component of current (the "Josephson current") which is controlled by conditions in the superconductors on either side of the junction. If the superconductors are connected together to form a loop closed by the junction, then the Josephson current I_s depends upon the magnetic flux ϕ linking the loop:

$$I_s = I_c \sin(2\pi\phi/\phi_0). \tag{2.1}$$

I_c depends on the degree of coupling for the particular contact. The quantity ϕ_0 is a fundamental constant of nature known as the flux quantum.

$$\phi_0 = h/2e = 2.0678538 \times 10^{-15} \text{ Wb} \tag{2.2}$$

where h is Planck's constant and e is the charge on the electron.

PRECEDING PAGE BLANK-NOT FILMED

This arrangement of a small superconducting loop closed by a Josephson junction is the basic form of the SQUID. Since this device is the heart of the whole system, we will analyze its properties a little further, following Silver and Zimmerman [9].

The total magnetic flux ϕ linking the loop is the sum of two terms

$$\phi = \phi_x + LI_s \tag{2.3}$$

where ϕ_x is the flux from some external source driving the device and L is the inductance of the loop. Strictly speaking, the current I_s in eq (2.3) is the total current (including leakage, etc.) flowing through the junction. However, SQUID's are usually designed so that the Josephson current eq (2.1) is the dominant term; thus we may obtain an approximate understanding of the action of the device by neglecting the other contributions to the current. We may, therefore, combine eq (2.1) and eq (2.3):

$$\phi = \phi_x + LI_c \sin(2\pi\phi/\phi_0) \tag{2.4}$$

or, alternatively,

$$I_s = I_c \sin[2\pi(\phi_x + LI_s)/\phi_0]. \tag{2.5}$$

Inspection of eq. (2.5) shows that the current I_s has a periodic dependence on the external magnetic flux ϕ_x. If we add any whole multiple of ϕ_0 to ϕ_x, the sine function is unchanged, and, therefore, the current I_s is unchanged also. Remembering that the EMF V around the loop is just $d\phi/dt$, we can see that the device presents a nonlinear impedance to alternating current which is also a periodic function of the applied magnetic flux ϕ_x.

The standard technique for using a SQUID as a sensor of magnetic flux is to monitor this variation in impedance by coupling the device inductively to a readout circuit operating at some convenient radio frequency, as shown in figure 2.1 [8,9,10]. (These references give the details of readout circuits operating at 30 MHz and the output signals that can be obtained.) In any circuit with stable geometry the magnetic flux ϕ_x is proportional to the current I. The flux quantum is therefore a natural repeating unit with which to measure current. The periodic response of the impedance of the SQUID to variations of magnetic flux driven by the current I in this circuit is monitored by a microwave system which detects variations in the microwave reflection coefficient of the SQUID.

The basic response of a SQUID system to the current to be measured is displayed in figure 2.2. This is an oscilloscope display obtained with a slowly varying I. Monitored in this way, the periodic response of the SQUID to magnetic flux has degenerated into a simple and remarkably pure sine function. This response is obtained for a specific pump frequency (1 GHz) level. Increasing the 1 GHz level further results in flattening of the upper portion of the interference pattern and eventually a null condition. Still further 1 GHz level increases cause the interference pattern to reappear with a 180 degree phase shift. This progression continues at higher 1 GHz levels, therefore, the SQUID response is periodic with 1 GHz pump level also.

When the input current I is an rf current, the system records an average over a segment of figure 2.2. The width of the segment is determined by the amplitude of the rf current, and its location can be moved by simultaneously applying a dc bias current. As
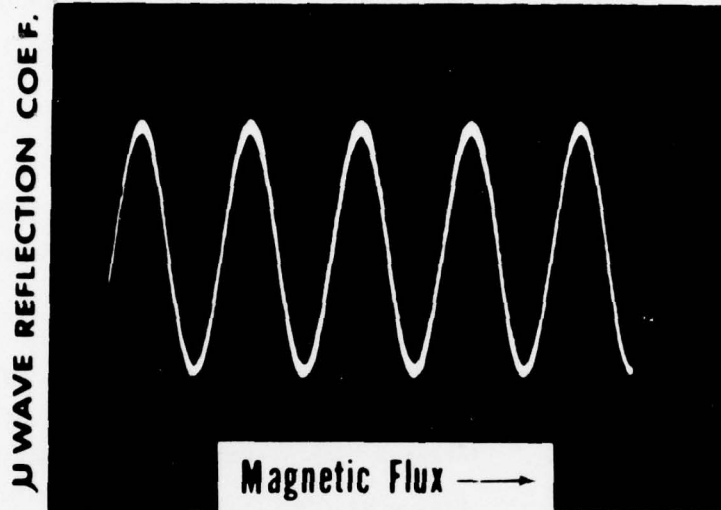
Figure 2.2.   SQUID response to current.
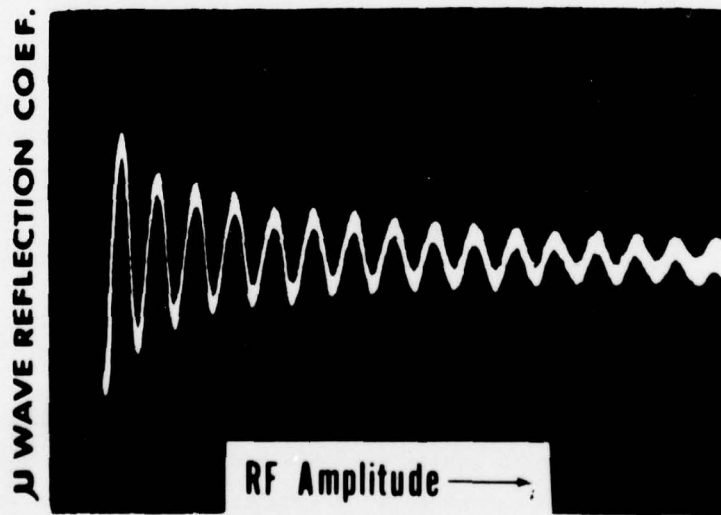
Figure 2.3.   SQUID averaged response to rf current.

the amplitude of the rf current varies, this averaged response reflects the basic periodicity of the SQUID. This is shown in figure 2.3, which is an oscilloscope display obtained by applying a slow amplitude modulation to an rf current applied to the SQUID. In the approximation, the basic response to current shown in figure 2.2 is proportional to $\cos(2\pi I/I_0)$, and the averaged response to rf current shown in figure 2.3 can be shown to be the zero-order Bessel function $J_0(2\pi I/I_0)$ [1]. In both expressions I_0 is the current required to drive one quantum of magnetic flux into the SQUID. It may be determined with a single measurement using dc. Notice that the frequency does not enter explicitly into these expressions.

2.3 Detailed Analysis of SQUID Operation Theory

Under certain predetermined conditions (to be elaborated upon later), the detected response of a SQUID to flux ϕ is approximately sinusoidal and may be written

$$V(\phi) = V\cos(2\pi\phi/\phi_0) \qquad (2.6)$$

recalling that ϕ_0 is the flux quantum ($\phi_0 = h/2e = 2.0678538 \times 10^{-15}$ Wb). The action of the system as an attenuator calibrator is illustrated by writing ϕ as $\phi_m \sin \omega_m t$ where the subscript m denotes "measuring." Taking a time average, eq (2.6) may then be written

$$V(\phi) = VJ_0(2\pi\phi_m/\phi_0). \qquad (2.7)$$

Since the zeros of the zeroth order Bessel function are well known, the ratios of the amplitudes ϕ_m at these zeros can be precisely determined. Attenuation is derived from a ratio of these amplitudes, and we thus have a means of calibrating attenuators.

One of the attractive features of the SQUID system is that the frequency of the ϕ_m signal is not restricted to a single value as it is for waveguide-below-cutoff attenuators. Instead, a 1-GHz biased SQUID system is usable from audio frequencies up through at least 100 MHz. The usable dynamic range decreases, however, as the frequency of the measured signal approaches the pump frequency (1 GHz).

Figure 2.4 illustrates the response characteristics of an rf biased SQUID as defined in eqs (2.6) and (2.7).

Since the performance of this system depends directly on the harmonic purity of the SQUID response, it is valuable to assess the effect of small variations from the ideal response. The purpose of this exercise is to illustrate that a good number of effects of nonideal response can be eliminated or greatly reduced by selecting proper bias conditions. Besides the pump signal at ω_c (1 GHz), the SQUID is subjected to the measuring signal at frequency ω_m (30 MHz for this work), a 1-kHz (ω_d) bias for phase sensitive location of nulls, and a dc bias.

In general, the detected response of the rf biased SQUID (including harmonic distortion) may be written

$$V(\phi) = \sum_{n=1}^{\infty} V_n \cos(2\pi n\phi/\phi_0), \qquad (2.8)$$

where $\phi = \phi_m \sin \omega_m t + \phi_d \sin \phi_d t + \phi_b$. The first term is the 30-MHz measuring signal, the second term is the 1-kHz modulation, and the final term is the dc bias. It is useful to study the complete response rather than to limit interest to the detection signal at 1 kHz. With the use of standard Bessel function expansions of terms of the form $\cos(A \sin X)$, we can write

$$V(\phi) = \sum_{n=1}^{\infty} V_n \left\{ \cos(nB) \left[J_0(nM) + 2 \sum_{k=1}^{\infty} J_{2k}(nM)\cos(2k\omega_m t) \right] \cdot \right.$$

$$\left. \left[J_0(nD) + 2 \sum_{j=1}^{\infty} J_{2j}(nD)\cos(2j\omega_d t) \right] \right\} + \ldots \tag{2.9}$$

where $J_n(X)$ is the nth order Bessel function of X and the quantities M, D, and B are $(2\pi\phi_m/\phi_0)$, $2\pi\phi_d/\phi_0)$, and $(2\pi\phi_b/\phi_0)$, respectively. Only the first of four similar terms is displayed. The depth of modulation at ω_m becomes quite large in normal operation, thus generating a large number of sidebands around ω_c. On the other hand, for the low-frequency modulation ω_d, optimum operation requires a unique value for D which results in very few sidebands at multiples of ω_d from each of the $n\omega_m$ sidebands of ω_c. Figure 2.5 depicts the nature of the frequency spectrum. The spectrum is for ideal SQUID response (no harmonic distortion), and half of the sidebands are eliminated if B = 0 or B = $\pi/2$. Phase information of eq (2.9) is not shown. Sideband A (fig. 2.5) is detected by the system to locate the zeros of J_0.

Consider first the signals which appear at the low-frequency sidebands of the carrier. Table 2.1 lists the first three terms of the harmonic expansion for the low-frequency sidebands about ω_c. The desired information is $J_0(M)$ as found in the very first term. Note that setting B = $\pi/2$ (i.e., adjusting the bias so that $\phi_b = \phi_0/4$) nulls even harmonic distortions of the SQUID response at this first sideband. In practice we locate two adjacent nulls on the ω_d detector and then use a specially designed resistive divider to bring the current midway between these. The nulling of the second harmonic term can be made more complete by the following process which minimizes V_2. Note that, at $2\omega_d$, the odd terms are zero and the second term is maximized for B = $\pi/2$. If the 1-GHz detector is linear, the even harmonic content of the interference pattern is almost solely dependent on the amplitude of the pump signal (at ω_c), and thus a detector of $2\omega_d$ provides an unambiguous method of adjusting the pump frequency amplitude. The effects of second harmonic distortion are then doubly nulled. The third harmonic term is nulled by adjusting D so that $J_1(3D) = 0$. To do this the 1-kHz amplitude is increased to null the ω_d signal, and the amplitude is then divided by 3. This value puts $J_1(D)$ near its first peak, thus maximizing sensitivity to the desired signal. It is also important to note that $J_3(3D)$ is now near a maximum. This makes the $3\omega_d$ sideband of interest. Referring to table 2.1, we note that the second term at $3\omega_d$ is zero because B = $\pi/2$ (dc bias properly set) and the first term contributes no error since it varies as $J_0(M)$ and thus has nulls in coincidence with the desired ω_d term. However, the third term at $3\omega_d$ is of concern because the argument is 3M and the term is nonzero when $J_0(M) = 0$. Ideally a phase-sensitive detector detects at a single frequency, but is is quite common for these detectors to have a significant sensitivity to odd harmonics
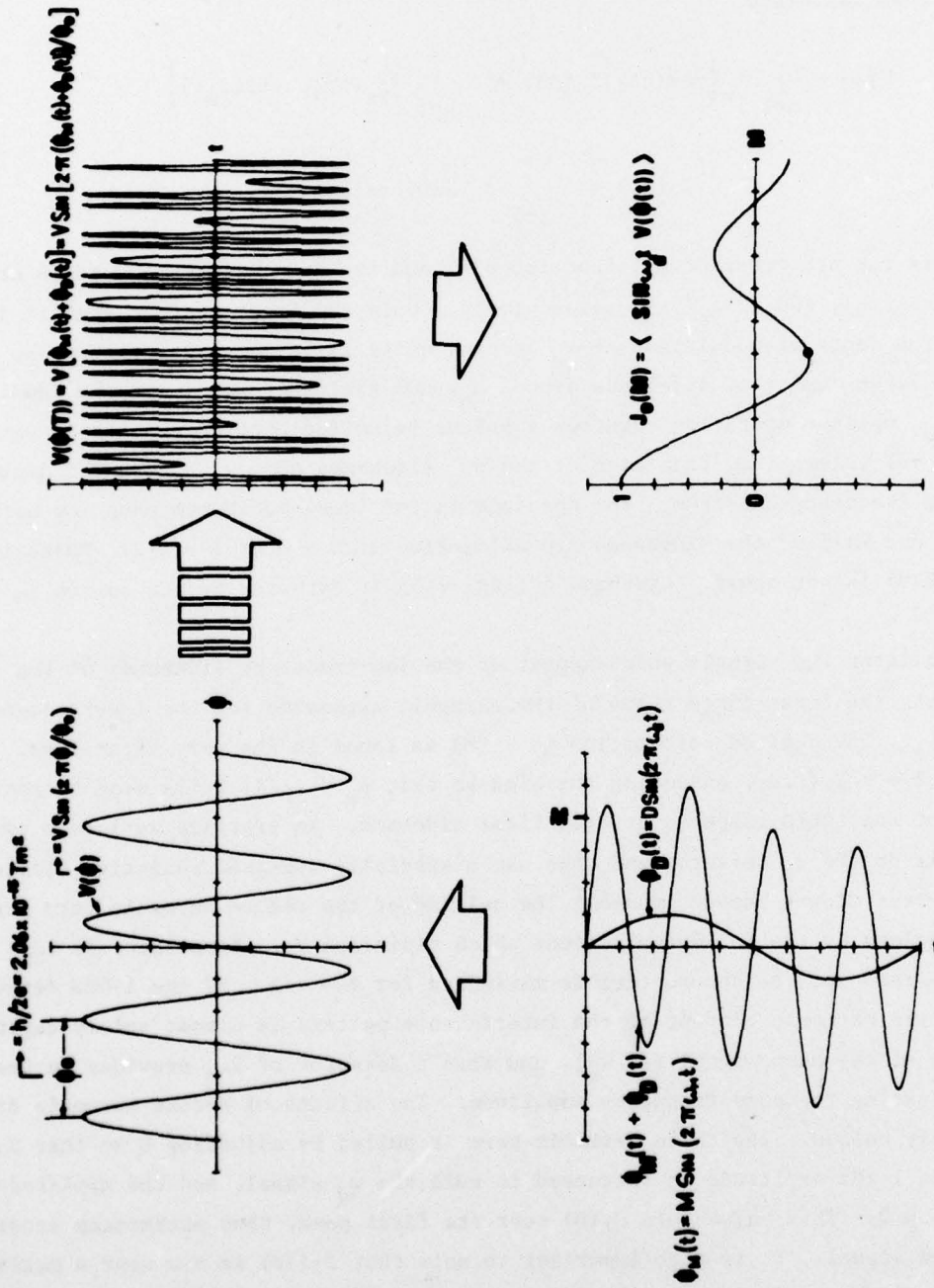
Figure 2.4. Response to microwave biased SQUID.

2-6

RELATIVE SIDEBAND AMPLITUDES OF THE SQUID RESPONSE
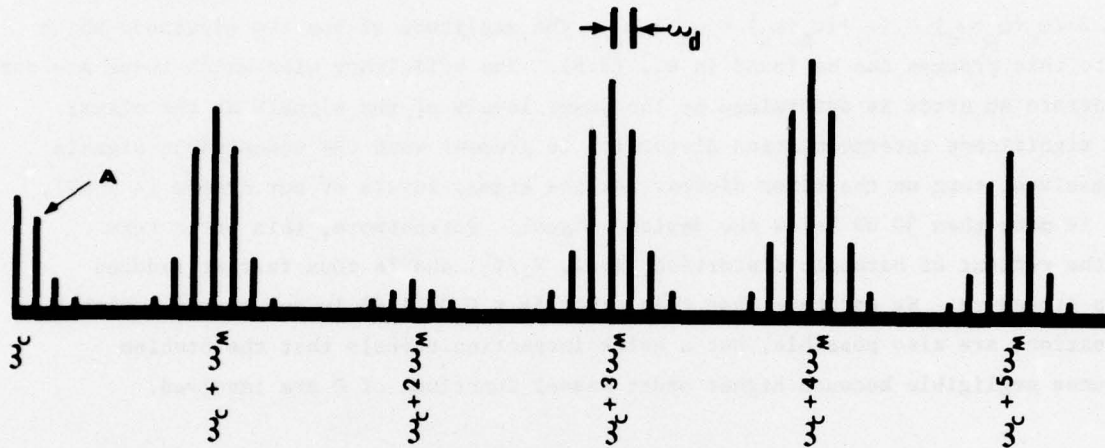
Figure 2.5.   Relative sideband amplitudes of the SQUID response.

Table 2.1

SIGNAL AND ERROR TERMS FROM THE SQUID

ANGULAR FREQUENCY	
$\omega_c \pm \omega_d$	$V_1 J_0(M)J_1(D)\sin B + V_2 J_0(2M)J_1(2D)\sin 2B + V_3 J_0(3M)J_1(3D)\sin 3B + \cdots$
$\omega_c \pm 2\omega_d$	$V_1 J_0(M)J_2(D)\cos B + V_2 J_0(2M)J_2(2D)\cos 2B + V_3 J_0(3M)J_2(3D)\cos 3B + \cdots$
$\omega_c \pm 3\omega_d$	$V_1 J_0(M)J_3(D)\sin B + V_2 J_0(2M)J_3(2D)\sin 2B + V_3 J_0(3M)J_3(3D)\sin 3B + \cdots$

of the signal frequency. One solution to this problem is simply to filter out harmonics of ω_d between the double-balanced mixer and phase-sensitive detector and to use a sinusoidal reference waveform in the PSD's multiplying circuit.

Another type of potential problem is the intermodulation distortion which is common to double-balanced mixers. All signals which reach the mixer are subject to harmonic generation and further mixing with the subsequent possibility of generating error signals at the detection frequency of $\omega_c + \omega_d$. The lowest order of these terms involves the combination $2 \cdot (\omega_c + \omega_m + \omega_d) - (\omega_c + 2\omega_m + \omega_d) = \omega_c + \omega_d$. The amplitude of the two sidebands which contribute to this process can be found in eq. (2.9). The efficiency with which these are combined to generate an error is determined by the power levels of the signals at the mixer; in essence, significant intermodulation distortion is present when the undesirable signals can, of themselves, turn on the mixer diodes. At the signal levels of our system (< 1 mW), this signal is more than 30 dB below the desired signal. Furthermore, this error term depends on the percent of harmonic distortion (i.e., V_2/V_1) and is thus further reduced by the setup procedure. We estimate that this error is < 0.0001 dB in our system. Higher order combinations are also possible, but a quick inspection reveals that the problem rapidly becomes negligible because higher order Bessel functions of D are involved.

2.4 Theory of the SQUID Measurement Process

The measurement process is depicted in figure 2.4. The response of the 1-GHz biased SQUID to flux is shown as $V(\phi)$ (upper left). ϕ is the input flux which, for this system, is illustrated immediately below $V(\phi)$ as $\phi_m(t) + \phi_d(t)$. The critical characteristic of $V(\phi)$ is its sinusoidal shape; i.e., $V(\phi)$ should be accurately described as $V(\phi) = V \sin(2\pi\phi/\phi_0)$.*
Any departure from this condition is a source of error in the measurement process. This effect will be discussed in section 4, Error Analysis of the System. We will assume here that the response is a sine function. The input flux is the algebraic sum of three fluxes, a dc flux, a 1-kHz or zero detecting flux, and a 30-MHz flux. While the flux at the 30-MHz signal frequency ω_m is injected by the signal coil, the dc and low frequency biases are introduced at the microwave readout coil. The dc flux is not explicitly depicted in figure 2.4; however, it is this flux which positions the 1-kHz and 30-MHz abscissas along the ϕ axis of the $V(\phi)$ function; i.e., the dc flux has the effect of moving $\phi_m(t) + \phi_d(t)$ to the left or right in figure 2.4.

Clearly, the dc flux determines whether or not $V(\phi) = V \sin \phi$ or $V(\phi) = V \sin(\phi + \delta)$ where δ is a measure of the error in the dc flux setting. In figure 2.4 the ratio of frequencies of $\phi_m(t)$ and $\phi_d(t)$ is, of course, not to scale. For $V(\phi)$ and ϕ as shown, the SQUID response is shown (upper right) as $V(\phi(t))$; i.e., the upper right picture is a reasonably accurate plot of $V(\phi) = f\left(\phi_m(t) + \phi_d(t)\right) = V \sin\left(2\pi(\phi_m(t) + \phi_d(t))/\phi_0\right)$ where $\phi_m(t) = M \sin(2\pi\omega_m t)$ and $\phi_d(t) = D \sin(2\pi\omega_d t)$. The time average of $V(\phi(t))$, after it has been multiplied by $\sin(\omega_d t)$, is shown in the lower right plot for $0 \le M \le 10$. For the particular case at hand (M = 4) a dot on the plot identifies the value of $\langle V(\phi(t)) \sin \omega_d t \rangle$. The analytic expression for this signal is the zeroth order Bessel function $J_0(M)$ [11]. Clearly, for those amplitudes of the 30-MHz measuring signal (M's)

*ϕ_0 = h/2e = 2.0678538 × 10^{-15} Wb.

where $\langle V(\phi(t))\sin \omega_d t\rangle$ is zero, M must have the tabulated values of the zeros of $J_0(x)$. For example, the first zero of $J_0(x)$ occurs at x = 2.4048 ... [11]; the second occurs at x = 5.52007 ... The ratios of the amplitudes (M's) at these two zeros must be (5.52 ...)/(2.40 ...) and this ratio represents 20 $\log_{10}$[(5.52 ...)/(2.40 ...)] dB or 7.217 ... dB. The distance between zeros is rather large for the first few zeros; however, consider the distance or dB difference between the 39th and 40th zeros: The 39th zero of $J_0(x)$ occurs at x = 121.73 ..., the 40th at x = 124.89 ..., and the dB difference for these two zeros is only .2213 dB. This difference continues to decrease (slowly) with increasing zero number which, of course, corresponds to higher and higher values of M, the 30-MHz measuring signal. Clearly, if one can vary the value of the 30-MHz signal smoothly from the ith to the rth zero, the ratio of signals M_r to M_i is given by the ratio of the arguments of $J_0(x)$ at its rth and i^{th} zeros, and if one can (by varying M smoothly) be certain of r and i, it is possible to measure a fairly wide range of attenuation. The present system will determine (i.e., count) over 1000 zeros. This corresponds to a range of over 60 dB. The system is equipped with a manual attenuator in the 30-MHz source. This attenuator is controlled by the front panel dial.

2.5 Attenuation Meaurements Using the SQUID System

The system as shown in figures 2.6(a) and 2.6(b) can be used to measure variations in attenuation without a conventional calibration standard. A stable signal generator is connected to the SQUID through the variable attenuator under test.

The SQUID is inductively coupled to the center conductor of a 50-Ω coaxial line, which passes through the SQUID. Variations in the current flowing in this line cause variations in the magnetic flux linking the super-conducting loop formed by the Josephson junction and the end of the cavity. Because of quantum mechanical interference, the microwave reflection coefficient of the device is sensitive to these variations in magnetic flux. For attenuation measurements, one end of the coaxial line is terminated with a 50-Ω load, and the other is connected to the rf system on which measurements are to be made.

Figure 2.6 shows the basic layout of the components used to realize this system. The microwave system is driven by an L-band signal generator delivering a few nanowatts of power to the 20-dB directional coupler. The power level at the SQUID is, therefore, of order 10^{-11} W. The reflected microwave signal is amplified by a solid-state amplifier, with a gain of about 50 dB, and detected by a double-balanced mixer. This millivolt level signal is applied to the lock-in detector, where it is amplified to an operating level of a few volts. An oscilloscope is used to monitor the dc bias and modulation levels in the SQUID. The modulation is a 1-kHz sine wave. Modulation and dc bias are applied to the SQUID via a low-pass filter connected to the microwave line. This must pass the bias and modulation, but present a significant attenuation at 1 GHz. The high degree of attenuation is required to prevent crosstalk between the microwave and measuring channels.

BASIC SYSTEM

RF SIGNAL SOURCE

ATTENUATOR UNDER TEST

MICROWAVE READOUT CIRCUIT

JOSEPHSON JUNCTION

SUPERCONDUCTING LOOP

LIQUID HELIUM

I_S
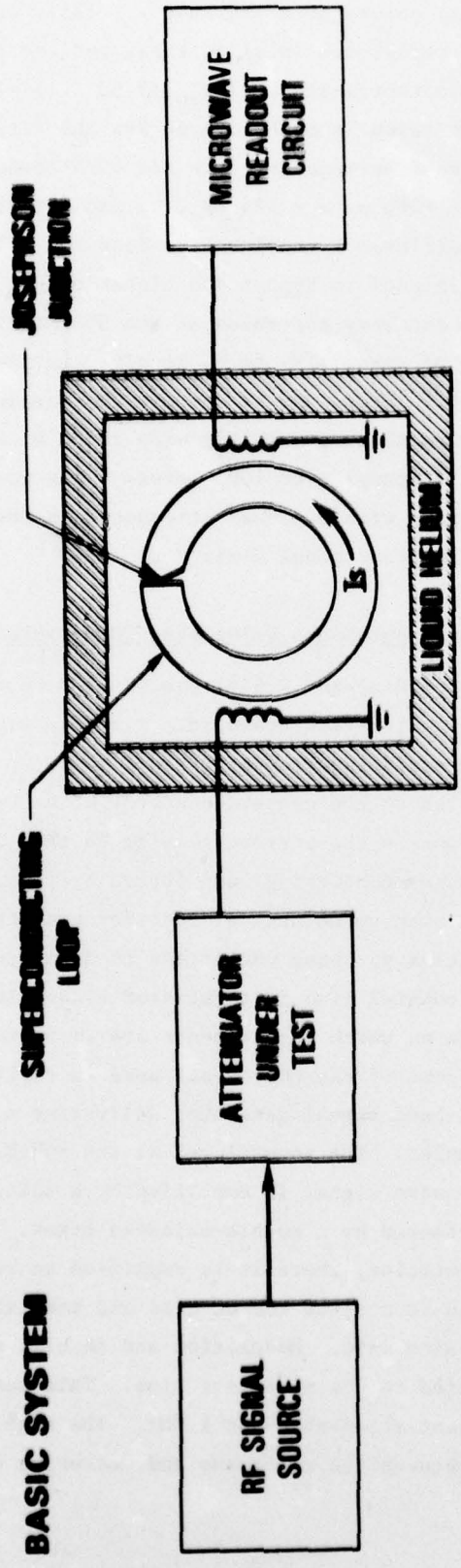
Figure 2.6(a). Basic block diagram of the SQUID attenuation measurement system.
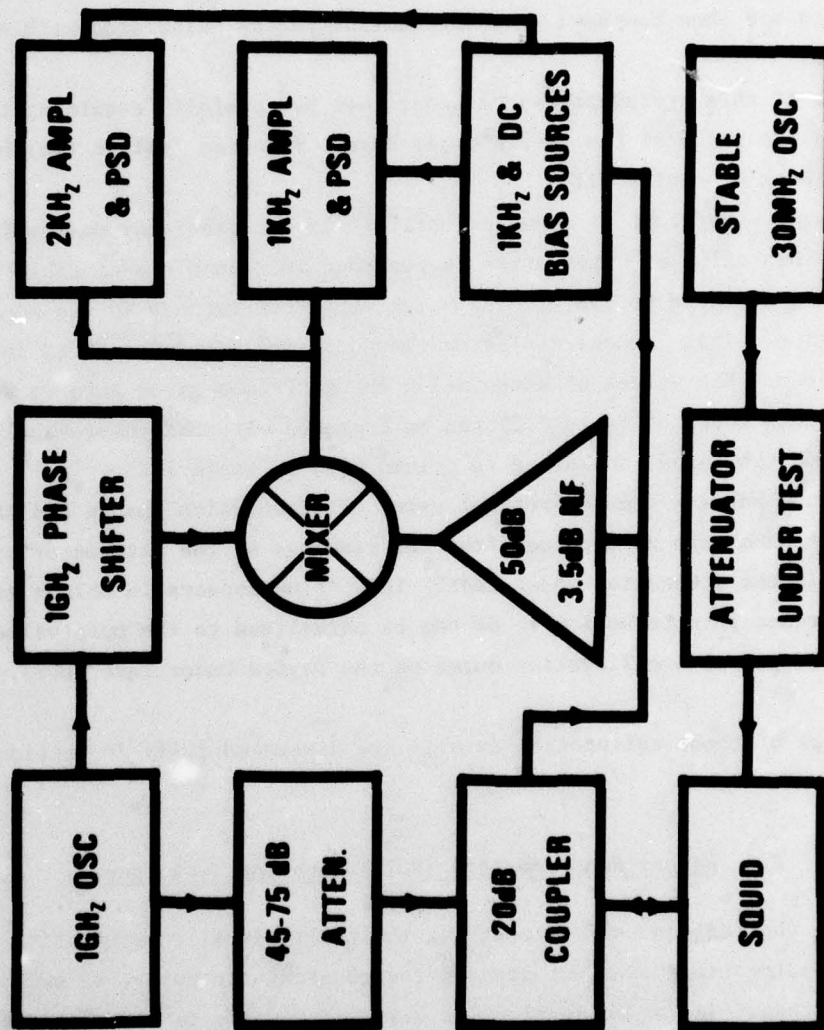
Figure 2.6(b). Block diagram of the complete system.

The 30-MHz source is a crystal-controlled solid-state oscillator. An amplifier of comparable stability raises this level to the maximum permitted by the attenuator under test. All connections are made with semirigid coaxial line (with solid conductors) or double-shielded flexible coaxial line (with braided conductors). With this precaution and some care with connectors, leakage does not appear to be a significant problem.

The null indicator on the phase sensitive detector is used to locate the nulls of the response function $J_0(2\pi I/I_0)$ as the attenuator under test is adjusted. The system is set on a sequence of these nulls, and the reading of the attenuator dial is noted at each null. The dial readings are then compared with attenuation ratios calculated with a table of Bessel functions.

The details of this procedure can be understood by carefully examining the contents of table 2.2, where the zeros of the zeroth order Bessel function (column two) have been obtained from a book of tables [11].

The attenuator under test is adjusted until it is set precisely on the first Bessel function zero. This value of attenuation is recorded in column six of table 2.2. The attenuator is then adjusted to the precise value which corresponds to the second zero of the Bessel function. This process can be continued to include any desired zero in the range of the system. The values of attenuation change from a given zero to another zero (appearing in column seven of table 2.2) can be compared with the theoretical change between those same two zeros (appearing in column five of table 2.2).

The difference between the theoretical value of attenuation change and the indicated value of attenuation change as obtained from the readings on the attenuator under test gives the error in the attenuator under test. This value appears in column eight of table 2.2. This difference in attenuation in dB can be normalized to the mean value of the difference and plotted as a calibration curve on the Device Under Test (DUT), as illustrated in figure 3.14.

The mechanics of these calibration details are discussed fully in section 3 "Operating Procedure."

2.6 Bessel Function Zero (Null) Counting Techniques

To eliminate the tedious task of counting the nulls visually by watching the null indicator, a semiautomatic system was devised for counting the nulls, as well as interpolating between them. (Refer to section 1.3.2.) This system is shown in figure 2.7. Nulls are counted by a digital counter, driven by the lock-in detector in the L-band readout system, as the incident rf power is slowly reduced from the working level to a very low level manually via the level control dial on the front panel of the RF Source Plug-in Module. The incident rf power is then restored to its working level slowly to the nearest null. The rf output power can be measured by a microwattmeter and a 3-dB coupler on the output port J4. The corresponding small change in rf power level from the level at which the measurement is being made (between nulls) to the nearest adjacent null can be measured. This value can then be compared to the change in rf power between the nulls on each side of

Table 2.2. Theoretical values of attenuation change between Bessel functional zeros compared to the attenuation values from a typical device under test.

Zero No. n	Zero of $J_0(X)$ X_n	X_n/X_1	$20 \log(X_n/X_1)$ dB	Spacing Between Zeros in dB	Typical Attenuator Reading dB	Spacing Between Zeros as Indicated on Device Under test (dB)	Difference in Theoretical and Indicated Values dB
1	2.4048				72.614		
2	5.5201	2.2954	7.2172	7.2172	65.397	7.235	-0.0178
3	8.6537	3.5985	11.1224	3.9052	61.496	3.901	+0.0042
4	11.7915	4.9033	13.8098	2.6874	58.801	2.695	-0.0076
5	14.9309	6.2088	15.8602	2.0504	56.757	2.044	0.0064
6	18.0711	7.5146	16.5181	1.6579	55.100	1.657	0.0009
7	21.2116	8.8205	18.9099	1.3918	53.708	1.392	-0.0002
8	24.3525	10.1266	20.1093	1.1994	52.505	1.203	-0.0036
9	27.4935	11.4328	21.1630	1.0537	51.454	1.051	0.0027
10	30.6346	12.7389	22.1026	0.9396	50.514	0.940	0.0004

the point in question with sufficient accuracy for interpolation between nulls. The circuit for controlling the rf output power level was developed after trying several commercial voltage-variable attenuators and modulators, which were rejected because of their high insertion loss and inconvenient control voltage characteristics. This manually variable-attenuator circuit is shown in figures 1.15 and 2.7. It consists of a well-balanced 180° hybrid junction with a variable piston capacitor acting as a variable termination on one of the side ports as described in section 1.3.2.

This technique to interpolate between nulls has not been used routinely since the system is more easily operated in a manual mode. The accuracy of interpolation between zeros using this technique has not been evaluted thoroughly although the resolution of the RF Level Control dial is nominally 0.01 dB which should be adequate for calibrating fixed attenuators.

The simpler technique of calibrating a fixed attenuator by placing it in series with a variable attenuator has been successful. The variable attenuator is first calibrated using the SQUID System; then the fixed attenuator is inserted as described in section 3.6.3. This technique eliminates the need to interpolate between Bessel Function Zeros in most cases.

The interpolation technique is included in the system to provide maximum flexibility and to allow the use of further semi-automatic data processing and control of the system if desired.
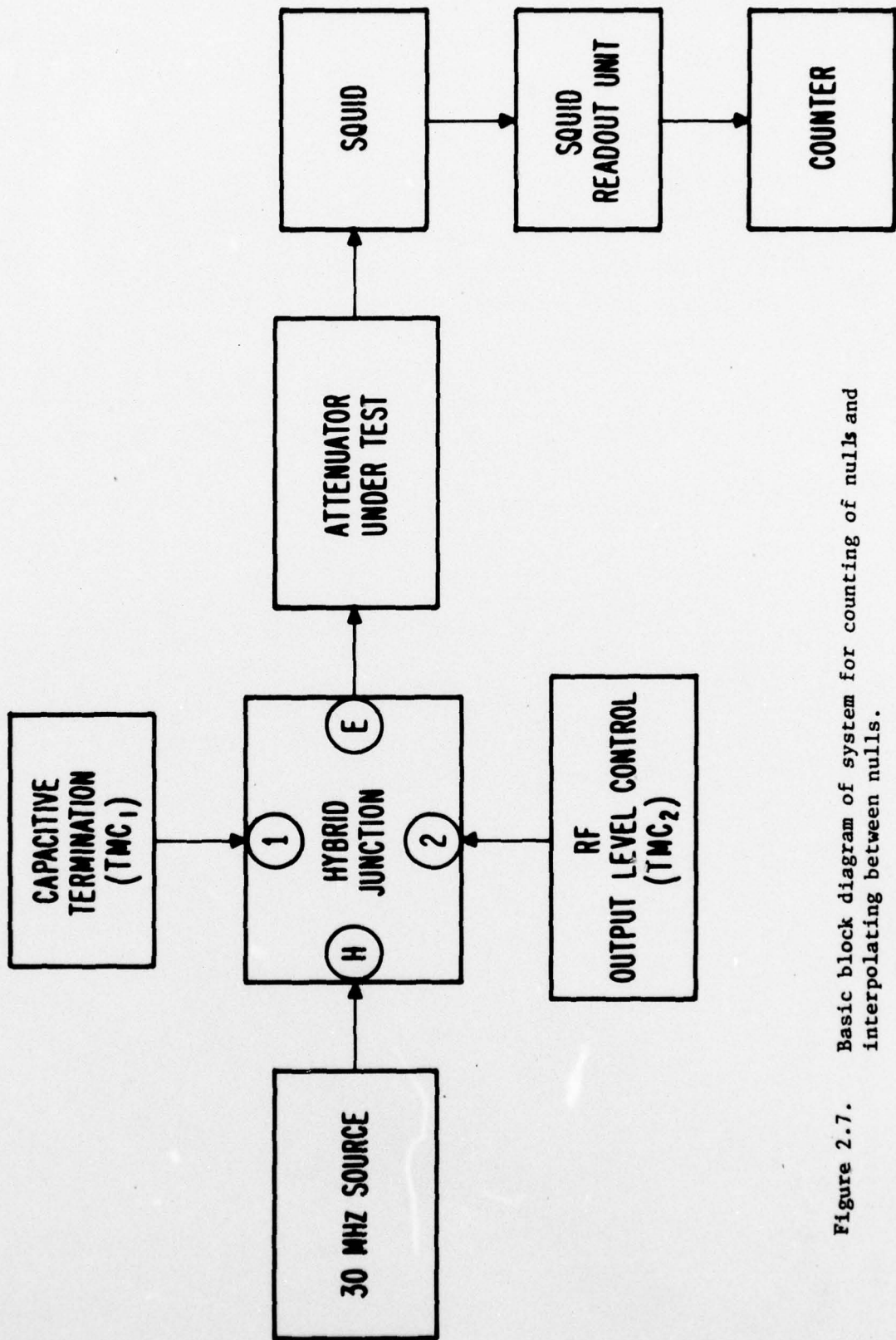
Figure 2.7. Basic block diagram of system for counting of nulls and interpolating between nulls.

3. OPERATING PROCEDURE

3.1 General

This section contains information on preparation for use, identification, and description of controls and indicators, and a step-by-step operating procedure.

3.2 System Components

The individual system components are described in table 3.1 and are identified by index numbers in figure 3.1 which is a view of the total system.

Table 3.1. Description of system components.

Item No.	Item	Description
1.	Dewar	This 30-liter Dewar contains the liquid helium bath in which the SQUID must be submerged for proper operation of the system.
2.	SQUID Control Unit	This unit contains the dc-bias circuits, the 1-kHz bias and modulation circuits, and the 1-GHz biasing circuits for the SQUID.
3.	Digital Counter	This counter provides a readout for the semiautomatic counting of the nulls at the Bessel function zeros.
4.	SQUID Readout Unit	This unit contains the dc power supplies, the null indicator circuitry for the phase-sensitive detector and the rf signal source which provides the calibration signal for the device under test.
5.	Oscilloscope	This device provides a visual representation of the SQUID interference pattern for use during system setup and operation.
6.	Device Under Test	This is a typical variable attenuator being calibrated by the SQUID Attenuation Measurement System.

3.3 Connectors, Controls, and Indicators

The SQUID Readout Unit connectors, controls, and indicators are described in table 3.2 and are identified in figures 3.2, 3.3, and 3.4 by index numbers. The SQUID Control Unit connectors and controls are described in table 3.3 and are identified in figures 3.5, 3.6, and 3.7 by index numbers.
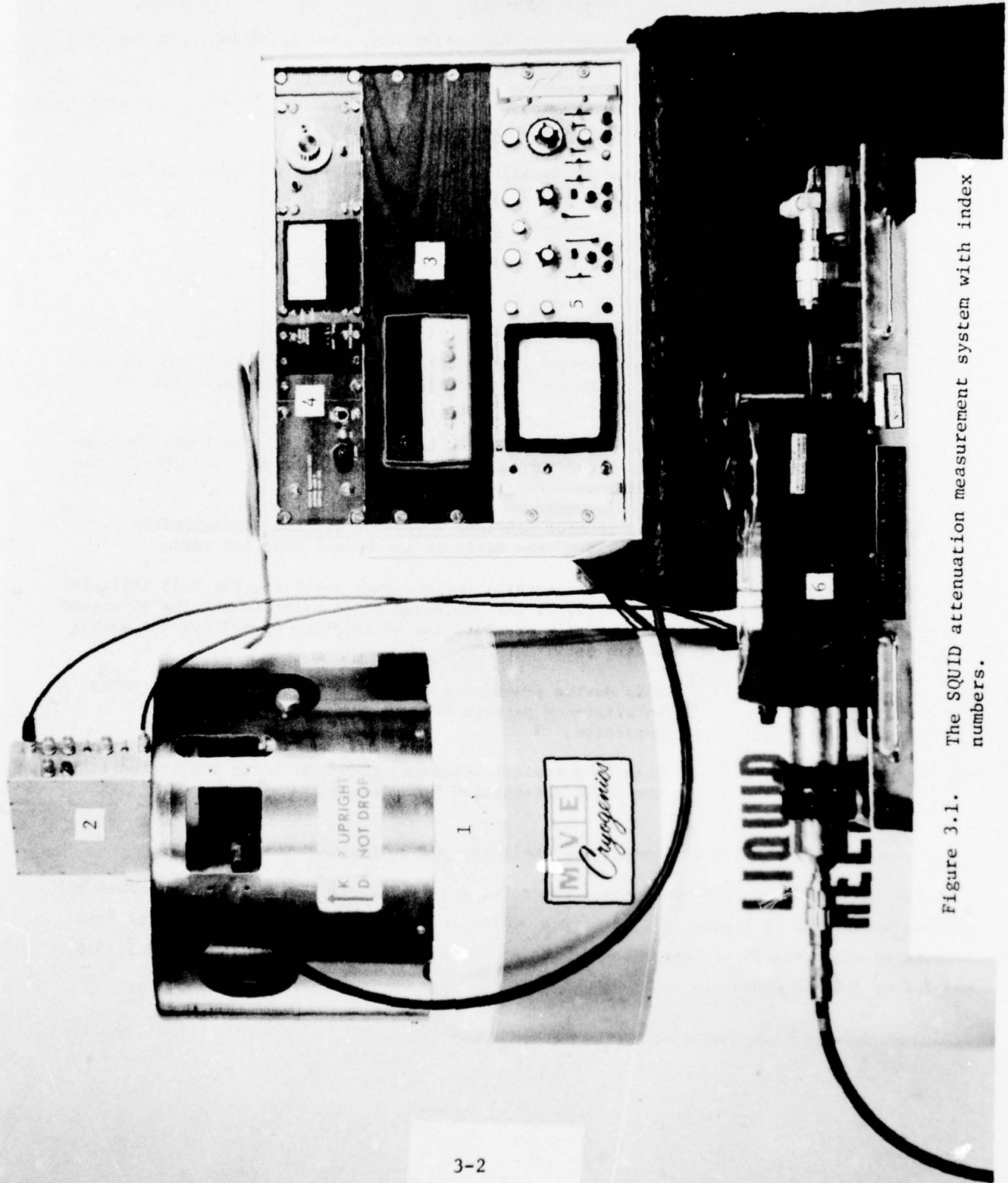
Figure 3.1. The SQUID attenuation measurement system with index numbers.
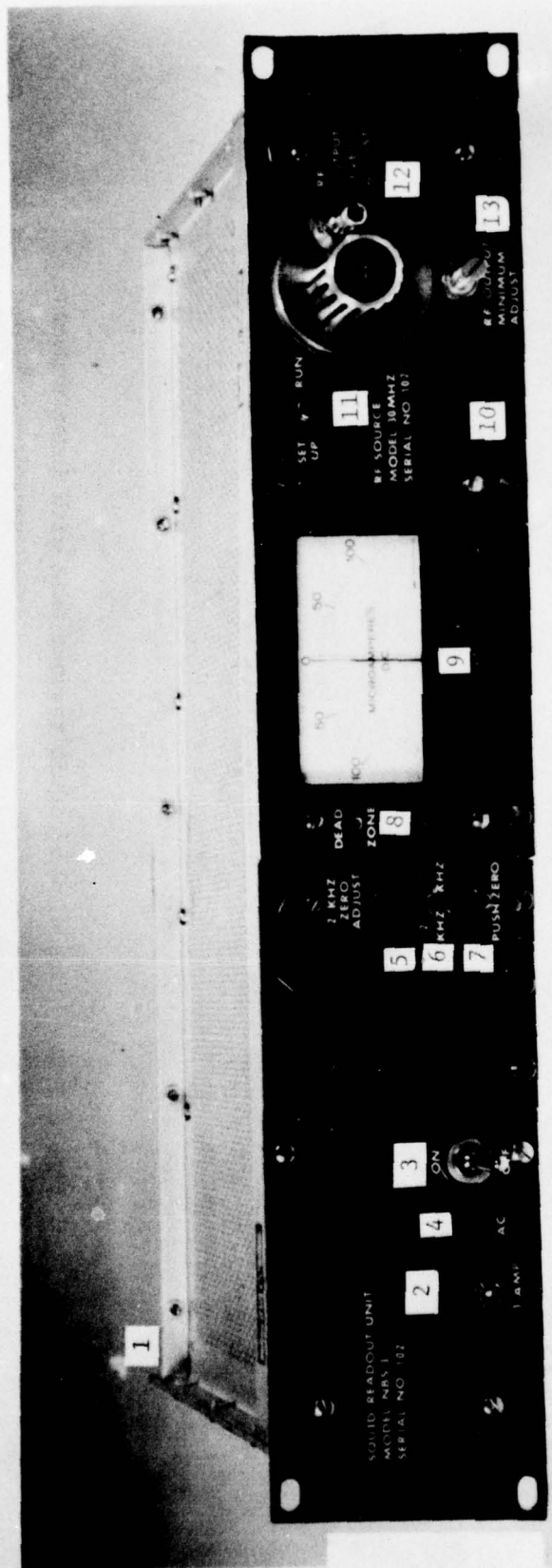
Figure 3.2. Front view of SQUID readout unit with index numbers.
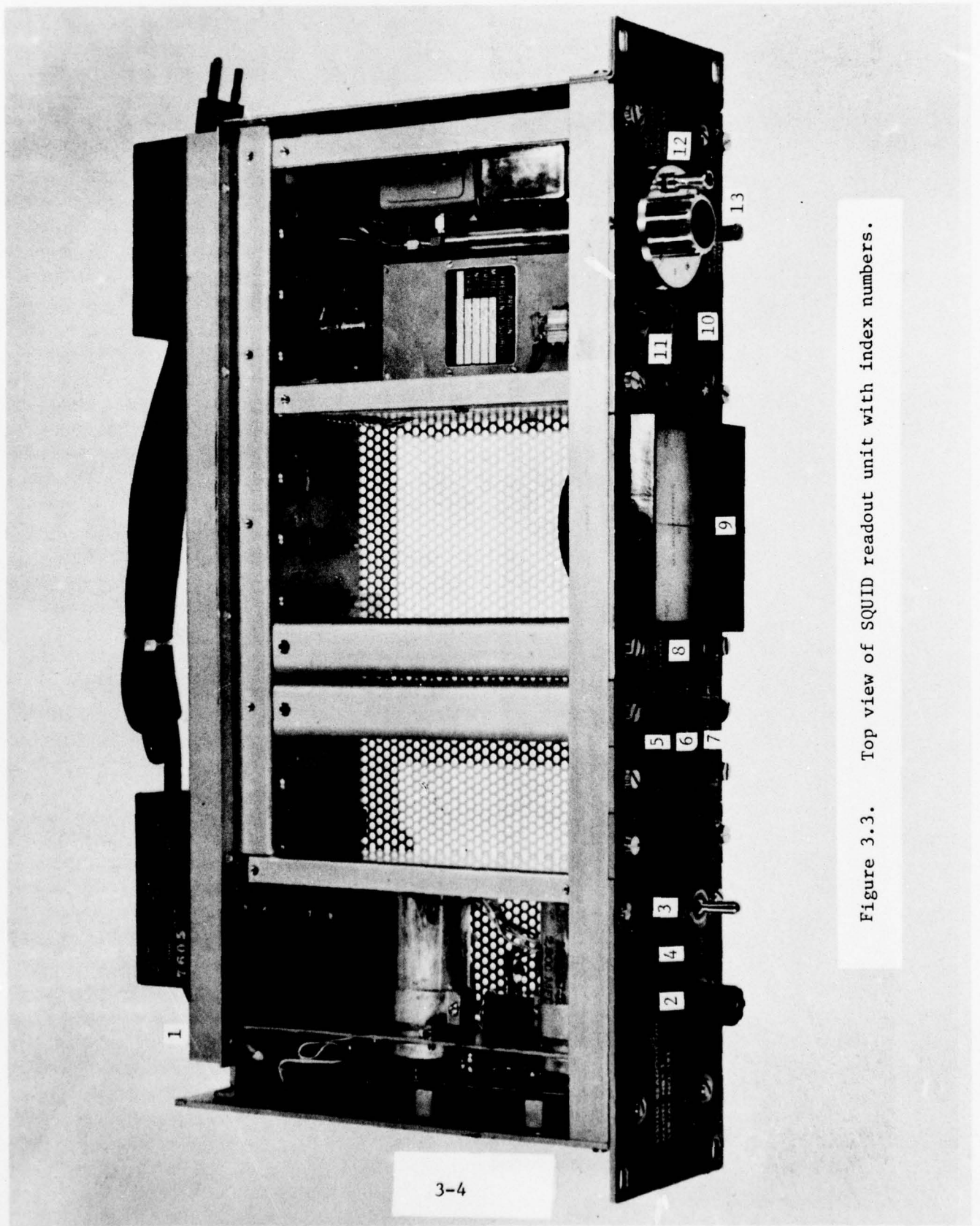
Figure 3.3. Top view of SQUID readout unit with index numbers.
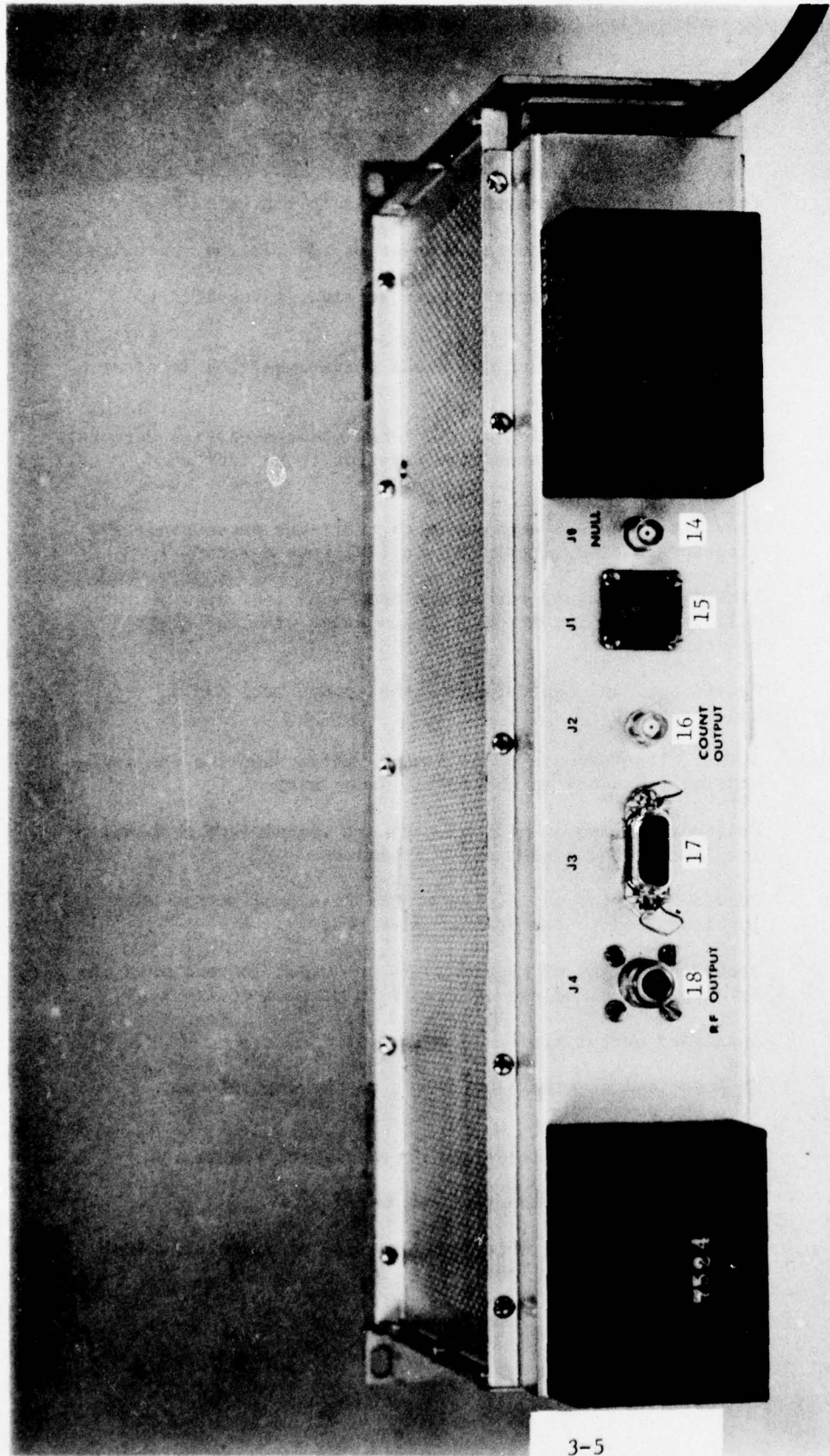
Figure 3.4. Rear view of SQUID readout unit with index numbers.

Table 3.2. Connectors, controls, and indicators on the SQUID readout unit.

Item No.	Item	Description
1.	AC Power Input (on rear panel)	Provides connection for 115-volt, 60-Hz power cable.
2.	Fuse	Protects circuits and power supplies in the unit.
3.	On/Off Switch	Connects and disconnects ac power to the internal circuits.
4.	Pilot Light	Provides visual indication when ac power is applied to the unit.
5.	2-kHz Zero Adjust	Provides adjustment of the 2-kHz phase-sensitive detector zero reference.
6.	Detector Selector Switch	Provides the selection of the 1-kHz phase-sensitive detector or the 2-kHz phase-sensitive detector to be indicated on the null meter.
7.	Zero Circuit Energizing Switch	Provides momentary engagement of the 2-kHz phase-sensitive detector zeroing circuit for initial system setup.
8.	Dead Zone Adjustment	Provides for adjustment of the dead zone near zero on the null indicator for proper null counting with the digital counter.
9.	Null Indicator	Provides visual indication of the system null during setup and operation.
10.	RF Source Plug-in Unit	30-MHz signal source plug-in unit, which supplies the calibrating frequency to the device under test.
11.	Setup/Run Switch	Provides a means of switching the rf signal into a 50-ohm load during the system setup procedure.
12.	RF Output Level Set Control	Provides vernier adjustment of the rf signal source output level applied to the device under test.
13.	RF Output Minimum Adjust	Provides a means of reducing the rf output to zero when the RF Output Level Adjust is turned to minimum (fully ccw).
14.	Jack J_0	Auxiliary output from null indicator.
15.	Jack J_1	DC power and ac signal connector to the control unit atop the dewar.
16.	Jack J_2	Output from count circuit to drive digital counter.
17.	Jack J_3	Auxiliary output connector (not used).
18.	Jack J_4	RF output connector which supplies the calibrating signal to the Device Under Test.
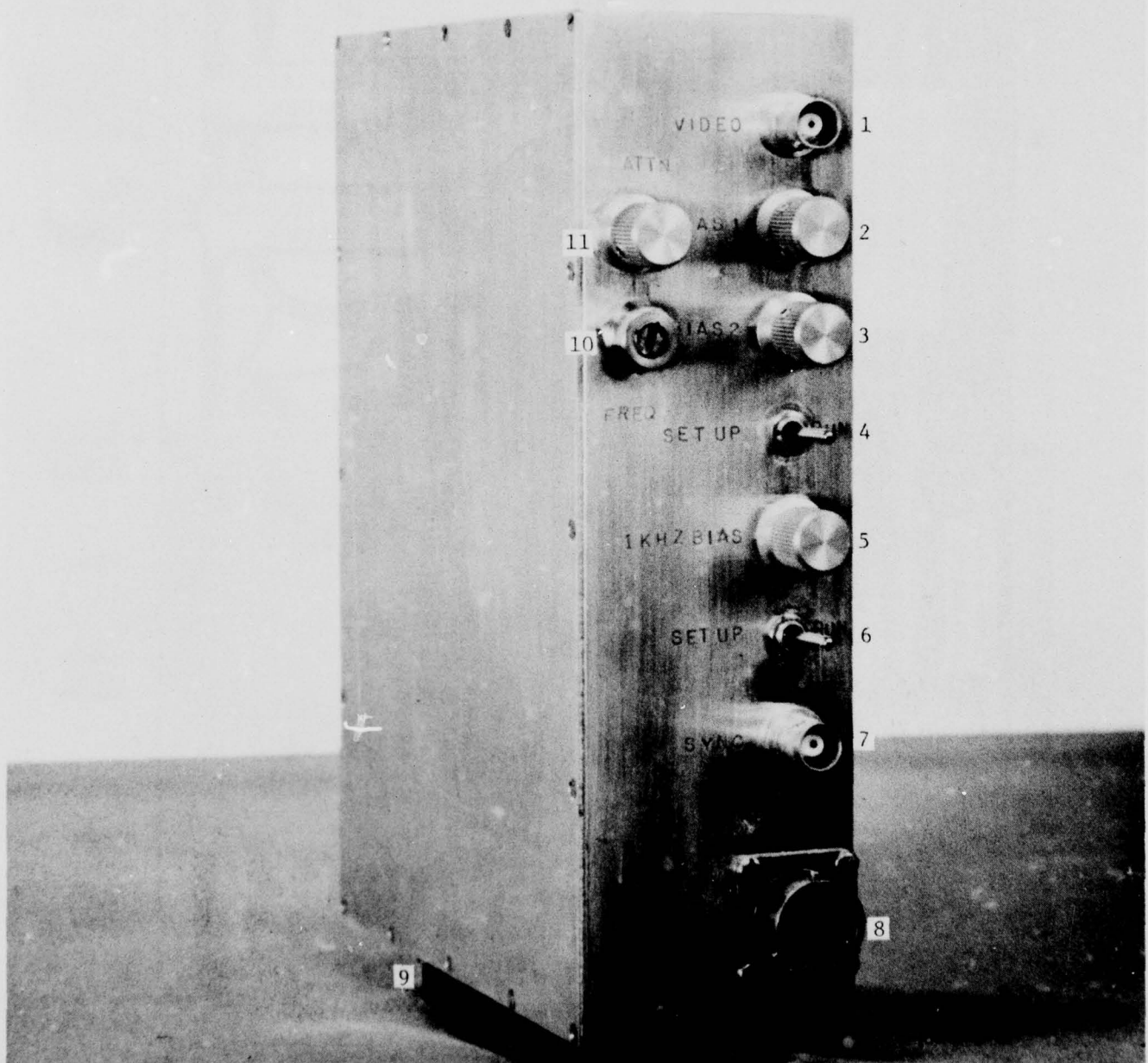
Figure 3.5.   Front view of SQUID control unit with index numbers.
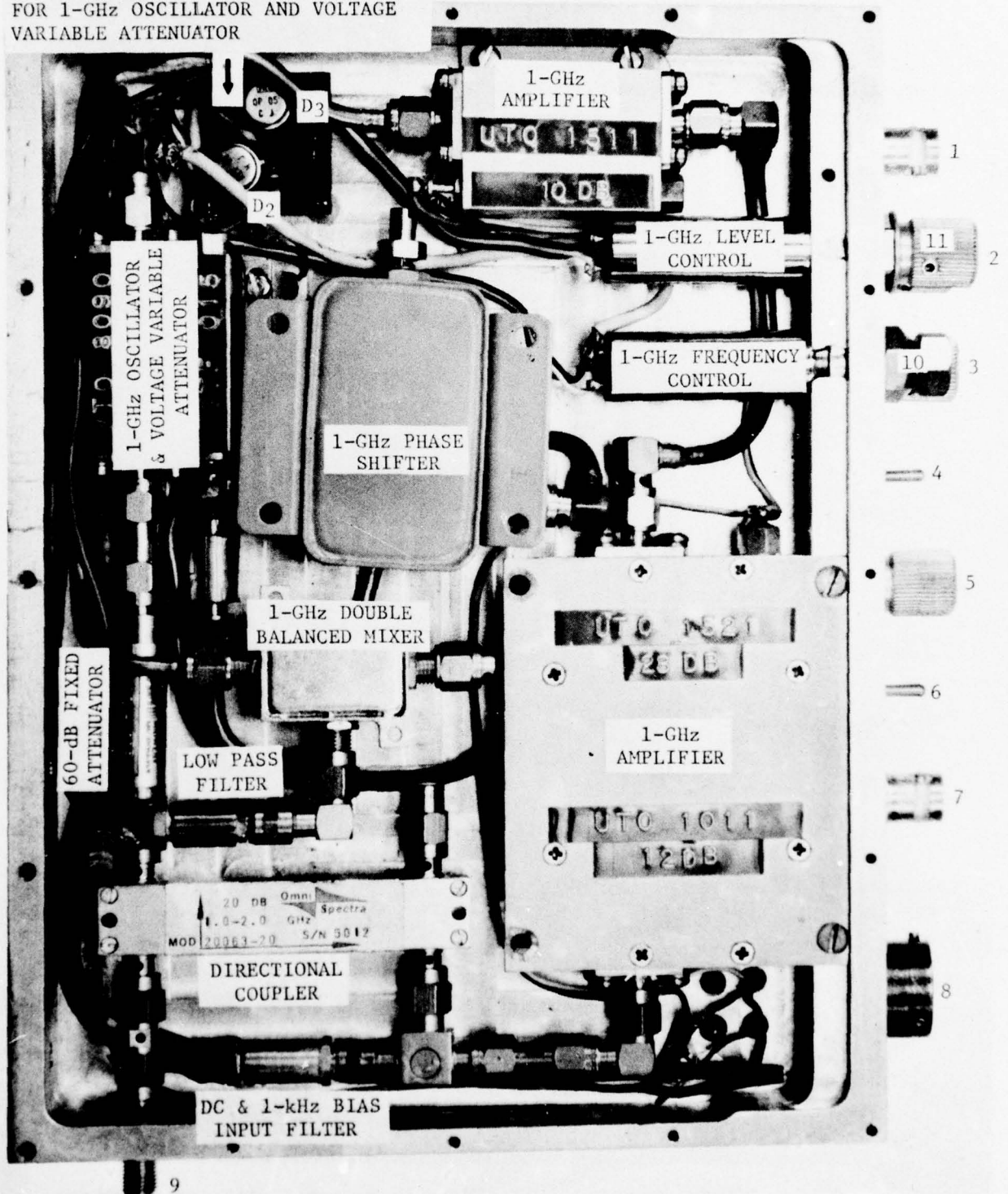
Figure 3.6.   Descriptive view of microwave bias (1 GHz) components
contained in SQUID control unit.
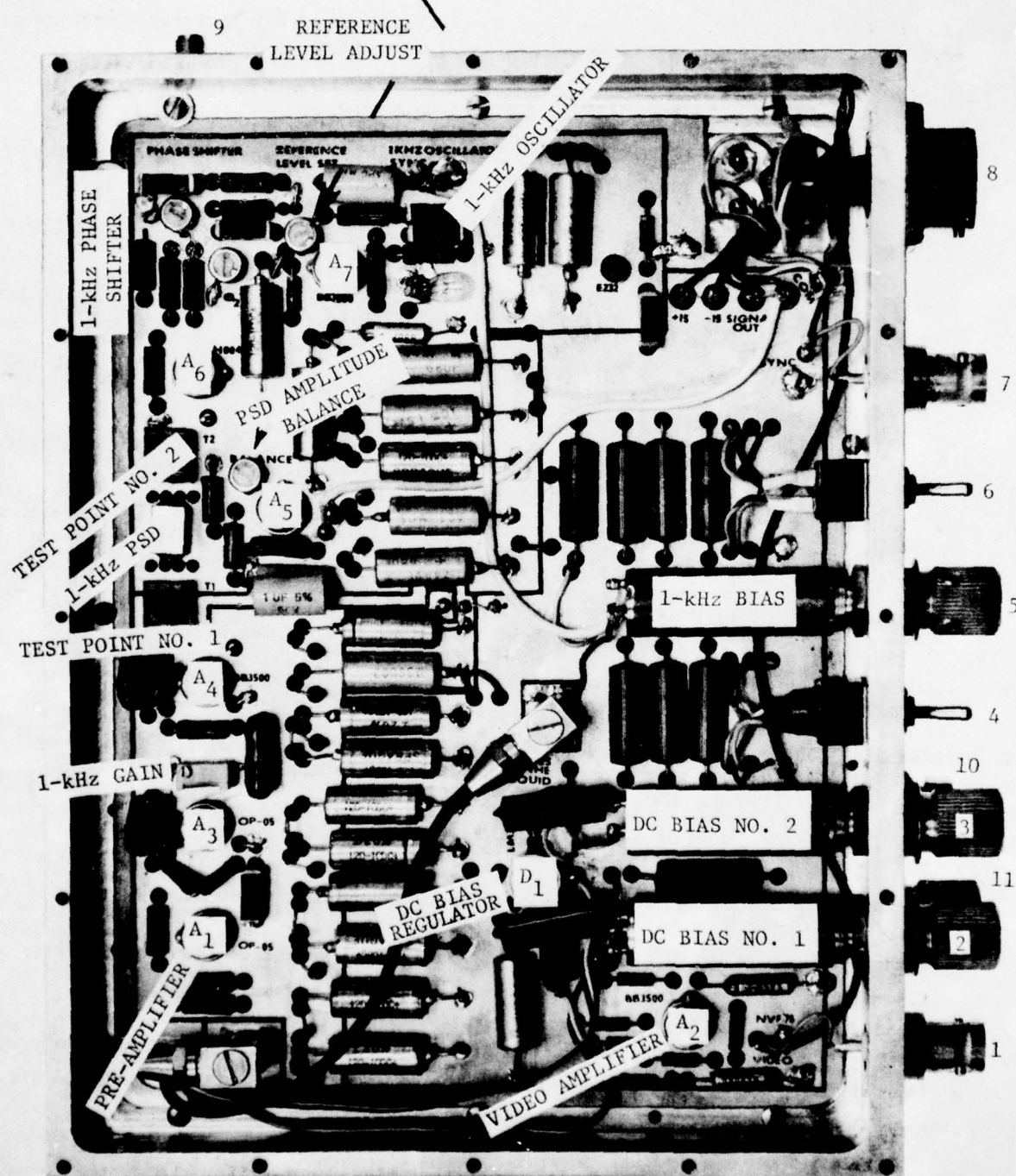
Figure 3.7. Descriptive view of 1-kHz and dc bias circuits contained in SQUID control unit.

Table 3.3. Connectors and controls on the SQUID control unit.

Item No.	Item	Description
1.	Video Output Connector	A BNC Connector provides the means for applying the SQUID interference pattern to the oscilloscope.
2.	DC Bias No. 1 Control	This control provides the means for setting the dc bias on the SQUID during system setup.
3.	DC Bias No. 2 Control	This control provides the means for setting the dc bias on the SQUID during system setup.
4.	DC Setup/Run Switch	This switch provides the proper circuit connections for the dc setup and operation of the system.
5.	1-kHz Bias Control	This control provides the means for setting amplitude of the 1-kHz bias on the SQUID during system setup.
6.	1-kHz Setup/Run Switch	This switch provides the proper circuit connections for the 1-kHz setup and operation of the system.
7.	1-kHz Sync Output	A BNC connector provides the signal to synchronize the oscilloscope with the 1-kHz SQUID interference pattern.
8.	DC Power/ac Signal Connector	This connector provides the means for applying dc power to the Control Unit from the Readout Unit and the proper connections for the 1-kHz signals between these two units.
9.	1-GHz Bias Connector	An SMA connector provides the interface between the SQUID control unit and the 1-GHz port on the SQUID.
10.	1-GHz Frequency Control	This control allows the adjustment of the microwave pump frequency for proper operation of the SQUID.
11.	1-GHz Bias Control	This control allows the proper setting of the 1-GHz amplitude for proper operation of the SQUID.

3.4 Preparation for Use

1. Bleed the pressure off the helium Dewar by opening the vent valve slowly.

2. When the pressure reaches zero, remove the mounting plate screws from the mounting plate which contains the filling valves, relief valves, pressure gauge, etc.

3. Remove the mounting plate mechanism from the Dewar and cover the hole immediately with a clean rag or similar item to contain the helium and prevent moisture from the air from entering the Dewar. Moisture in the Dewar will freeze and cause problems.

4. Verify that the helium Dewar contains sufficient liquid helium for the system to operate using the dip tube provided. Ten liters is adequate for several days running time.

5. Remove the rag from the Dewar neck and insert the SQUID probe a few inches and quickly wrap the rag around the SQUID probe.

6. Slowly lower the SQUID until helium gas starts escaping around the rag.

7. Continue to lower the SQUID probe very slowly to prevent excessive boil-off of the liquid helium.

8. Fasten the SQUID probe mounting plate to the Dewar's neck flange with the mounting screws provided.

9. Attach the SQUID control chassis to the mounting bracket on the mounting plate (fig. 3.1). Care should be exercised during this process to avoid damaging the SMA connectors on the semirigid coaxial cable which connects the SQUID Control Unit to the SQUID probe mounting flange.

10. Connect the dc/signal cable to jack J1 (fig. 3.4) on the rear panel of the SQUID Readout Unit and to jack J1 (connector 8 in figs. 3.5, 3.6, and 3.7) on the SQUID Control Unit located on top of the Dewar.

11. Connect a 25-cm long coaxial cable (with BNC connectors) from jack J2 on the rear panel of the SQUID Readout Unit to the signal input jack on the rear panel of the digital counter in the SQUID Readout Unit cabinet.

12. Connect a two-meter length of RG9B/u coaxial cable having precision Type N male connectors on each end, between the rf signal output jack J4 on the rear of the SQUID Control Unit and the input port on the Device Under Test.

13. Connect an RG9B/u cable three meters in length with precision Type N connectors from the output of the Device Under Test to the SQUID input port at the mounting bracket on the Dewar.

14. Connect an appropriate length rf cable (RG55/u) having BNC connectors on each end from the SYNC output jack on the SQUID Control Unit to the HORIZ input jack on the rear panel of the oscilloscope in the SQUID Readout Unit cabinet.

15. Connect the special rf cable (RG55/u with a BNC connector on one end and the oscilloscope rear panel vertical input connector on the other) from the "Video" output jack on the SQUID Control Unit to the "VERT A" input jack on the rear panel of the oscilloscope contained in the SQUID Readout Unit cabinet.

16. Connect the ac power cord housed in the rear of the SQUID Readout Unit to a 115 V, 60 Hz power source.

17. Turn on the digital counter, the SQUID Readout Unit, and the oscilloscope.

18. Connect the Device Under Test to the proper ac source if appropriate.

3.5 Preliminary Setup and Adjustments

1. Turn on power switches on the SQUID Readout Unit, the oscilloscope, and the digital counter.

2. Allow approximately one-half hour for the system to stabilize.

3. Adjust oscilloscope for five mV/div sensitivity.

4. Set the oscilloscope sweep speed to .2 ms/div.

5. Set oscilloscope sweep sync to external.

6. Throw all setup, run switches to setup.

7. Turn all bias controls (two dc bias controls and the 1-kHz bias control) to full CCW.

8. Turn 1-kHz bias control three turns CW.

9. Put control panel setup, run switch on rf source plug-in to setup.

10. Adjust the #1 dc bias control for a zero indication on the phase-sensitive detector output meter (null indicator).

11. Adjust #2 dc bias for the next zero and throw the dc bias toggle switch from setup to run.

12. Turn the 1-kHz bias control CW until the null meter reads zero, throw the 1-kHz setup, run toggle from setup to run.

13. Switch the null indicator switch to the 2-kHz position.

14. Depress the meter zero button and zero the null indicator using the 2-kHz zero adjust control.

15. Adjust the rf bias control (1-GHz amplitude) for zero on the null indicator.

16. Switch the null indicator switch back to the 1-kHz position.

17. Throw the 1-kHz toggle to setup and adjust the 1-kHz bias for zero on the null meter and return toggle to run.

18. Throw dc bias toggle to setup, turn both dc bias controls full CCW. Now adjust #1 dc bias (CW) for zero on the null meter, adjust #2 dc bias (CW) for the next zero on the null meter.

19. Throw the dc bias toggle to run.

20. Throw the 1-kHz bias toggle to setup and adjust the 1-kHz bias for zero on the null meter. Throw the 1-kHz toggle to run.

21. Switch the null indicator to the 2-kHz position.

22. Adjust the rf bias (1-GHz amplitude) for zero (second harmonic) on the null indicator.

23. Switch the null indicator back to the 1-kHz position.

24. Throw the 1-kHz toggle to setup, adjust the 1-kHz bias for zero on the null meter, and throw the toggle to run.

25. Throw setup, run toggle on the control panel of the rf source plug-in to run.

26. The system is now set up and ready to operate.

3.6 Operating Procedure

3.6.1 Introduction

The attenuator to be calibrated will be referred to as the Device Under Test (DUT). A good quality 10-dB fixed attenuator (VSWR $\leq$ 1.01) should be placed on the input of any attenuator calibrated with this system. This will make certain the DUT is terminated in nominally 50 + j0 ohms to eliminate any system caused mismatch error.

3.6.2 Calibration of a Variable Attenuator

1. Set the DUT to a value near its maximum attenuation setting.

2. Go through the preliminary setup procedure as outlined in section 3.5 of this document to make certain the system is properly set up, adjusced, and ready for operation.

3. Prepare a data sheet similar to the one shown in figure 3.8 to cover the range of attenuation values desired.

   NOTE: The first 10 Bessel Function Zeros cover a range of nominally 20 decibels. The first 100 Bessel Function Zeros cover a range of nominally 40 decibels. The first 200 Bessel Function Zeros cover a range of nominally 48 decibels.

   The sensitivity of the SQUID used in this system is nominally -80 dBm which means that the first Bessel Function Zero occurs at approximately 100 dB below the 250 mW being applied to the DUT. Thus, if the initial insertion loss of the DUT is nominally 30 decibels, the first Bessel Function Zero would occur at an attenuator setting of approximately 70 decibels.

   RECALL: The Bessel Function Zero number increases as the signal level applied to the SQUID increases which means the attenuator setting in dB goes down as the zero number goes up! See figure 3.9.

4. Adjust the DUT in the direction of decreasing attenuation until the Null Indicator reads zero. This indicates the first Bessel Function Zero has been reached. Set the DUT very carefully to a value which sets the Null Indicator precisely on Zero.

    CAUTION: If the DUT is moved to a setting past the value which provides a zero indication on the null meter, the attenuator under test should be returned to a higher reading, and the zero reading approached again from the high side. That is, when calibrating a variable attenuator, the indicated null on the meter should always be approached by turning the DUT in the same direction for every reading. This will eliminate the effect of any backlash in the attenuator under test and thus improve the repeatability of the measurements.

5. Repeat the reading at the first zero several times to check the system repeatability. The readings should repeat to within 0.001 to 0.002 dB.

6. Record the attenuator readings and proceed onto the second Bessel Function Zero which is approximately 7.2 dB from the first zero.

7. Record this attenuator setting and proceed to the next zero and so on.

8. The operator may count the zeros manually or the digital counter may be used.

    CAUTION: The automatic Bessel Function Zero counting circuitry cannot recognize the difference in an up count and a down count. This means if a zero null indication is overshot the counter will register one additional count each time the Bessel Function Zero is crossed. Thus, getting back to a given attenuator setting to approach the zero from the correct direction will cause errors in the automatic counter readout.

9. Continue taking readings on the DUT at the desired Bessel Function Zeros until the series is complete.

10. Return to zero number 1 and repeat the original reading. This will indicate the stability of the system and the repeatability of the system and the DUT.

    NOTE: A minimum of three sets of readings should be taken for the calculation of the mean value of attenuation at each setting for the particular Device Under Test. This will provide measurements with the minimum desired statistical control. More measurements should be taken on different days to provide attenuation mean values with a higher confidence level.

11. A different range of values may be calibrated on a Device Under Test by placing fixed attenuators in series with the input and output of the DUT.

3.6.3 Calibration of a Fixed Attenuator

A fixed attenuator may be calibrated by placing it between two good quality 10-dB fixed attenuators (VSWR < 1.01) in series with a variable attenuator which has been previously calibrated on this system. The block diagram in figure 3.10 illustrates this procedure. The insertion loss of the fixed attenuator may be obtained by making a short calibration run on the variable attenuator (with the fixed attenuator in the system) and comparing these results with the original results on the variable attenuator. This process is illustrated in figures 3.10, 3.11(a), and 3.11(b). Figures 3.11(c) and 3.11(d) illustrate the calibration of a fixed attenuator without the use of a precalibrated precision variable attenuator.

If the VSWR of the fixed attenuator under test is significant (VSWR > 1.05), then the error due to mismatch must be calculated and included in the sources of error for the calibration results. See figure 3.12 for an example of this.

3.6.4 Reduction of Calibration Data

Calibration results may be calculated from the raw data manually using a book of tables containing Bessel Functions or with the aid of a programmable calculator or a computer.

3.7 Data Reduction

The choice of computers and data reduction techniques is virtually unlimited in today's world of advanced technology. The following discussion presents a few suggested methods for calculating the calibration results from the measurements made using the SQUID System. These techniques are certainly not the only ones available but have been convenient for our purposes.

3.7.1 Data Reduction Using a Table of Bessel Functions

Recall that the SQUID response is of the form $[V(\phi)] = VJ_0(2\pi\phi_m/\phi_0)$ where ϕ_m is the flux applied to the SQUID from the output of the Device Under Test, and 2π and ϕ_0 are constants. The zeros of the zeroth order Bessel Function can be taken from a Book of Tables [11]. Taking the ratio of the tabulated value of any two Bessel Function Zeros as amplitudes allows the calculation of the attenuation change between those two zeros. This theoretical value is then compared with the indicated change in attenuation as obtained from the readings on the Device Under Test which produced the two respective Bessel Function Zeros.

Let us consider the first and twentieth zeros from the Book of Tables [11],

$$J_{0,20} = 62.04846 \ \& \ J_{0,1} = 2.40482.$$

So the attenaution change between the first and twentieth zeros is

$$20 \ \log\left(\frac{62.04846}{2.40482}\right) = 28.233 \ dB.$$

Now looking at the measured values of attenuation from the data taken on the DUT which appear in figures 3.9 and 3.15, we see that the value at the twentieth zero is 44.386 dB and

LOG SHEET   U.'S. DEPARTMENT OF COMMERCE   DATE _____
                     NATIONAL BUREAU OF STANDARDS   SHEET NO. _____

                                                          OBSERVER _____

KIND OF MEASUREMENT   RF ATTENUATION

INSTRUMENT TESTED _____

Mfg. _____   Model _____   S/N _____

	ZERO NO.					
Run No. ➡						
Time ➡						
	1					
	1					
	2					
	3					
	4					
	5					
	6					
	7					
	8					
	9					
	10					
	12					
	15					
	20					
	25					
	30					
	40					
	50					
	60					
	80					
	100					
	1	Figure 3.8.	Sample calibration data sheet. _____			
Special Conditions {						
			3-16			

Figure 3.8.   Sample calibration data sheet.

LOG SHEET

U. S. DEPARTMENT OF COMMERCE
NATIONAL BUREAU OF STANDARDS

DATE 5 MAY 1977

SHEET NO. 1

OBSERVER RTA

KIND OF MEASUREMENT RF ATTENUATION

INSTRUMENT TESTED Variable Attenuator

Mfg. NBS   Model VII   S/N 3

	ZERO NO.	ATTEN READING				
Run No. ➔		1				
Time ➔		0930				
	1	72.619				
	1	72.619				
	2	65.397				
	3	61.498				
	4	58.802				
	5	56.760				
	6	55.099				
	7	53.709				
	8	52.504				
	9	51.454				
	10	50.514				
	12	48.893				
	15	46.923				
	20	44.386				
	25	42.423				
	30	40.825				
	40	38.310				
	50	36.359				
	60	34.764				
	80	32.257				
	100	30.311				
	1	72.621	Figure 3.9.	Typical calibration data sheet.		
Special Conditions				3-17		

NBS-255A
(8-72)

USCOMM-NBS-DC

Figure 3.10. Basic block diagram of fixed attenuator calibration setup.

CALIBRATION OF A FIXED ATTENUATOR USING ONE ZERO

ZERO USED	FIXED ATTENUATOR POSITION	RUN NO. 1	RUN NO. 2	RUN NO. 3	RUN NO. 4	RUN NO. 5	MEAN $\overline{X}$	STANDARD DEVIATION S_X	STANDARD ERROR $S_{\overline{X}}$
3	OUT	42.442	42.445	42.445	42.442	42.442			
	IN	32.577	32.578	32.573	32.573	32.569			
	DIFFERENCE	9.865	9.867	9.872	9.869	9.873	9.869	0.0034 dB	0.0015 dB

THE UNCORRECTED VALUE WHEN USING ZERO NO. 3 IS 9.869 dB.

A SMOOTH CURVE THROUGH THE DATA POINTS PLOTTED IN FIGURE 3.15 SHOWS T-M=-0.002 dB AT 42 dB INDICATED ON THE VARIABLE ATTENUATOR AND T-M=+0.002 dB AT 32 dB INDICATED ON THE VARIABLE ATTENUATOR.

THUS (T-M) DIFFERENCE = -0.002 - (+0.002) = -0.004 dB WHICH MEANS THE MEASURED (OR INDICATED) VALUE IS 0.004 dB MORE THAN THE ACTUAL (OR THEORETICAL) ATTENUATION CHANGE. TO CORRECT FOR THIS ERROR IN THE VARIABLE ATTENUATOR THE FIXED ATTENUATOR VALUE INDICATED ABOVE FOR ZERO NO. 3 MUST BE DECREASED BY 0.004 dB.

THEN THE 10 dB FIXED ATTENUATOR CORRECTED VALUE IS 9.869 - 0.004 = 9.865 dB (MISMATCH ERROR HAS NOT BEEN ACCOUNTED FOR HERE BUT CONNECTOR REPEATABILITY HAS BEEN INCLUDED).

Figure 3.11(a). Sample calculation of fixed attenuator calibration results using a previously calibrated variable attenuator as a readout device.

CALIBRATION OF A FIXED ATTENUATOR
USING SEVERAL ZEROS AT ONCE

ZERO NO.	FIXED ATTENUATOR POSITION		DIFFERENCE
	OUT	IN	dB
1	53.542	43.679	9.863
1	53.542	43.680	9.862
2	46.346	36.480	9.866
3	42.444	32.577	9.867
4	39.764	29.900	9.864
5	37.701	27.836	9.865
6	36.050	26.187	9.863
7	34.652	24.792	9.860
8	33.458	23.599	9.859
9	32.399	22.536	9.863
10	31.466	21.606	9.860
1	53.545	43.675	9.870

MEAN VALUE OF DIFFERENCE = $\overline{X}$ = 9.8635 dB

= 9.864 dB

STANDARD DEVIATION = S_X = 0.00318 dB

STANDARD ERROR = $S_{\overline{X}}$ = 0.00092 dB

This mean value is incorrect only by the amount of nonlinearity in the variable attenuator being used as the readout. This value includes only one connect and disconnect operation. The average of more runs should be taken to include a better random sample of the connector repeatability.

Also mismatch error at the insertion point has not been accounted for here.

The average value of the NBS calibration of this 10 dB fixed attenuator over the past three years is 9.858 dB.

Figure 3.11(b). Sample calculation of fixed attenuator calibration using a previously calibrated variable attenuator.

CALIBRATION OF A FIXED ATTENUATOR WITHOUT USING
A PRECALIBRATED PRECISION VARIABLE ATTENUATOR

EXAMPLE OF A 20 dB FIXED ATTENUATOR CALIBRATION

1. Select the portion of the SQUID scale to use [from figure 3.11(d)] based on fixed
    attenuator nominal value and resolution desired.

    For this example, zeros 3 and 28 will be selected giving an attenuation range of
    31.1867 dB - 11.1224 dB = 20.0643 dB. (Note the spacing between zeros 27 and 28
    is 0.3188 dB.)

2. Insert the Device Under Test, the insertion point fixed pads, and a variable
    attenuator which permits coverage of the desired range (as in figure 3.10).

3. Set the variable attenuator to a value greater than that required to obtain the
    first Bessel Function Zero. Reduce the attenuation of this attenuator until zero
    number 3 is reached. Record the zero number and the variable attenuator reading.
    These numbers are a, and α_a.

4. Remove the Device Under Test from the system and reconnect the system at the
    insertion point.

5. Slowly adjust the variable attenuator for <u>less attenuation</u> until the closest Bessel
    Function Zero is reached. You're at zero b, and α_b. Note, the exact number of
    zero b is yet to be determined. Record α_b.

6. Carefully adjust the variable attenuator for <u>more attenuation</u> until the closest Bessel
    Function Zero above b is reached. Read the attenuation value from the variable
    attenuator and record it as α_{b+1}. Note the exact zero number b+1 is yet to be
    determined. (Take care to compensate for backlash in the variable attenuator.)

7. Set the variable attenuator approximately midway between α_b and α_{b+1} and reset the
    Bessel Function Zero counter to zero.

8. Increase the attenuation of the variable attenuator until zero number 1 is passed.
    The zero counter now indicates the number of zero b. Record this number and b+1.

9. The attenuation of the Device Under Test = attenuation difference between zeros a
    and b from figure 3.11(d) + the interpolated attenuation value between zeros b and
    b+1 from figure 3.11(d) and the variable attenuator readings.

10. Calculate α_{DUT}.

| ZERO NUMBER | ATTENUATION VALUE IN dB | |
	FROM VARIABLE ATTENUATOR	FROM FIGURE 3.11(d)
a = 3	α_a = 24.644	$T\alpha_a$ = 11.1224
b = 27	α_b = 24.790	$T\alpha_b$ = 30.8679
b+1 = 28	α_{b+1} = 24.472	$T\alpha_{b+1}$ = 31.1867

Attenuation of Device Under Test = α_{DUT}

$$\alpha_{DUT} = (T\alpha_b - T\alpha_a) + (T\alpha_{b+1} - T\alpha_b)\left(\frac{\alpha_b - \alpha_a}{\alpha_b - \alpha_{b+1}}\right)$$

$$\alpha_{DUT} = 19.7455 + (0.3188)\left(\frac{0.146}{0.318}\right) = 19.892 \text{ dB}$$

Considerable care must be exercised during the counting operation since the error of one zero count will introduce a gross error in the final attenuation value.

Note, mismatch error has not been accounted for yet.

Figure 3.11(c). Example of fixed attenuator calibration without using a previously calibrated precision variable attenuator.

ZERO NUMBER	ATTENUATION BETWEEN ZEROS	ZERO NUMBER	ATTENUATION BETWEEN ZEROS
1	0.0000	51	36.4301
2	7.2172	52	36.5996
3	11.1224	53	36.7658
4	13.8098	54	36.9289
5	15.8601	55	37.0890
6	17.5180	56	37.2462
7	18.9098	57	37.4007
8	20.1092	58	37.5524
9	21.1629	59	37.7015
10	22.1026	60	37.8481
11	22.9504	61	37.9923
12	23.7229	62	38.1341
13	24.4322	63	38.2736
14	25.0880	64	38.4109
15	25.6977	65	38.5461
16	26.2674	66	38.6793
17	26.8020	67	38.8104
18	27.3056	68	38.9395
19	27.7817	69	39.0668
20	28.2329	70	39.1922
21	28.6619	71	39.3159
22	29.0707	72	39.4378
23	29.4612	73	39.5580
24	29.8348	74	39.6766
25	30.1930	75	39.7936
26	30.5370	76	39.9090
27	30.8679	77	40.0229
28	31.1867	78	40.1353
29	31.4942	79	40.2463
30	31.7912	80	40.3559
31	32.0783	81	40.4642
32	32.3563	82	40.5711
33	32.6256	83	40.6767
34	32.8869	84	40.7810
35	33.1405	85	40.8841
36	33.3869	86	40.9860
37	33.6265	87	41.0867
38	33.8597	88	41.1863
39	34.0868	89	41.2847
40	34.3081	90	41.3820
41	34.5239	91	41.4783
42	34.7345	92	41.5734
43	34.9401	93	41.6676
44	35.1409	94	41.7607
45	35.3372	95	41.8529
46	35.5292	96	41.9441
47	35.7170	97	42.0343
48	35.9008	98	42.1237
49	36.0808	99	42.2121
50	36.2572	100	42.2996

Figure 3.11(d). Theoretical values of attenuation as determined by the first 100 zeros of the zeroeth order Bessel function.

END
DATE
FILMED
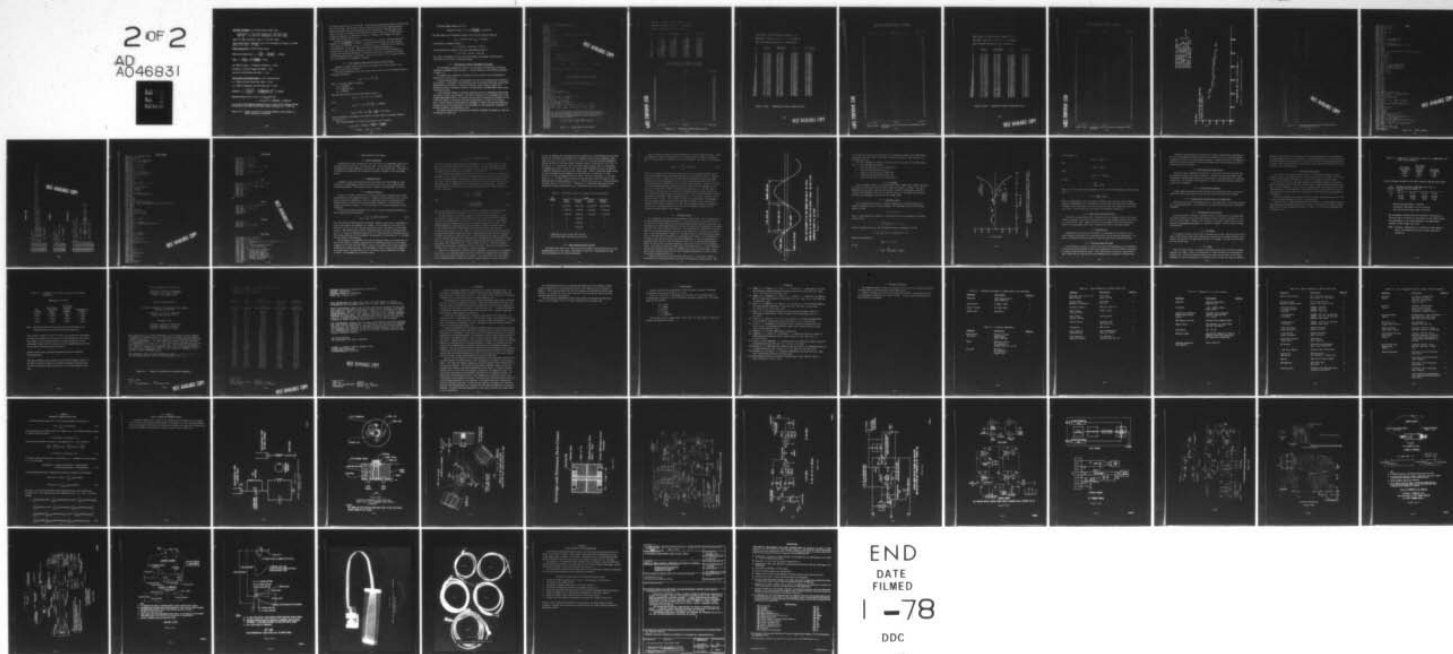
I -78

DDC

MEASURED IMPEDANCE of 10 dB Attenuator Under Test

     Female End   Z = 48.5 @ 0° Terminated in 50.0 @ 0° ohms
     Male End   Z = 49.3 @ 0° Terminated in 50.0 @ 0° ohms

Model VII WBCO Attenuator Input Z = 50.0 @ 0° ohms

SQUID System Output Impedance with 20 dB Attenuator on Output of 30 MHz
Source = Z = 50.5   -2° ohms.

VSWR CALCULATION For SQUID System Output

$$\text{Reflection Coefficient} = \rho = \frac{Z - Z_o}{Z + Z_o} = \frac{50.5 - 50}{50.5 + 50} = 0.00497$$

$$\text{VSWR} = \sigma = \frac{1 + |\rho|}{1 - |\rho|} = \frac{1 + 0.00497}{1 - 0.00497} = 1.010$$

and VSWR at Input to Variable Attenuator = 1.000

Similarly, 10 dB DUT Female End VSWR = 1.031

and the 10 dB DUT Male End VSWR = 1.014

CALCULATION OF MISMATCH ERROR at the Insertion Point

σ_1 = VSWR of Device Under Test (DUT) = 1.031

σ_2 = VSWR of Impedance the DUT Looks Into = 1.010

$$\text{Mismatch} = F = \left(\frac{\sigma_1 \sigma_2 - 1}{\sigma_1 \sigma_2 + 1} \right)^2 = \left(\frac{1.031 \times 1.01 - 1}{1.031 \times 1.01 + 1} \right)^2 = 0.000409$$

Maximum Mismatch Error in dB = $10 \, \text{Log}_{10}(1 + F)$ dB

$$= 10 \, \text{Log} \, (1 + 0.000409) = 0.0018 \text{ dB}$$

So the Worst Case Maximum Mismatch Error For This 10 dB Attenuator Being
Calibrated in the SQUID System Under These Conditions is ± 0.002 dB.

Figure 3.12. Sample calculation of maximum mismatch error present in
                fixed attenuator calibration.

the value at the first zero is 72.619 dB. The difference between these values is 72.619-44.386 which is 28.233 dB. This indicates that the theoretical value and the measured value of attenuation between the first and twentieth zeros are identical. This then states that there is no error in the Device Under Test (to the overall accuracy of the SQUID system) between the settings of 72.619 dB and 44.386 dB. Similarly, let's examine the results between the third and twelfth zeros.

The Book of Tables states $J_{0,12}$ = 36.91709 and $J_{0,3}$ = 8.65372. Thus the theoretical change is 20 log$\left(\dfrac{36.91709}{8.65372}\right)$ = 12.600 dB. The measured values between the same two zeros (from figures 3.9 and 3.15) are $J_{0,3}$ = 61.498 dB and $J_{0,12}$ = 48.893 dB, so the difference is 61.498-48.893 = 12.605 dB. Then the difference T-M (theory-measured) is 12.600-12.605 = -0.005 dB which indicates an error in the DUT of 0.005 dB between the settings of 61.498 dB and 48.893 dB. A calibration curve can be constructed for the DUT using the measurement data in this manner. The curve in figure 3.15 is a typical calibration curve plotted by a programmable calculator.

3.7.2 Data Reduction Using Calculated Bessel Function Values

Arguments of Bessel Function Zeros may be calculated when a Book of Tables is not available or sufficiently inclusive.

The close approximation of any zeroth order Bessel Function can be calculated using the following relationship:

$$J_{0,S} = S\pi - \alpha_0 + \frac{\alpha_1}{S} + \frac{\alpha_2}{S^2}$$

where S = the zero number of interest,

α_0 = 0.78540566,

α_1 = 0.04055529, and

α_2 = 0.00808324.

Thus the first zero of the zeroth order Bessel Function is

$$J_{0,1} = \pi - \alpha_0 + \alpha_1 + \alpha_2 = 2.40482552$$

also

$$J_{0,2} = 2\pi - \alpha_0 + \frac{\alpha_1}{2} + \frac{\alpha_2}{(2)^2} = 5.52007810$$

and

$$J_{0,100} = 100\pi - \alpha_0 + \frac{\alpha_1}{100} + \frac{\alpha_2}{(100)^2} = 313.374266.$$

Values calculated in this manner can be used in the data reduction techniques explained in section 3.7.1.

The following example is a further illustration of this technique:

$$J_{0,30} = 30\pi - 0.785406 + \frac{0.040555}{30} + \frac{0.0080832}{(30)^2}$$

$$= 93.4610 \quad \text{and } J_{0,1} = 2.4048.$$

So the dB change between the two is

$$\text{Theoretical Value} = T = 20 \log\left(\frac{93.4610}{2.4048}\right) = 31.7910 \text{ dB}.$$

Now from figure 3.15 the measured values at the first and thirtieth zeros are

$$J_{0,1} = 72.619 \text{ dB} \quad \text{and} \quad J_{0,30} = 40.825 \text{ dB}.$$

The difference in measured values is

$$M = 72.619 \text{ dB} - 40.825 \text{ dB} = 31.794 \text{ dB}.$$

Then the difference between the theoretical and measured values is

$$T - M = 31.791 - 31.794 = -0.003 \text{ dB}.$$

This, then, is the amount of error in the DUT between the readings of 40.825 dB and 72.619 dB (to the accuracy of the SQUID System).

3.7.3 Data Reduction Using a Programmable Calculator

The relationship presented in section 3.7.2 can easily be solved with a relatively inexpensive programmable desk calculator. A typical program for the HP 9830 is presented in figure 3.13.

The results can be displayed in tabular form and in graphic form as illustrated in figures 3.14, 3.15, and 3.16.

A further sophistication of this process is the use of the plotter which is driven by the calculator. A laboratory type calibration curve on the Device Under Test can be drawn automatically on the plotter. A typical calibration curve is shown in figure 3.17. Calibration values at convenient attenuator settings between the measurement points can be read from this curve.

A more convenient method of obtaining calibration values at intermediate points along the curve is to query the calculator. The curve in figure 3.17 is a polynomial fit to the original measurement results. The operator has the option of asking the calculator for the calibration results for any given attenuator setting within the limits of the plotted curve. Typical results of this process are displayed in figure 3.18 along with additional information such as the coefficients of the polynomial fit and statistical information on the data contained in the calibration curve.

The plotter program which generated the information appearing in figures 3.17 and 3.18 is presented in figure 3.19.

```
10 DIM N[50],M[50],T[50],S[50]
20 DISP "TYPE IN NUMBER OF DATA POINTS";
30 INPUT N0
40 S=G=0
50 FOR K=1 TO N0
60 READ N[K],M[K]
70 I=N[K]
80 J1=2.40483
90 J=I+3.14159265358-0.78540566+0.0405529/I+0.00808324/I↑2
100 T[K]=20*LGT(J/J1)
110 NEXT K
120 A=T[6]+M[6]
130 FOR K=1 TO N0
140 T[K]=A-T[K]
150 S=S+T[K]-M[K]
160 G=G+(T[K]-M[K])↑2
170 FORMAT F4.0,F13.4,F11.3,F13.4,F13.4
180 NEXT K
190 A=S/N0
200 S1=SQR(G/N0-A↑2)
210 PRINT
220 PRINT
230 PRINT "    THE NUMBER OF DATA POINTS TAKEN IS"N0
240 PRINT
250 PRINT "    THE MEAN VALUE OF (T-M) IS   "A
260 PRINT
270 PRINT "    THE STANDARD DEVIATION IS"S1
280 PRINT
290 PRINT
300 PRINT "   I       THEORY      MEASURED      T-M     (T-M)-MEAN"
310 PRINT "   -      -------     --------      ---     ----------"
320 PRINT
330 FOR K=1 TO N0
340 WRITE (15,170)N[K];T[K];M[K];T[K]-M[K];(T[K]-M[K])-S/N0
350 NEXT K
360 PRINT
370 PRINT
380 PRINT
390 PRINT "              DEVIATION FROM THE MEAN IN DECIBELS"
400 PRINT "              VERSUS ATTENUATOR SETTING IN DECIBELS"
410 PRINT
420 PRINT
430 PRINT
440 PRINT "        -0.025 DB "TAB34" 0.000"TAB59"+0.025 DB"
450 PRINT "         +----+----+----+----+----0----+----+----+----+----+"
460 PRINT
470 I=INT(T[N0])
480 FOR L=1 TO N0
490 K=N0+1-L
500 IF I+0.5>T[K] THEN 540
510 PRINT TAB5,I,TAB36".",TAB64,I
520 I=I+1
530 GOTO 500
540 IF ABS((T[K]-M[K])-A)>0.0005 THEN 570
550 PRINT TAB5,I,TAB36"*",TAB64,I
560 GOTO 630
570 IF (T[K]-M[K])-A<0 THEN 620
580 IF (T[K]-M[K])-A<0.025 THEN 600
590 M[K]=T[K]-0.025-A
600 PRINT TAB5,I,TAB36"."TAB(36+1000*((T[K]-M[K]-A)))"*"TAB64,I
610 GOTO 630
620 PRINT TAB5,I;TAB(36+1000*((T[K]-M[K])-A))"*"TAB36"."TAB64,I
630 I=I+1
640 NEXT L
650 DATA 1,72.338,2,65.142,3,61.213,4,58.524,5,56.474,6,54.82,7,53.419
660 DATA 8,52.226,9,51.168,10,50.231,12,48.605,15,46.629,20,44.093,25,42.132
670 DATA 30,37.806,40,35.288,50,33.337,60,31.749,80,29.238,100,27.292
680 DATA 150,15.972,200,13.473,300,9.946,400,7.447,500,5.508,600,3.922
690 DATA 700,2.582,800,1.421,900,0.399
700 PRINT
710 PRINT "         +----+----+----+----+----0----+----+----+----+----+"
720 PRINT "        -0.025 DB "TAB34" 0.000"TAB59"+0.025 DB"
730 PRINT
740 PRINT
750 PRINT
760 PRINT
770 STOP
```

Figure 3.13.   Typical program for data reduction.

THE NUMBER OF DATA POINTS TAKEN IS 12

THE MEAN VALUE OF (T-M) IS   7.23981E-04

THE STANDARD DEVIATION IS 2.16831E-03

I	THEORY	MEASURED	T-M	(T-M)-MEAN
1	72.6100	72.610	0.0000	-0.0007
2	65.3928	65.390	0.0028	0.0021
3	61.4876	61.482	0.0056	0.0049
4	58.8002	58.803	-0.0028	-0.0035
5	56.7499	56.750	-0.0001	-0.0008
6	55.0920	55.092	0.0000	-0.0007
7	53.7002	53.698	0.0022	0.0015
8	52.5008	52.502	-0.0012	-0.0019
9	51.4471	51.445	0.0021	0.0014
10	50.5074	50.507	0.0004	-0.0003
12	48.8871	48.889	-0.0019	-0.0026
15	46.9124	46.911	0.0014	0.0006

DEVIATION FROM THE MEAN IN DECIBELS
VERSUS ATTENUATOR SETTING IN DECIBELS

```
         -0.025 DB                      0.000                    +0.025 DB
         +----+----+----+----+----+----0----+----+----+----+----+----+
    46                                  . *                              46
    47                                  . *                              47
    48                                  .                                48
    49                              *   .                                49
    50                            .     :                                50
    51                                * .                                51
    52                                  .*                               52
    53                              * . :                                53
    54                                  .*                               54
    55                                * .                                55
    56                                  :                                56
    57                                * :                                57
    58                                  .                                58
    59                            *     .                                59
    60                                  :                                60
    61                                  .   *                            61
    62                                  :                                62
    63                                  .                                63
    64                                  :                                64
    65                                  .  *                             65
    66                                  :                                66
    67                                  :                                67
    68                                  :                                68
    69                                  :                                69
    70                                  :                                70
    71                                  :                                71
    72                                  :                                72
    73                                * :                                73
         +----+----+----+----+----+----0----+----+----+----+----+----+
         -0.025 DB                      0.000                    +0.025 DB
```
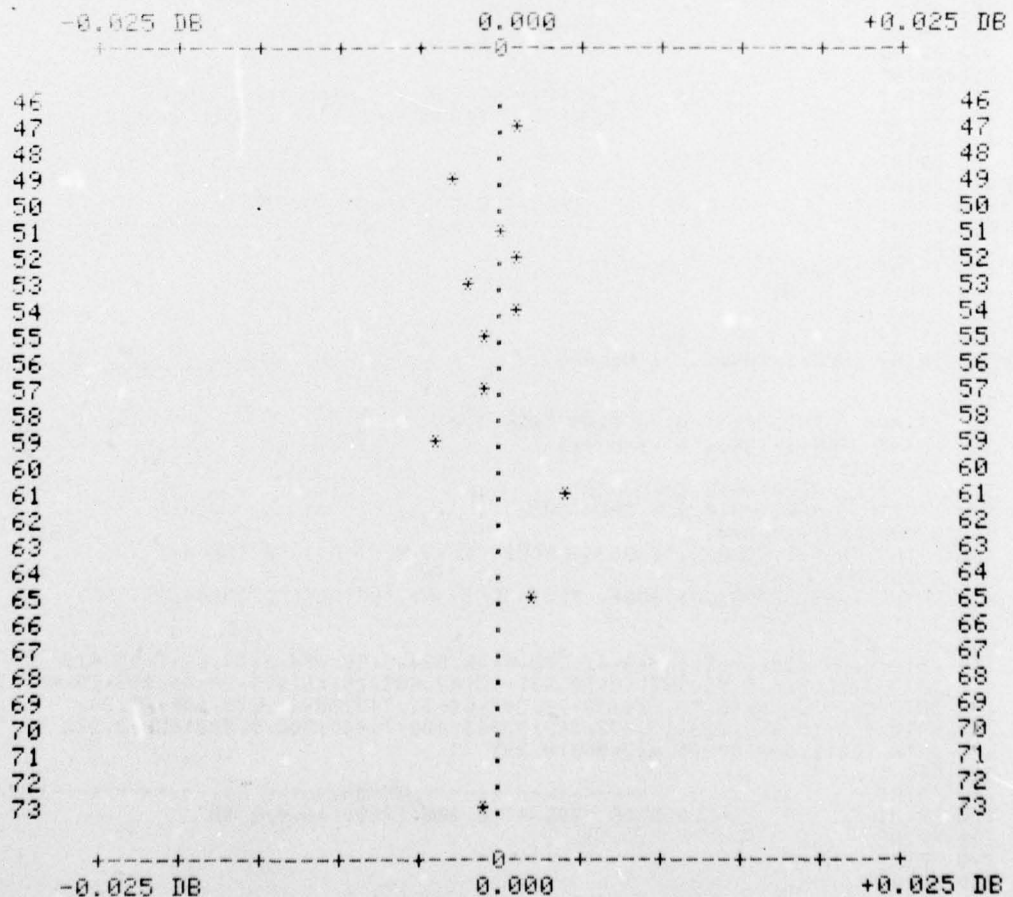
Figure 3.14.   Calibration results using 15 zeros.

THE NUMBER OF DATA POINTS TAKEN IS 24

THE MEAN VALUE OF (T-M) IS   1.77836E-03

THE STANDARD DEVIATION IS 3.62580E-03

I	THEORY	MEASURED	T-M	(T-M)-MEAN
1	72.6170	72.619	-0.0020	-0.0037
2	65.3998	65.397	0.0028	0.0010
3	61.4946	61.498	-0.0034	-0.0052
4	58.8072	58.802	0.0052	0.0035
5	56.7569	56.760	-0.0031	-0.0048
6	55.0990	55.099	0.0000	-0.0018
7	53.7072	53.709	-0.0018	-0.0036
8	52.5078	52.504	0.0038	0.0020
9	51.4541	51.454	0.0001	-0.0017
10	50.5144	50.514	0.0004	-0.0013
12	48.8941	48.893	0.0011	-0.0006
15	46.9194	46.923	-0.0036	-0.0054
20	44.3841	44.386	-0.0019	-0.0037
25	42.4240	42.423	0.0010	-0.0008
30	40.8258	40.825	0.0008	-0.0009
40	38.3089	38.310	-0.0011	-0.0029
50	36.3598	36.359	0.0008	-0.0010
60	34.7689	34.764	0.0049	0.0031
80	32.2611	32.257	0.0041	0.0023
100	30.3174	30.311	0.0064	0.0047
120	28.7302	28.721	0.0092	0.0074
150	26.7884	26.781	0.0074	0.0056
175	25.4474	25.440	0.0074	0.0056
200	24.2860	24.282	0.0040	0.0022

Figure 3.15(a).   Calibration results using 200 zeros.

3-29

DEVIATION FROM THE MEAN IN DECIBELS
VERSUS ATTENUATOR SETTING IN DECIBELS

```
      -0.025 DB                  0.000                  +0.025 DB
      +----+----+----+----+----+----0----+----+----+----+----+----+
24                                      *                          .
25                                   .     *                          .
26                                   .
27                                   .     *
28                                   .
29                                   .        *
30                                   .     *
31                                   .
32                                   *
33                                   .
34                                   .
35                                   *
36                               *   .
37                                   .
38                          *        .
39                                  .
40                                  .
41                               *  .
42                               *  .
43                                  .
44                          *       .
45                                  .
46                                  .
47                      *           .
48                                  .
49                               *  .
50                                  .
51                            *     .
52                            *     .
53                               *
54                         *   *    .
55                            *     .
56                                  .
57                     *            .
58                                  .
59                               *  .
60                                  .
61                    *             .
62                                  .
63                                  .
64                                  .
65                               *  .
66                                  .
67                                  .
68                                  .
69                                  .
70                                  .
71                                  .
72                                  .
73                  *               .
      +----+----+----+----+----+----0----+----+----+----+----+----+
      -0.025 DB                  0.000                  +0.025 DB
```

Figure 3.15(b).   Calibration curve for attenuation measurements using
                    200 zeros.

3-30

```
THE NUMBER OF DATA POINTS TAKEN IS 24

THE MEAN VALUE OF (T-M) IS    2.77462E-03

THE STANDARD DEVIATION IS 5.71733E-03
```

I	THEORY	MEASURED	T-M	(T-M)-MEAN
1	72.9670	72.980	-0.0130	-0.0157
2	65.7498	65.752	-0.0022	-0.0050
3	61.8446	61.847	-0.0024	-0.0052
4	59.1572	59.155	0.0022	-0.0005
5	57.1069	57.112	-0.0051	-0.0078
6	55.4490	55.449	0.0000	-0.0028
7	54.0572	54.057	0.0002	-0.0026
8	52.8578	52.856	0.0018	-0.0009
9	51.8041	51.806	-0.0019	-0.0047
10	50.8644	50.865	-0.0006	-0.0033
12	49.2441	49.241	0.0031	0.0004
15	47.2694	47.267	0.0024	-0.0004
20	44.7341	44.730	0.0041	0.0013
25	42.7740	42.772	0.0020	-0.0008
30	41.1758	41.173	0.0028	0.0001
40	38.6589	38.655	0.0039	0.0011
50	36.7098	36.705	0.0048	0.0020
60	35.1189	35.115	0.0039	0.0011
80	32.6111	32.602	0.0091	0.0063
100	30.6674	30.660	0.0074	0.0047
150	27.1384	27.132	0.0064	0.0036
200	24.6360	24.625	0.0110	0.0082
300	21.1105	21.099	0.0115	0.0088
400	18.6099	18.595	0.0149	0.0122

Figure 3.16(a).   Calibration results using 400 zeros.

DEVIATION FROM THE MEAN IN DECIBELS
VERSUS ATTENUATOR SETTING IN DECIBELS

```
    -0.025 DB                 0.000                 +0.025 DB
    +----+----+----+----+----+----0----+----+----+----+----+----+
18                                     .           *              18
19                                     .                          19
20                                     .                          20
21                                     .        *                 21
22                                     .                          22
23                                     .                          23
24                                     .                          24
25                                     .      *                   25
26                                     .                          26
27                                   * .                          27
28                                     .                          28
29                                     .                          29
30                                     .                          30
31                                    *.                          31
32                                     .                          32
33                                      *                         33
34                                     .                          34
35                                  . *                           35
36                                     .                          36
37                                   * .                          37
38                                     .                          38
39                                  . *                           39
40                                     .                          40
41                                  *  .                          41
42                                     .                          42
43                                *.                              43
44                                     .                          44
45                                 .*                             45
46                                     .                          46
47                                 *   .                          47
48                                     .                          48
49                                 *   .                          49
50                                     .                          50
51                             *   .                              51
52                           *       *.                           52
53                              *.                                53
54                             *                                  54
55                             *                                  55
56                                     .                          56
57                         *           .                          57
58                                     .                          58
59                              *.                                59
60                                     .                          60
61                                     .                          61
62                          *          .                          62
63                                     .                          63
64                                     .                          64
65                                     .                          65
66                          *          .                          66
67                                     .                          67
68                                     .                          68
69                                     .                          69
70                                     .                          70
71                                     .                          71
72                                     .                          72
73                *                    .                          73
    +----+----+----+----+----+----0----+----+----+----+----+----+
    -0.025 DB                 0.000                 +0.025 DB
```
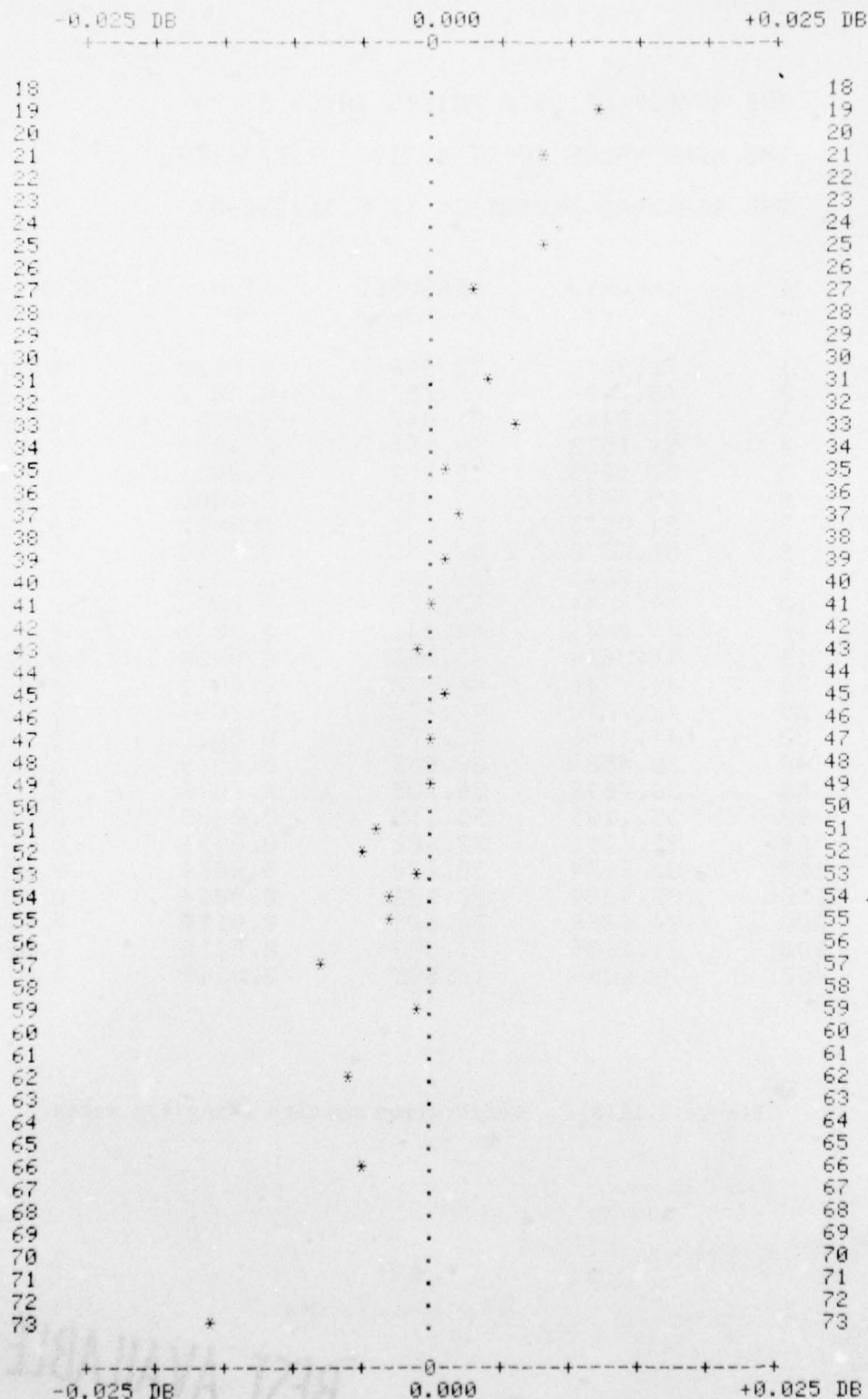
Figure 3.16(b).   Calibration curve for attenuation measurements using
                  400 zeros.

3-32

ATTENUATOR CALIBRATION
USING SQUID SYSTEM
ATTENUATOR MODEL NO. VII
ATTENUATOR SERIAL NO. 3
DATE OF CALIBRATION: 5-17-76
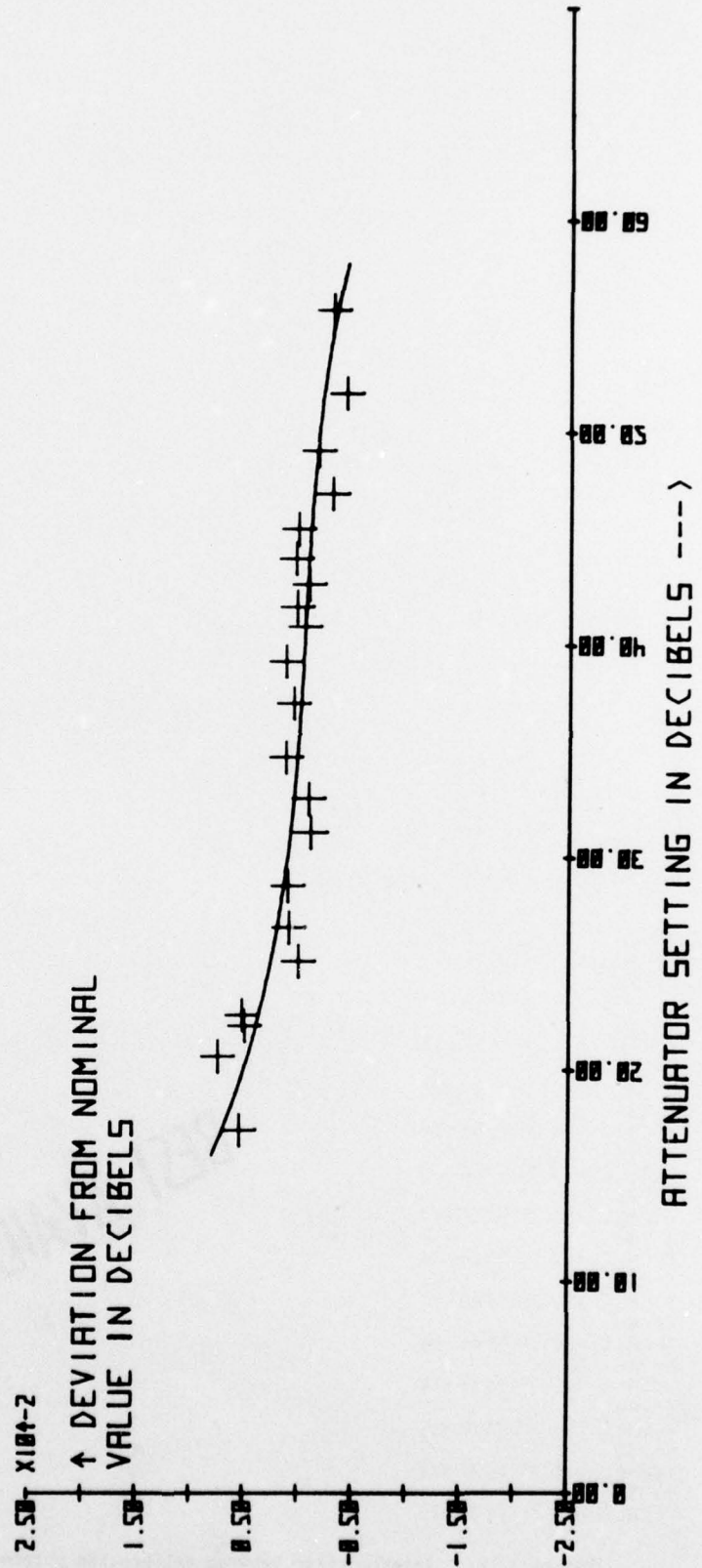DEGREE OF POLYNOMIAL FIT: 3
SYSTEM OPERATOR: RTA

ATTENUATOR SETTING IN DECIBELS --->

Figure 3.17. Calibration curve plotted by computer.

```
PT.NO.          X              Y

    1          17.1540        0.0054
    2          20.6810        0.0074
    3          22.0990        0.0049
    4          23.6370        0.0051
    5          25.1400       -0.0001
    6          26.7300        0.0008
    7          30.6740        0.0003
    8          31.1950       -0.0012
    9          32.7930       -0.0010
   10          34.7540        0.0011
   11          37.2900        0.0011
   12          39.3640        0.0011
   13          40.3860       -0.0006
   14          41.9250        0.0001
   15          43.8800       -0.0010
   16          44.0780        0.0002
   17          45.4730       -0.0003
   18          47.1310        0.0001
   19          49.1300       -0.0015
   20          51.3700       -0.0014
   21          55.7740       -0.0002
   22          63.3310       -0.0110

NO. POINTS = 22

X: MEAN = 39.571373    ST.DEV.= 12.265419
Y: MEAN = 3.09091E-05  ST.DEV.= 4.19051E-03

CORR.COEF. = 0.852154623


COEFFICIENTS

B( 0)=     0.0414
B( 1)=    -0.0032
B( 2)=     0.0001
B( 3)=    -0.0000

R SQUARE =  0.880765126


X=220
Y(CALC)=-5.10487E-03
X=225
Y(CALC)= 3.19426E-03
X=230
Y(CALC)= 6.83008E-04
X=232
Y(CALC)= 0.53684E-04
X=234
Y(CALC)= 1.20610E-04
X=236
Y(CALC)=-3.50973E-05
X=238
Y(CALC)=-1.57523E-04
X=240
Y(CALC)=-2.77953E-04
X=242
Y(CALC)=-4.30872E-04
X=244
Y(CALC)=-6.50464E-04
X=246
Y(CALC)=-9.70915E-04
X=248
Y(CALC)=-1.42641E-03
X=250
Y(CALC)=-2.05113E-03
X=255
Y(CALC)=-4.57765E-03
```

Figure 3.18.   Interpolation between calibration points using computer
curve fit shown in figure 3.17.

3-34

```
1000 DIM C[66],B[11]              START
1010 FOR I=1 TO 11
1020 C[I]=B[I]=0
1030 NEXT I
1040 FOR I=12 TO 66
1050 C[I]=0
1060 NEXT I
1070 B[1]=1
1080 W=N=S1=S2=S3=S4=S5=0
1090 DISP "MAX.DEGREE=";9
1100 D2=9
1110 IF D2>9 THEN 1090
1120 DISP "XMIN,XMAX,INCRM.=";0,80,10
1130 X1=0
1140 X2=80
1150 X3=10
1160 DISP "YMIN,YMAX,INCRM.=";-0.025,+0.025,0.01
1170 Y1=-0.025
1180 Y2=+0.025
1190 Y3=0.01
1200 I=(X2-X1)/27
1210 J=(Y2-Y1)/17
1220 Y5=Y1-2*J
1230 Y6=Y2+J
1240 SCALE -8,90,-0.045,0.055
1242 XAXIS -0.025,10,0,80
1244 YAXIS 0,0.005,-0.025,0.02
1250 PLOT X2,Y1
1260 PLOT X1,Y1
1270 PLOT X1,Y2,-1
1280 U=Y1
1290 V=Y2
1300 T=Y3
1310 Z=FNL0
1320 U=X1
1330 V=X2
1340 T=X3
1350 Z=FNL1
1360 X3=I
1370 Y3=J
1380 Z=FNK0
1390 LABEL (*,3,1,0,2/3)
1400 DISP "ENTER 1 TO PRINT DATA";
1410 INPUT P9
1420 IF P9#1 THEN 1460
1430 PRINT
1440 PRINT "PT.NO."TAB14"X"TAB28"Y"
1450 PRINT
1460 DISP "PRESS 'ENTER DATA' KEY"
1470 END
1480 FORMAT 2F7.2
1490 DEF FNL(Z)
1500 X=ABSU
1510 Y=ABSV
1520 P=INTLGT(X+(Y-X)*(Y>X))
1530 P0=(P<-1 OR P>2)
1540 LABEL (*,1.5,2,Z*ATN1E+99,2/3)
1550 FOR K=U TO V STEP T
1560 PLOT X1* NOT Z+K*Z,K* NOT Z+Y1*Z,1
1570 CPLOT -7.3,-0.3
1580 LABEL (1480)K/( NOT P0+P0*10↑P)"-";
1590 NEXT K
1600 IF P0=0 THEN 1630
1610 LABEL (*)" X10↑"P;
1630 RETURN 0
```

Figure 3.19.   Plotter program.

3-35

ENTER DATA

```
1000 IF W THEN 1100
1010 READ B[2],Y
1050 DATA 46.892,0.0009,48.867,0.0007,50.488,0.51.426,0.0016,52.48,0.0014
1060 DATA 53.684,-0.0032,55.074,-0.0014,56.729,0.0015,58.78,0.0008,61.47,-0.0019
1070 DATA 65.374,-0.0006,72.591,-0.0004
1080 IF FNX1,THEN 1010
1090 END
1100 DISP "NOT ALLOWED"
1110 END
```

CORRECT

```
1000 IF W THEN 1050
1010 DISP "WRONG X,Y=";
1020 INPUT B[2],Y
1030 IF FNX(-1) THEN 1010
1040 END
1050 DISP "NOT ALLOWED"
1060 END
```

STATISTICS

```
1000 S8=SQR((S2-S1↑2/N)/(N-1))
1010 S9=SQR((S4-S3↑2/N)/(N-1))
1020 R9=(S5-S1*S3/N)/(N-1)/S8/S9
1030 PRINT "NO. POINTS ="N
1040 PRINT "NO. POINTS ="N
1050 PRINT
1060 PRINT "X:   MEAN="S1/N;TAB25"ST.DEV.="S8
1070 PRINT "Y:   MEAN="S3/N;TAB25"ST.DEV.="S9
1080 PRINT
1090 PRINT "CORR.COEFF.="R9
1100 PRINT
1110 END
```

SELECT DEGREE

```
1000 IF N <= D2-W THEN 1250
1010 DISP "DEG.REG.=";
1020 INPUT D1
1030 IF D1 <= D2-W THEN 1060
1040 DISP "MAX DEG=";D2-W
1050 END
1060 IF W=0 THEN 1240
1070 T=0
1080 FOR I=1 TO D1+1
1090 B[I]=0
1100 FOR J=1 TO D1-I+2
1110 R=(I+J-1)*(D2+2-0.5*(I+J))
1120 B[I]=B[I]+C[T+J]*C[R]
1130 NEXT J
1140 T=I*(D2+(3-I)/2)
1150 NEXT I
1160 R1=0
1170 FOR I=2 TO D1+1
1180 R1=R1+C[I*(D2+(3-I)/2)]↑2
1190 NEXT I
1200 T0=C[(D2+1)*(D2+2)/2]
1210 T0=T0-C[D2+1]↑2
1220 DISP "DONE"
1230 END
1240 IF N>D2 THEN 1270
1250 DISP "NOT ENOUGH POINTS"
1260 END
1270 P=W=1
1280 D2=D2+1
1290 FOR J=1 TO D2
1292 IF C[P] >= 0 THEN 1300
1294 PRINT "MATRIX UNSTABLE-USE LOWER MAXIMUN DEGREE !"
1296 PRINT
1297 PRINT
1298 END
1300 C[P]=SQRC[P]
1310 FOR I=1 TO D2-J+1
1320 C[P+I]=C[P+I]/C[P]
1330 NEXT I
1340 R=P+I
1350 S=R
1360 FOR L=1 TO D2-J
1370 P=P+1
1380 FOR M=1 TO D2+2-J-L
1390 C[R+M-1]=C[R+M-1]-C[P]*C[P+M-1]
1400 NEXT M
1410 R=R+M-1
1420 NEXT L
1430 P=S
1440 NEXT J
1450 T=(D2+1)*(D2+2)/2
1460 FOR I=1 TO D2-1
1470 T=T-1-I
1480 C[T]=1/C[T]
1490 FOR J=1 TO D2-I
1500 P=D2+1-I+J
1510 P=P*(D2+1-(P-1)/2)-I
1520 R=P-J
1530 S=0
1540 U=I+J+1
1550 V=P
1560 FOR K=1 TO J
1570 V=V+U-K
1580 S=S-C[R+K]*C[V]
1590 NEXT K
1600 C[P]=S/C[R]
1610 NEXT J
1620 NEXT I
1630 C[1]=1/C[1]
1640 GOTO 1070
```

3-37

COEFFICIENTS

```
1000 IF W=0 THEN 1110
1010 PRINT
1020 PRINT "COEFFICIENTS"
1030 PRINT
1040 FORMAT F3.0,F12.4
1050 FOR I=1 TO D1+1
1060 WRITE (15,1040)"B("I-1")="B[I]
1070 NEXT I
1080 PRINT
1090 PRINT "R SQUARE = "R1/T0
1100 PRINT
1110 END
```

PLOT

```
1000 FOR X=X1 TO X2 STEP (X2-X1)/100
1010 Y=FNZX
1020 IF Y<Y5 OR Y>Y6 THEN 1050
1030 PLOT X,Y
1040 GOTO 1060
1050 PEN
1060 NEXT X
1070 Z=FNK0
1080 END
```

LETTER

```
1000 DISP "CHARACTER HEIGHT(%)";
1010 INPUT H
1020 LABEL (*,H,2,0,2/3)
1030 LETTER
1040 Z=FNK0
1050 END
```

ESTIMATE

```
1000 DISP "X=";
1010 INPUT X
1020 DISP "Y(CALC)="FNZX
1030 END
```

LABEL GRAPH

```
990 SCALE 0,60,-2.75,2.75
1000 LABEL (*,2,1.7,0,10/15)
1010 PLOT 15,-2.25,1
1020 LABEL (*)"ATTENUATOR SETTING IN DECIBELS --->"
1030 PLOT 5,0.75,1
1040 LABEL (*)"↑ DEVIATION FROM NOMINAL"
1050 LABEL (*)"VALUE IN DECIBELS"
1060 PLOT 35,3,1
1070 LABEL (*)"ATTENUATOR CALIBRATION"
1080 LABEL (*)"USING SQUID SYSTEM"
1090 LABEL (*)"ATTENUATOR MODEL NO."
1100 LABEL (*)"ATTENUATOR SERIAL NO."
1110 LABEL (*)"DATE OF CALIBRATION:"
1120 LABEL (*)"DEGREE OF POLYNOMIAL FIT:"
1130 LABEL (*)"SYSTEM OPERATOR:"
1135 LETTER
1140 END
```

4. ERROR ANALYSIS OF THE SYSTEM

4.1 General Information

Determining the exact contribution to the total error in a measurement system of all possible sources of error is a very difficult task. This section will be limited to a discussion of the major significant contributors to the total system error. The errors in any system may be separated into two general categories; systematic errors and random errors.

4.2 Systematic Errors

Systematic errors can be defined as the errors which cause the average of a well defined set of measurements to differ from the true value by a constant amount during repeated measurements. The systematic error is common to each measurement in the set.

4.2.1 Harmonic Distortion

Section 2.3 provides a description of the Fourier frequency components which result from distortion of the interference pattern. (Details of the derivation of eq. (2.9) are given in section 10, appendix A.) Section 2.3 describes bias set-up procedures which eliminate many of the errors resulting from harmonic distortion. In this section we consider such errors in detail. Eq. (2.9) and table 2.1 are useful references for this discussion.

The first low frequency sideband of the carrier contains the desired information as well as some effects of distortion.

$$V_{\omega_c \pm \omega_d} = \sum_{n=1}^{\infty} 2V_n \cdot J_0(nM) J_1(nD) \sin nB \quad . \tag{4.1}$$

The first term of the series contains the desired response, $J_0(M)$, and it is desirable to reduce other terms in the expansion to a minumum. If B is selected so that $\sin 2B = 0$, that is $B = \frac{\pi}{2}$ (or $I_b = I_o/4$), then the second term, and for that matter all even terms, are zero. The third term of the series can be made equal to zero by a judicious choice for D. $D = 2\pi I_d/I_o$ is adjusted so that $J_1(3D) = 0$, a situation which fortunately puts the first term, $J_1(D)$, near its first maximum. Unfortunately, the odd terms at $n = 5$ and above are not nulled by this technique.

This procedure, the adjustment of dc and low frequency biases, is the method used to null out the effects of harmonic distortion of the interference pattern, but one should recognize that at least the even harmonic content of the pattern can be nearly completely eliminated by a simple procedure. The even harmonic content is almost solely dependent on the amplitude of the pump signal (ω_c) if the detector used to demodulate the signal is linear. The sidebands at $2\omega_d$ from the carrier

$$V_{\omega_c \pm 2\omega_d} = \sum_{n=1}^{\infty} 2V_n \cdot J_o(nM) J_2(nD) \cos nB \qquad (4.2)$$

can be used to affect the adjustment of this amplitude. If one starts with $B = \pi/2$ as before, then the odd terms in this series are nulled. The even terms appear at large amplitude and one can adjust the ω_c amplitude to null this term. Having done this, the even harmonic terms are doubly nulled (small V_n and $\sin nB \approx 0$).

Even though we can minimize certain terms in eq. (4.1), it is useful to estimate the magnitude of errors which could arise, thus indicating just how much care must be exercised in the bias setup procedure. In the limit of small distortion (which we assume is the usual case), that is, small values for the quantities V_n/V_1, one can make a rather simple approximation for the magnitude of the errors produced by the distortion. Noting the identity $dJ_0(M)/dM = -J_1(M)$ and using a linear approximation for the Bessel functions it is easy to show that

$$\Delta M_{k,n} \approx \alpha_n \frac{J_0(nj_{o,k})}{J_1(j_{o,k})} \qquad (4.3)$$

where

$$\alpha_n = \frac{V_n J_1(nD) \sin(nB)}{V_1 J_1(D) \sin(B)} \qquad (4.4)$$

and $j_{o,k}$ is the kth zero of J_0. Thus, the deviations ΔM depend on the harmonic number n of the distortion and on the number k of the particular Bessel function zero.

For even values of n, it will in general be possible to doubly minimize α_n. That is, the setup procedure allows one to minimize both V_n/V_1 and $\sin(nB)/\sin(B)$. However, consider the situation where α_n is not zero. For a fixed even value of n, the quantity $J_0(nj_{o,k})/J_0(j_{o,k})$ alternates in sign as k is increased in integer units from 1. The absolute magnitude of this quantity quickly approaches a constant for larger values of k. One normally works with a logarithmic scale so that the errors take the form $20 \log[1 + (\Delta M_{k,n}/j_{o,k})]$. For n = 2 and $\alpha_2 = 0.01$, the error is 0.017 dB at the first zero and oscillates in sign at higher order zeros. Expressed in decibels, the error decreases at higher zeros since $j_{o,k}$ increases with k. At the seventh zero the error is 0.002 dB. V_2/V_1 is typically less than 0.1 and the magnitude of $\sin(2B)/\sin B \approx 2B$ can readily be kept below 0.01. V_n/V_1 gets smaller as n takes on higher even values while $\sin(nB)/\sin B \approx nB$ gets larger (for a fixed error in B). The net result is that $\alpha_n < .001$ can be readily achieved and this results in negligible error at even zeros. Note that a resolution and stability of $B = 2\pi I_b/I_o = 0.01$ or $I_b/I_o \approx 0.001$ is required.

Errors due to odd harmonic distortions do not alternate in sign and are of considerably more concern. The underdamped SQUID interference pattern is triangular and this develops into a sinusoidal pattern as damping is increased. It is quite likely that some remnants of the triangular behavior persist even when the visual appearance is nearly sinusoidal,

in fact, we speculate that the higher order odd harmonics are attenuated more than the lower order ones. The Fourier coefficients for a triangular pattern take the geometric series values of $V_3/V_1 = 1/9$, $V_5/V_1 = 1/25$, $V_7/V_1 = 1/49$, etc. The setup procedure dramatically reduces the effect of the third harmonic distortion since D is selected so that $J_1(3D) \simeq 0$ and thus $\alpha_3 \simeq 0$. Odd terms of order 5 and higher remain, however, and it is instructive to estimate their effect. Since we don't have accurate estimates for V_n/V_1, we take the triangular values given above as a worst possible case. Table 4.1 lists the decibel errors for the 5th through 11th odd harmonics for this worst case. As before $B = \pi/2$ and $J_1(3D) = 0$ so that 3rd harmonic errors are nulled. Note that errors for $n = 7$ are worse than for $n = 5$. To show how well D must be set we note that at the first zero, if D is displaced from its proper setting by 1.5% ($\alpha = .044$) the error is $\Delta M_{1,3} = .0028$ or 0.010 dB (for worst case, i.e., $V_3/V_1 = 1/9$). Development of a sinusoidal interference pattern dramatically reduces the quantities V_n/V_1, thus making these errors insignificant.

Table 4.1. Odd harmonic errors for triangular interference pattern.

ZERO NUMBER	ERROR			
	Fifth Harmonic	Seventh Harmonic	Ninth Harmonic	Eleventh Harmonic
k	$V_5/V_1=1/25$	$V_7/V_1=1/49$	$V_9/V_1=1/81$	$V_{11}/V_1=1/121$
1	− 0.005 dB	0.004 dB	0.003 dB	− 0.002 dB
2	− 0.001 dB	0.006 dB	0.001 dB	− 0.001 dB
3	*	0.004 dB	*	*
4	*	0.003 dB	*	*
5	*	0.002 dB +	*	*

* Magnitude of error is less than 0.001 dB

+ Error drops below 0.001 dB at the 12th zero

4.2.2 Phase Sensitive Detector Errors

Any signal which adds to the 1-kHz null detecting signal and which does not go to zero simultaneously with it will cause a displacement of that null. Possibilities for such errors are examined in the following discussion.

The low frequency signal is amplified and applied to a phase sensitive detector (PSD). The signal and a reference voltage $V_r(t)$ at 1-kHz are applied to a mixer, the output of which is passed through a low-pass filter and then amplified. The output can be expressed as

$$V_{psd} = 1/T \int_{-T/2}^{T/2} V_r(t)V_s(t)dt \qquad (4.5)$$

where T is one period of the 1-kHz oscillation and $V_s(t)$ is the signal derived from the 1-GHz double balanced mixer and intermediate amplifier (this signal has all the components given in eq. (2.9)). Ideally, if $V_r(t)$ were purely sinusoidal, the output V_{psd} would contain only the 1-kHz components of eq. (2.9) which are given explicitly in eq. (4.1). This follows from the orthogonality of the sine and cosine functions. However, in practice $V_r(t)$ does contain significant harmonics particularly odd value ones and these can be a concern. The third line of table 2.1 displays the response at $3\omega_d$. The first term of this causes no concern since its zeros are in coincidence with the desired response and the second term is doubly nulled by the setup process. But the third term which represents third harmonic distortion is near a maximum ($J_3(3D) \approx 0.42$ for $J_1(3D) = 0$) and is thus a potential source of error. This problem is resolved by a simple means. The bandwidth of the low frequency amplifier which precedes the PSD is narrowed so that only the 1-kHz component of the signal is applied to the PSD. This eliminates response to sidebands at $2\omega_d$, $3\omega_d$, etc. The signal applied to the 2-kHz PSD is similarly filtered at $2\omega_d$ to eliminate the same problem at that frequency.

4.2.3 Null Meter Offset

It is essential that the null indicating meter read zero when a null is obtained with the Device Under Test (variable attenuator). If this condition is not satisfied, that is, if there is a dc offset signal from the phase-sensitive detector amplifier A_5 (see fig. 3.7) when there is no 1-kHz signal being sent into the 1-kHz amplifier, the data will be erroneous (see fig. 4.1). The net effect of this type of error shows up as a "splitting" of the data. That is, the indicated zeros are alternately to the right then to the left of the correct zeros. This is illustrated in figure 4.1. The amplifier A_5 is a very low drift-type amplifier, and the PSD diodes are matched so as to minimize this offset. It is occasionally re-assuring to check the zero offset of the PSD and amplifier A_5. This is accomplished by turning the gain control in the 1-kHz amplifier (see fig. 3.7) counterclockwise approximately 25 turns or until the rather indistinct clicks occur at the end of its adjustment range. This operation removes any 1-kHz signal from the PSD driver A_4. If the null meter does not read precisely zero adjust the "BALANCE" pot near A_5 to zero the meter. After this is done, the gain control must be turned clockwise approximately 25 turns to bring the system to maximum sensitivity.

A similar situation occurs with the 2-kHz PSD circuit. In this case, instead of affecting the zero locations directly, the effect is through the 1-GHz bias level. That
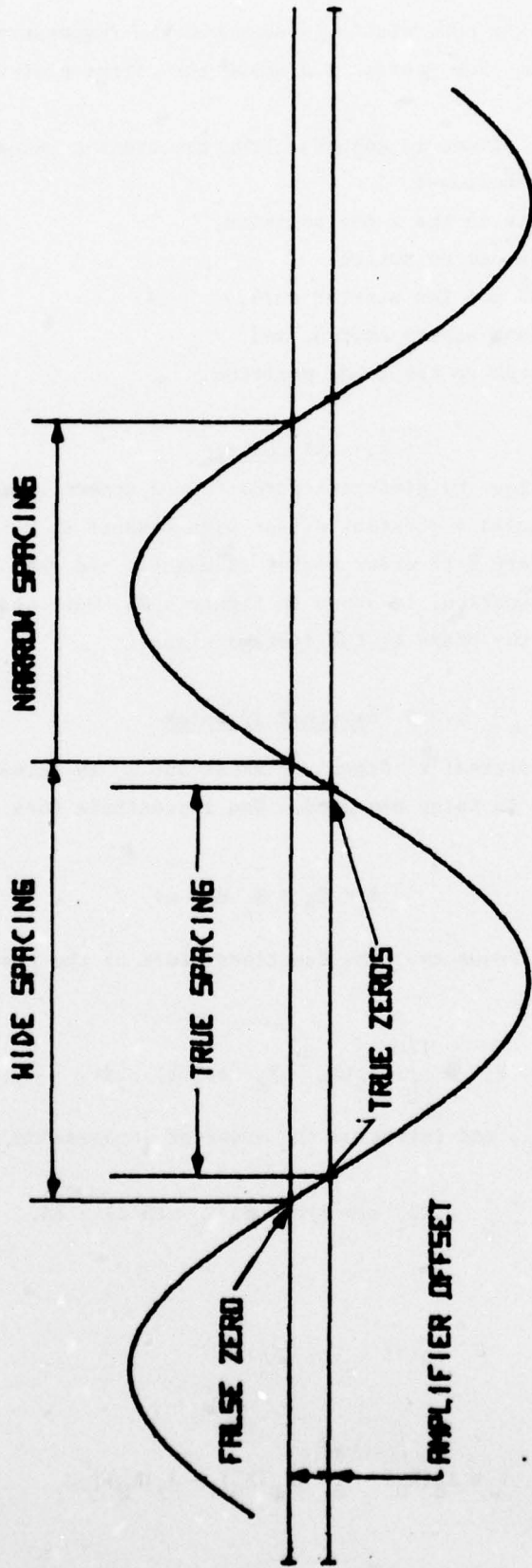
NOTE THE ALTERNATE WIDE AND NARROW SPACING OF THE FALSE

ZEROS DUE TO THE PSD AMPLIFIER OFFSET, HENCE, THE SPLITTING

(SPREADING APART) OF THE DATA.

Figure 4.1. Error due to PSD amplifier offset.

is, a false zero from the 2-kHz PSD results in an asymetric response of the SQUID because of improper 1-GHz bias level. See section 2.3 where the effect of 1-GHz bias error is discussed more fully.

The 2-kHz PSD amplifier offset is adjusted from the front panel of the SQUID Readout Unit. It is accomplished as follows:

1.   throw the PSD switch to the 2-kHz position,

2.   press the ZERO push-button switch,

3.   adjust the NULL ADJ pot for a meter null,

4.   release the ZERO push-button switch, and

5.   return the PSD switch to the 1-kHz position.

4.2.4 RF Leakage

Since rf signals traveling by different paths from a common source combine coherently, this source of error also causes a constant offset with respect to current. The errors measured in dB, therefore, vary with order number in exactly the same way as the error caused by third harmonic distortion, as shown in figure 4.2. Once again, this error has arbitrary sign depending on the phase of the leakage signal.

4.2.5 External rf Noise

Let us assume that an external rf signal of amplitude X_1 is interfering with the signal of amplitude X_0 which is being measured. The approximate form of the resulting signal X is then

$$X = X_0 + X_1 \cos \omega t$$

where ω is the angular beat frequency. The functional form of the response of the SQUID system is then

$$V \sim \omega \int_0^{1/\omega} J_0(X_0 + X_1 \cos \omega t) \cdot dt.$$

Using the integral form of J_0, and inverting the order of integration, we find

$$V \sim \frac{1}{\pi} \int_0^\pi J_0(X_1 \sin \phi) \cdot \cos(X_0 \sin \phi) \cdot d\phi.$$

Making the approximation

$$J_0(X) \simeq 1 - 1/4 \, X^2$$

we find

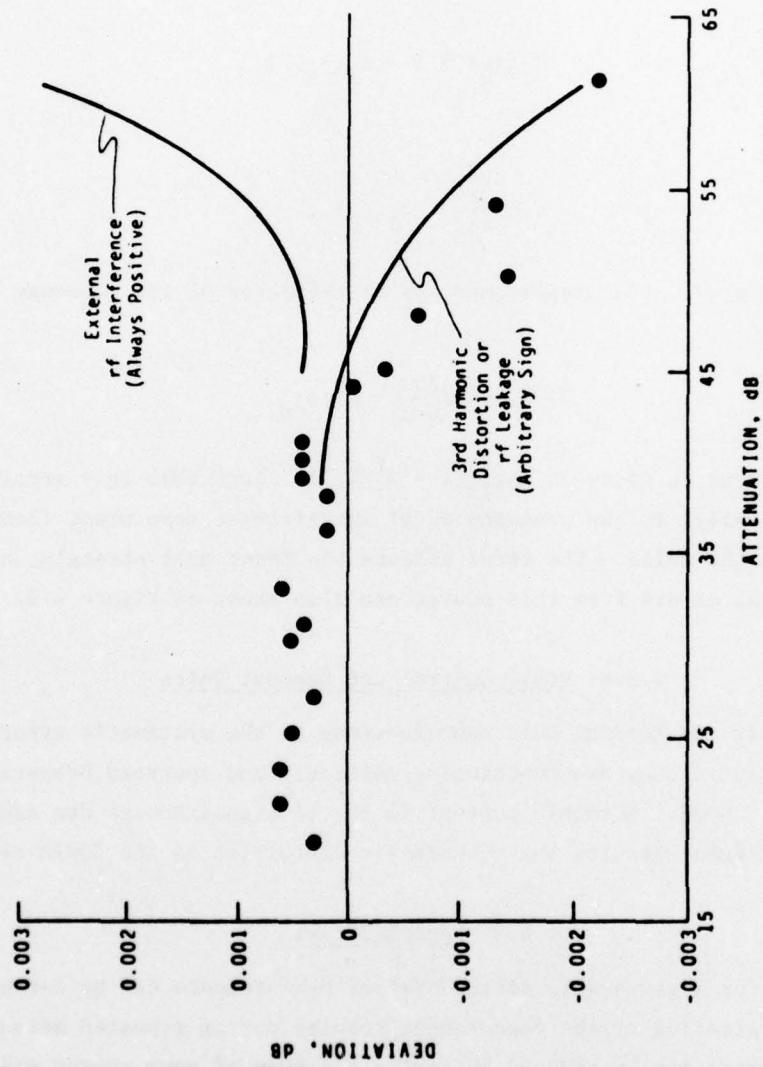$$V \sim J_0(X_0) - \frac{X_1^2}{8} [J_0(X_0) - J_2(X_0)] \, .$$

Figure 4.2. The calculated effects of various sources of systematic error compared with the experimental results of a typical "bad" run.

4-7

At the zeros of J_0,

$$J_0(X_0) = J_0(j_0) = 0$$

and

$$V \sim X_1^2 \cdot J_2(j_0)/8.$$

Since

$$J_2(j_0) = 2 \cdot J_1(j_0)/j_0$$

we find

$$V \sim \frac{X_1^2}{4j_0} \cdot J_1(j_0) .$$

Hence, to the first order, the displacement δX of the zeros of the response by this perturbation is

$$\delta X = -V/\frac{dV}{dX_0} \simeq X_1^2/4j_0 .$$

Hence, the displacement in dB is $20 \log_{10}(1 + X_1^2/4j_0^2)$. Note that this error is always positive. Paradoxically, in the presence of rf interference more power (less attenuation) is needed to set on the nulls. The error affects the first null strongly, and the others very little. Typical errors from this source are also shown on figure 4.2.

4.2.6 SQUID Control and Readout Units

The Control Unit and Readout Unit contributions to the systematic error of the total system are negligible if they are functioning correctly and operated properly (see sections 3.4, 3.5, and 3.6). NOTE: Harmonic content in the rf signal source can cause serious errors in the measurement results due to harmonic distortion in the SQUID response.

4.3 Random Errors

Random errors for a given well defined set of measurements can be defined as the errors causing a scattering of the measurement results during repeated measurements. The effect of random errors may be reduced by taking the mean of many repeat measurements.

4.3.1 The Device Under Test (DUT)

Any such device is subject to random errors due to nonrepeatability of the mechanical drive and positioning mechanism, as well as the mechanical or optical readout and possible rf leakage at high attenuation values. After these devices are used for long periods of time, normal wear can cause poorly fitting components which contribute to random errors.

Calibration (which provides an evaluation of linearity and mechanical tolerances, as well as the repeatability) of these devices is the primary function of the SQUID system. Calibration of DUT's on a regular basis will greatly increase the ability of a laboratory to maintain an accurate record of the device's performance and find any sudden occurrence of excessive errors in the device.

4.3.2 SQUID Control and Readout Units

These units have a negligible contribution to the system total error (provided they are operating properly as previously discussed). However, any significant power supply fluctuations or ground-loop currents have the potential of causing these units to generate random error. Any noticeable errors generated in these units would indicate a malfunction in one or more components.

4.3.2.1 RF Source and Amplifier

Normal random fluctuations in these devices have no significant effect on the total system error since these units are well regulated and well isolated from the SQUID.

4.3.2.2 Coaxial Switch (Set-Run relay in rf signal path)

This device will have no significant effect on the random error of the system provided it is functioning properly. Its repeatability and VSWR characteristics were investigated thoroughly.

4.3.3 Phase-Sensitive Null Detector

This device should contribute a negligible amount of random error to the system when it is given sufficient warm-up time and operated properly as stated in sections 3.4, 3.5, and 3.6 of this document. However, this instrument could produce random error if it were subjected to abnormally high levels of rf signals, rf leakage, rf noise, and line voltage irregularities.

4.3.4 RF Leakage

RF leakage is always a real threat in any measurement system. When sufficient care is taken in using correct cables and in making each connector secure (tighten carefully with a wrench), this system is not appreciably affected by rf leakage. This was verified during the final system check.

4.3.5 Noise

Electrical noise consists of unwanted disturbances which tend to obscure the desired component of a signal. Noise is characterized by a random distribution of amplitude and frequency [12]. Within the operating range of the system, the net effect of the noise components in this system averages to a negligible value, provided the system is operated

properly. Noise effects in the system (at high sensitivities) will only be noticeable on the phase-sensitive detector null indicator. This random fluctuation of the null indicator has been reduced to the optimum level by presetting the gain of the appropriate amplifier. The useful limit of the system is reached when the noise obscures the signal which produces a distinct null count indication.

4.4 Total System Uncertainty

The accuracy of the composite system can only be determined by adding the uncertainties caused by all possible sources. This is not an easy task since the actual value of each of these separate uncertainties is difficult to express as a fixed number.

All sources of error in this system appear to be negligible compared to the uncertainty contributed by the Device Under Test provided the system Setup and Operation procedure is strictly adhered to. Thus the total systematic error of the system is well within the design goal of $\pm$ 0.005 dB/20 dB. The principal sources of the random errors are the repeatability of the Device Under Test and the effect of the noise on the phase-sensitive null detector.

When fixed attenuators are calibrated with this system, any uncertainties due to such sources as mismatch and phase shift must be accounted for.

Tables 4.2 and 4.3 compare calibration results obtained on the NBS primary standard to those obtained on the system discussed in this report. In table 4.2, the DUT was a NARDA Model 779 10-dB fixed attenuator, S/N 01066. In table 4.3, the DUT was an NBS Model VII attenuator, S/N 3.

Table 4.2. Comparison of calibration results for a NARDA Model 779 10-dB fixed attenuator.

DUT Values Using SQUID System dB	DUT Values Using NBS Primary Standard dB	Difference in Results dB
9.861	9.858	0.003

Actual readings obtained on the SQUID System at NBS are given below.

DUT Position	Variable Attenuator (NBS Model VII, S/N, 3) Settings (at zero Number 2) dB			
out	56.577	56.574	56.576	56.575
in	46.712	46.709	46.709	46.708
	9.865	9.865	9.867	9.867

Uncorrected Mean Value = 9.866 dB.

Correction from figure 3.15 is -0.005 dB.

Thus the Corrected Mean Value = 9.861 dB.

The discrepancy between these two methods of calibration is 0.003 dB, which is within the uncertainty of the SQUID System. The uncertainty on the value measured by the NBS primary standard is much larger than this.

NOTE: Connector repeatability is included in these measurements, but mismatch error has not been calculated separately.

Table 4.3. Comparison of calibration results for variable
attenuator.

(NBS Model VII, S/N 3)

DUT Settings dB	DUT Values Using SQUID System dB	DUT Values Using NBS Primary Standard dB	Differences in Results dB
20-30	10.000	9.996	0.004
30-40	10.001	10.002	0.001
40-50	10.002	9.999	0.003

NOTE: These SQUID System values were obtained from figure 3.18.
The NBS System values were obtained from figure 4.3.

These results (tables 4.2 and 4.3) verify the accuracy of this system
as being well within the accuracy goal of the system over the attenua-
tion range of 20 to 50 dB (50-80 dB of actual attenuation in the
measurement channel which includes the 30 dB minimum insertion loss in
the variable attenuator being calibrated).

Similar results were obtained during many different laboratory
intercomparisons.

This same procedure can be applied to any desired range of values on
the DUT by inserting fixed (or variable) attenuators in series with
the DUT to preset the attenuation value at the first Bessel Function
zero.

U.S. DEPARTMENT OF COMMERCE

NATIONAL BUREAU OF STANDARDS
INSTITUTE FOR BASIC STANDARDS
BOULDER, COLORADO 80301

REPORT OF CALIBRATION

VARIABLE WAVEGUIDE BELOW-CUTOFF ATTENUATOR,
COAXIAL CONNECTORS

NATIONAL BUREAU OF STANDARDS
MODEL VII, SERIAL NO. 3

SUBMITTED BY:

NATIONAL BUREAU OF STANDARDS
ELECTROMAGNETICS DIVISION
CIRCUITS STANDARDS SECTION

THE MEASUREMENTS ON THIS ATTENUATOR WERE PERFORMED UNDER AMBIENT
CONDITIONS OF APPROXIMATELY 23 DEGREES CENTIGRADE AND 40 PERCENT
RELATIVE HUMIDITY. THE POWER PRESENTED TO THE ATTENUATOR WAS LESS
THAN 200 MILLIWATTS. THE ATTENUATOR WAS TERMINATED AT EACH END
IN APPROXIMATELY 50 +J0 OHMS. THE CALIBRATION FREQUENCY OF 30 MHZ
WAS ACCURATE TO ONE PART IN 1,000,000. THE CHANGE IN INSERTION
LOSS WHEN THE COUNTER IS INCREASED FROM A 00000 REFERENCE SETTING
AND THE DIAL IS INCREASED FROM A 0.000 REFERENCE SETTING IS IN-
DICATED IN THE ATTACHED TABLE.

THE INSERTION LOSS OF THIS ATTENUATOR WITH THE COUNTER SET AT 00000
AND THE DIAL SET AT 0.000 IS APPROXIMATELY 30.4 DECIBELS.

Figure 4.3.   Report of calibration on variable attenuator.

VARIABLE WAVEGUIDE BELOW-CUTOFF ATTENUATOR,
COAXIAL CONNECTORS
NATIONAL BUREAU OF STANDARDS
MODEL VII, SERIAL NO. 3

COUNTER SETTING	DIAL SETTING	CHANGE IN INSERTION LOSS	LIMIT OF SYSTEMATIC ERROR	MAXIMUM UNCERTAINTY
		DECIBELS	DECIBELS	DECIBELS
******	******	**************	**********	***********
11011	1.111	0.997	0.006	0.008
11020	1.111	1.994	0.006	0.008
11030	1.111	2.993	0.007	0.009
11040	1.111	3.992	0.007	0.009
11050	1.121	4.991	0.008	0.010
11060	1.111	5.933	0.008	0.010
11071	1.111	6.927	0.009	0.011
11080	1.111	7.976	0.009	0.011
11091	1.111	8.977	0.010	0.012
11140	1.111	9.976	0.010	0.012
11110	1.111	10.974	0.011	0.014
11120	1.111	11.973	0.011	0.014
11130	1.111	12.973	0.012	0.015
11140	1.111	13.933	0.012	0.015
11150	1.111	14.932	0.013	0.016
11161	1.111	15.932	0.013	0.016
11171	1.111	16.932	0.014	0.017
11181	1.111	17.933	0.014	0.017
11191	1.111	18.933	0.015	0.018
11200	1.111	19.933	0.015	0.018
11250	1.111	24.931	0.018	0.021
11300	1.111	29.979	0.020	0.024
11350	1.111	34.932	0.023	0.026
11411	1.111	39.931	0.025	0.029
11450	1.111	44.931	0.028	0.032
11511	1.111	49.930	0.030	0.034
11550	1.111	54.931	0.033	0.037
11510	1.111	59.979	0.035	0.039
11650	1.111	64.973	0.038	0.042
11700	1.111	69.973	0.040	0.045
11750	1.111	74.973	0.043	0.048
11800	1.111	79.971	0.045	0.053

PAGE 2 OF 3
TEST NO.   103306
DATE OF CALIBRATION: AUGUST 23, 1975
REFERENCE: PROJECT NO. 2763446

4-14

BEST AVAILABLE COPY

VARIABLE WAVEGUIDE BELOW-CUTOFF ATTENUATOR,
COAXIAL CONNECTORS
NATIONAL BUREAU OF STANDARDS
MODEL VII, SERIAL NO. 3

THIS CALIBRATION IS VALID ONLY WHEN THE ATTENUATOR IS SET BY
APPROACHING THE INDICATED VALUE FROM A LOWER VALUE OF ATTENUATION.

THREE MEASUREMENTS WERE MADE AT EACH ATTENUATOR SETTING TO FIND THE
MEAN VALUE OF "CHANGE IN INSERTION LOSS" AND TO ESTIMATE THE STAND-
ARD DEVIATION (S.D.) OF THIS MEAN. EXCEPT AS NOTED BELOW, A COM-
BINED ESTIMATE OF S.D. (RMS VALUE OF ALL THE S.D.'S ABOVE) HAS BEEN
ASSIGNED TO EACH MEAN. THE MAXIMUM UNCERTAINTY IS THE SUM OF THE
LIMIT OF SYSTEMATIC ERROR AND THE RANDOM ERROR WHERE THE LATTER IS
DEFINED AS THREE TIMES THE ESTIMATE OF THE S.D. OF THE MEAN.

FOR CONVENIENCE, USUALLY ONE OR MORE INTERMEDIATE REFERENCE SETTINGS
ARE USED DURING CALIBRATION. TO DETERMINE THE ESTIMATE OF STANDARD
DEVIATION OF THE MEAN FOR A SPECIFIC INSERTION LOSS SETTING WHICH
WAS MEASURED WITH RESPECT TO AN INTERMEDIATE SETTING, THE S.D. OF
THE INTERMEDIATE SETTING AND THE S.D. OF THE SPECIFIC SETTING WERE
POOLED (VARIANCES ADDED).

FOR THE DIRECTOR,
THE INSTITUTE FOR BASIC STANDARDS

ROBERT A. KAMPER, ACTING PROGRAM CHIEF
GUIDED WAVE METROLOGY
ELECTROMAGNETICS DIVISION

PAGE 3 OF 3
TEST NO.   100006
DATE OF CALIBRATION: AUGUST 20, 1976
REFERENCE: PROJECT NO. 2763446

5. CONCLUSIONS

This RF Attenuation Measurement System meets the original performance goals. The system has a measurement range of nominally 80 dB including any minimum insertion loss associated with the Device Under Test (DUT). The system is quite accurate for calibrating attenuators over a 50-dB range above their minimum insertion loss.

The optimum use of this system lies in calibrating waveguide below-cutoff attenuators when the best accuracy attainable is desired. Phase shift and mismatch errors may occur when it is used to calibrate fixed resistive attenuators or step resistive attenuators, if a buffer pad is not used at the input (as shown in figure 3.10). A thorough investigation of these errors should be performed before this system is used to calibrate attenuators other than the types discussed in this report.

We have used the SQUID system to calibrate a high quality piston attenuator. Our results consistently show deviations of 0.003 dB (rms) or less. The reproducibility of a given zero of J_0 is 0.001 dB or better for a fixed set of operating parameters. It appears that the deviations are systematic in nature, depending in part on microwave frequency, phase of the mixer reference signal, etc.

We want to emphasize that in utilizing the detailed shape of the interference pattern of the rf-biased SQUID, extreme care must be exercised in both the signal handling and the fabrication of the junction. A close study of eq (2.4) clarifies the nature of a number of possible error-causing interferences. An awareness of these problems provides guidance in the design of the readout system. A study of the equation also shows how one can reduce errors due to harmonic distortion of the interference response. While these error-reducing methods are a necessary part of the system operation, it should be recognized that best results will be obtained when the harmonic distortion of the interference response is minimized. That is, the proper setting of bias levels can only provide a certain reduction in errors due to distortion, and thus such distortions should be minimized. We therefore conclude that the contact parameters are crucial to the concept and that further improvements will require a deeper understanding of the junction operation.

The fact that the junction in our system operates in the nonhysteretic mode means that the SQUID response is derived primarily from a modulation of the phase of the microwave signal. This makes the frequency response of the entire system a rather important part of the detection linearity. Reflections in the microwave components, phase of the double-balanced-mixer reference, and SQUID resonances each contribute to a nonlinear frequency response which in turn affects the linearity of detection. We suggest that this is at least partly responsible for the systematic deviations in our calibration results. We believe that the calibration accuracy of such systems will be improved to better than 0.001 dB when these problems are resolved. One step in this direction would be the use of a cold microwave amplifier in close proximity to the SQUID, which would eliminate the effect of microwave reflections. Another approach might be to operate in the hysteretic mode where the phase modulation is a minimum, and thus reduce the importance of frequency response. To date we have been unsuccessful in this type of operation for reasons which we do not understand.

As a final demonstration of the usefulness and simplicity of the technique, we have turned the system over to a technician who was not at all familiar with the principle of operation. After some coaching in the use of the system, quite satisfactory results were obtained. Our intention is to put this system into routine calibration use and thus gain long term experience in its operation.

This RF Attenuation Measurement System, using a SQUID, was designed and constructed under CCG Project Number 72-72C. The project objectives are successfully met.

6. ACKNOWLEDGMENTS

7. REFERENCES

[1] Kamper, R. A., Simmonds, M. B., Hoer, C. A., and Adair, R. T., Measurement of rf power and attenuation using superconducting quantum interference devices, Nat. Bur. Stand. (U.S.), Tech. Note 643, 12-63 (Aug. 1973).

[2] Kamper, R. A., Simmonds, M. B., Adair, R. T., and Hoer, C. A., Advances in the measurement of rf power and attenuation using SQUIDS, Nat. Bur. Stand. (U.S.), Tech. Note 661, 27 pages (Sept. 1974).

[3] Adair, R. T., Simmonds, M. B., Kamper, R. A., and Hoer, C. A., RF attenuation measurement using quantum interference in superconductors, IEEE Trans. Instrum. Meas., Vol. IM-23, No. 4, 375-381 (Dec. 1974).

[4] Kamper, R. A., Superconducting Devices for Metrology and Standards, Chapter 5 in Superconductor Applications: Squids & Machines (Plenum Publishing Corp., N.Y., N.Y, 1977).

[5] Petley, B. W., Morris, K., Yell, R. W., and Clarke, R. N., Moulded microwave SQUID for rf-attenuator calibration, Electronics Letters, Vol. 12, 237-238 (1976).

[6] Strait, S. F., Development of mechanically stable, thermally cyclicably point contacts for use in superconducting devices, Report #1636, Cornell Materials Science Center, Ithaca, New York (1971).

[7] Simmonds, M. B., private communication (unpublished).

[8] Zimmerman, J. E., Thiene, P., and Harding, J. T., Design and operation of stable rf-biased superconducting point-contact quantum devices, J. Appl. Phys, Vol. 41, 1572-1580 (1970).

[9] Silver, A. H. and Zimmerman, J. E., Quantum states and transitions in weakly connected superconducting rings, Phys. Rev., Vol. 157, No. 2, 317 (1967).

[10] Sullivan, D. B., Superconducting quantum interference devices: An operational guide for rf-biased systems, Nat. Bur. Stand. (U.S.), Tech. Note 629, 3-10 (Nov. 1972).

[11] Abramowitz, M. and Stegun I. A., Handbook of mathematical functions, Nat. Bur. Stand. (U.S.), Applied Math Series 55, 409 (June 1964).

[12] IEEE Standard Dictionary of Electrical and Electronics Terms, IEEE STD 100-1972 (Wiley and Sons, N.Y., N.Y., 1972).

8. COMPONENT INFORMATION

The components listed in tables 8.1 through 8.6 are the major electrical and mechanical components used in this RF Attenuation Measurement System.

Commonly available stock items such as connectors, switches, interconnecting cables, and miscellaneous hardware are not listed in detail. Critical items are detailed on the appropriate circuit diagrams.

Table 8.1. Components contained in SQUID readout unit mainframe.

Component	Description	Quantity
Mainframe	AMCO Engineering Co. APDM 14-WA-C-H	1
Oscilloscope	HP Model 1200B	1
Digital Counter	HP Model 5301A	1
Readout Unit	NBS Model 3	1

Table 8.2. Cryogenic Components.

Component	Description	Quantity
Helium Dewar (30 litre)	Minnesota Valley Engineering Model USHE-30A	1
SQUID	NBS Model CTG-30 See Appendix B Figures 10(b),(c), & (d)	1
Dip Tube	NBS Model 3 See Appendix B Figure 10(o)	1

Table 8.3. Major Components in SQUID readout unit.

Component	Description	Quantity
Mainframe with ±15V dc, 1A Power Supply	Burr-Brown Model 506/16A	1
Plug-In Module Hardware & Connectors	Burr-Brown Model/16	6
RF Source Plug-In	NBS (See Table 8.4)	1
Power Supply ±15V dc, 90 mA	Lambda LZD-22	1
Power Supply ±15V dc, 150 mA	Lambda LZD-23	1
Coaxial Switch	HP 8761A with SMA Connectors	1
Termination	SMA 50 ohm	1
Null Indicator (100-0-100 μA)	API Instruments Co. Model 447-101R3	1
Phase Sensitive Detector Circuits	See Appendix B Figures 10(e) and (j)	-

Table 8.4. Components in rf source plug-in.

Component	Description	Quantity
Amplifier	Greenray Industries, Model X-133A	1
Attenuator	3 dB, 2 watts, Narda, Model 4778-3	1
Capacitive Termination and RF Output Level Control	Variable Piston Capacitor Johanson Type JMC 190C 0.7 - 30 pF	2
180° Hybrid Junction	Merrimac Model CHTM-30/13291	1
Signal Source	CTS Knights, Inc. Model VCXO Part No. 970-3367-0	1
Termination	SMA 50 ohm	1
Assorted Cables	Appropriate Lengths of 0.358 cm diameter semi-rigid cable with SMA Connectors on Each End	4
Assorted Connectors and Adapters	SMA as Required	

Table 8.5. Major components in SQUID control unit.

Component	Description	Quantity
Master Circuit Board	DC & 1 kHz Bias Circuits See Figures 3.7 and 10 (e)	1
DC Bias Voltage Reference Circuit Board	Ultra Stable DC Bias Supply, See Figure 10 (g)	1
1 GHz Oscillator & Voltage Variable Attenuator	AVANTEC VTO 8090 AVANTEC UTF 015 AVANTEC CASE TC2M	1 1 1
1 GHz Amplifier 40 dB Gain	AVANTEC UTO 1011 (12 dB Gain) AVANTEC UTO 1521 (28 dB Gain) AVANTEC CASE UCS2M	1 1 1
1 GHz Amplifier 10 dB Gain	AVANTEC UTO 1511 (10 dB Gain) AVANTEC CASE USCIM	1 1
1 GHz Oscillator Output Attenuator	Midwest Microwave Model 205-60 dB	1
1 GHz OSC REF Output Attenuator	Midwest Microwave Model 205-3 dB	1
Directional Coupler 1 GHz, 20 dB	OMNI Spectra Model 20063-20	1
RF Detector	Merrimac Double Balanced Mixer Model DMM-2-500	1
1 GHz Phase Shifter	Merrimac Model PSM-2/22401	1
Coaxial Low Pass Filter	NBS Fabricated See Appendix B, Figure 10(n)	2
SMA Tee	OMNI Spectra Model 20200-2	1
SMA Adapters	SMA Double Male SMA Elbow	3 2
Coaxial Cables	Semirigid With SMA Connectors (Length As Necessary)	4

Table 8.6. List of suggested external coaxial cables & adapters.

Component	Description	Quantity
RF Cable (CBL-1)	1.5 Meters RG-9B/U With Male Precision Type N Connector on Each End (Input to DUT)	1
RF Cable (CBL-2)	2 Meters RG-9B/U With Male Precision Type N Connector on Each End (From DUT to SQUID RF Port)	1
Microwave Cable (CBL-3)	8 Centimeters 0.358 cm diameter Semirigid Coax With a Male SMA Connector on Each End	1
DC Power & AC Signal Cable (CBL-4)	See Appendix B Figures 10(k) and (q)	1
Digital Counter Input Cable (CBL-5)	0.5 Meter RG-55/U With a BNC Male Connector on Each End	1
Oscilloscope Vertical Input Cable (CBL-6)	2 Meters RG-55/U With a BNC Male Connector on One End & Rear Panel Input Connector Supplied With Oscilloscope on One End	1
Oscilloscope Sync Signal Cable (CBL-7)	2 Meters RG-55/U With a BNC Male Connector on Each End	1
Assorted Adapters	Precision 14 mm to Precision Type N Male	1
	Precision 14 mm to Precision Type N Female	1
	Precision 7 mm to Precision Type N Male	1
	Precision 7 mm to Precision Type N Female	1
	Other Adapters As Appropriate For Calibrating Various Devices Under Test	--

9. APPENDIX A

FREQUENCY SPECTRUM FROM THE SQUID

The SQUID response given by eq. (2.8) (including harmonic distortion) is

$$V(\phi) = \sum_{n=1}^{\infty} V_n \cos(2\pi n\phi/\phi_o) \quad . \tag{9.1}$$

The flux applied to the SQUID consists of a signal at ω_m, a low frequency bias at ω_d, and a dc bias, the sum of which is

$$\phi = \phi_m \sin(\omega_m t) + \phi_d \sin(\omega_d t) + \phi_b \quad . \tag{9.2}$$

Using notation introduced in section 2, the argument in eq. (9.1) is written

$$n \frac{2\pi\phi}{\phi_o} = n\left(\frac{2\pi\phi_m}{\phi_o} \sin(\omega_m t) + \frac{2\pi\phi_d}{\phi_o} \sin(\omega_d t) + \frac{2\pi\phi_b}{\phi_o}\right)$$

$$= nM \sin(\omega_m t) + nD \sin(\omega_d t) + nB \quad . \tag{9.3}$$

To simplify notation let $M\sin(\omega_m t) = m$ and $D\sin(\omega_d t) = d$. Expansion of the cos term in eq. (9.1) then gives

$$\cos(nm+nd+nB) = \cos(nB)[\cos(nm)\cos(nd) - \sin(nm)\sin(nd)]$$
$$- \sin(nB)[\sin(nm)\cos(nd) + \cos(nm)\sin(nd)] \quad . \tag{9.4}$$

The following Bessel function identities are required to complete the derivation.

$$\cos(Z \sin \theta) = J_0(Z) + 2 \sum_{k=1}^{\infty} J_{2k}(Z)\cos(2k\theta)$$

$$\sin(Z \sin \theta) = 2 \sum_{k=0}^{\infty} J_{2k+1}(Z)\sin(2k+1)\theta \quad . \tag{9.5}$$

Note that, if m and d are replaced by their sinusoidal values, all 8 terms in the brackets in eq. (9.4) have the form of the identities in eq. (9.5). Eq. (9.4) thus becomes

$$V = \sum_{n=1}^{\infty} V_n\left\{\cos(nB)[J_0(nM) + 2\sum_{k=1}^{\infty} J_{2k}(nM)\cos(2k\omega_m t)][J_o(nD) + 2\sum_{j=1}^{\infty} J_{2j}(nD)\cos(2j\omega_d t)]\right\}$$

$$- \sum_{n=1}^{\infty} V_n\left\{\sin(nB)[J_0(nM) + 2\sum_{k=1}^{\infty} J_{2k}(nM)\cos(2k\omega_m t)][2\sum_{j=0}^{\infty} J_{2j+1}(nD)\sin(2j+1)\omega_d t]\right\}$$

$$- \sum_{n=1}^{\infty} V_n\left\{\sin(nB)[2\sum_{k=0}^{\infty} J_{2k+1}(nM)\sin(2k+1)\omega_m t][J_o(nD) + 2\sum_{j=1}^{\infty} J_{2j}(nD)\cos(2j\omega_d t)]\right\}$$

$$- \sum_{n=1}^{\infty} V_n\left\{\cos(nB)[2\sum_{k=0}^{\infty} J_{2k+1}(nM)\sin(2k+1)\omega_m t][2\sum_{j=0}^{\infty} J_{2j+1}(nD)\sin(2j+1)\omega_d t]\right\} \quad . \tag{9.6}$$

10. APPENDIX B
CIRCUIT DIAGRAMS AND COMPONENT DETAILS

A detailed, itemized list of parts is not included in this document since its primary use is to aid in the operation and maintenance of the system. The critical parts necessary for the fabrication of this system are listed on the drawings in figures 10(a) through 10(q). Non-critical common stock items, such as machine screws, are not listed here.
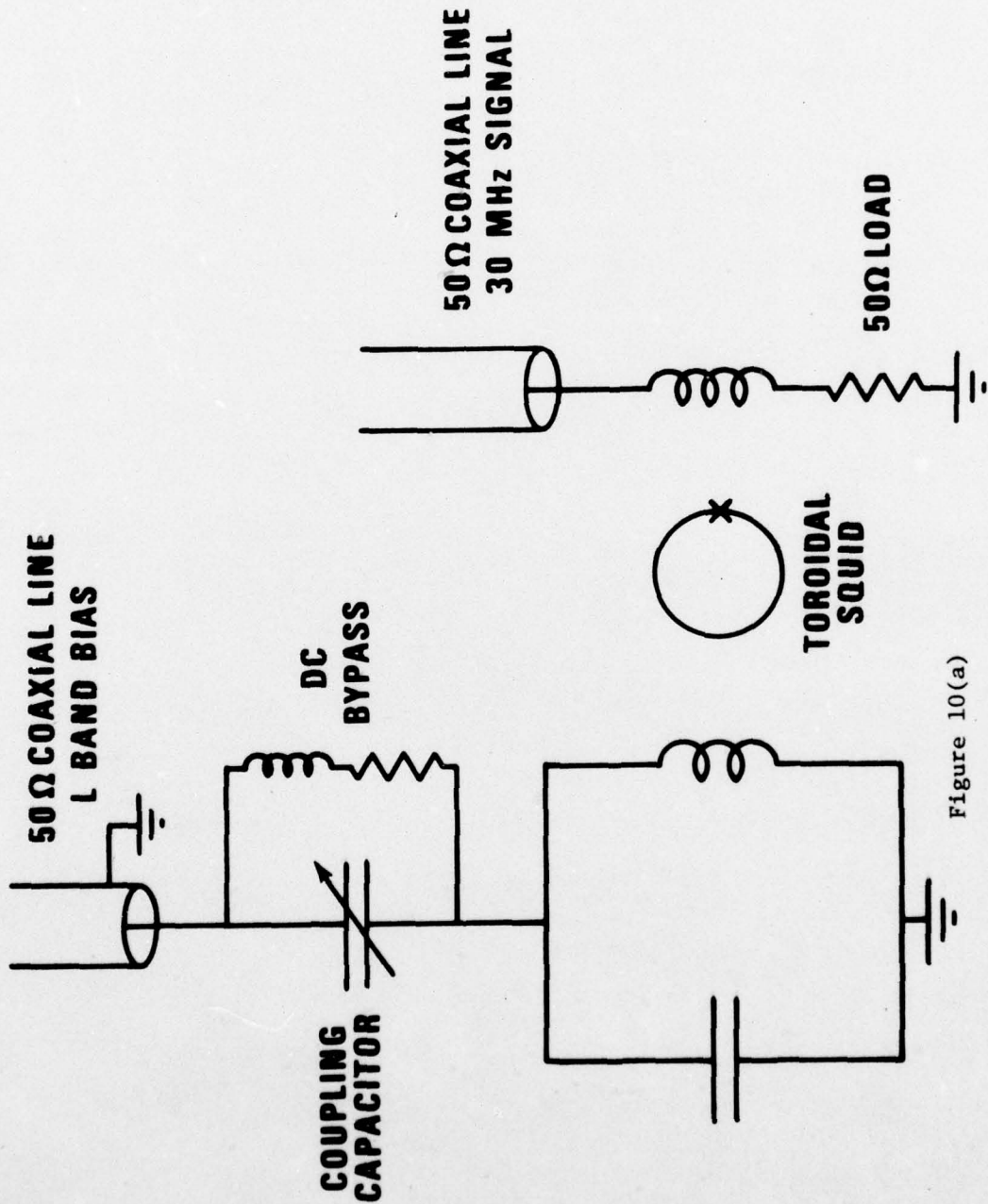
50 Ω COAXIAL LINE
30 MHz SIGNAL

50 Ω LOAD

50 Ω COAXIAL LINE
L BAND BIAS

DC
BYPASS

TOROIDAL
SQUID

COUPLING
CAPACITOR

Figure 10(a)

SCHEMATIC DIAGRAM OF MICROWAVE BIASED SQUID
NBS MODEL CTG-30
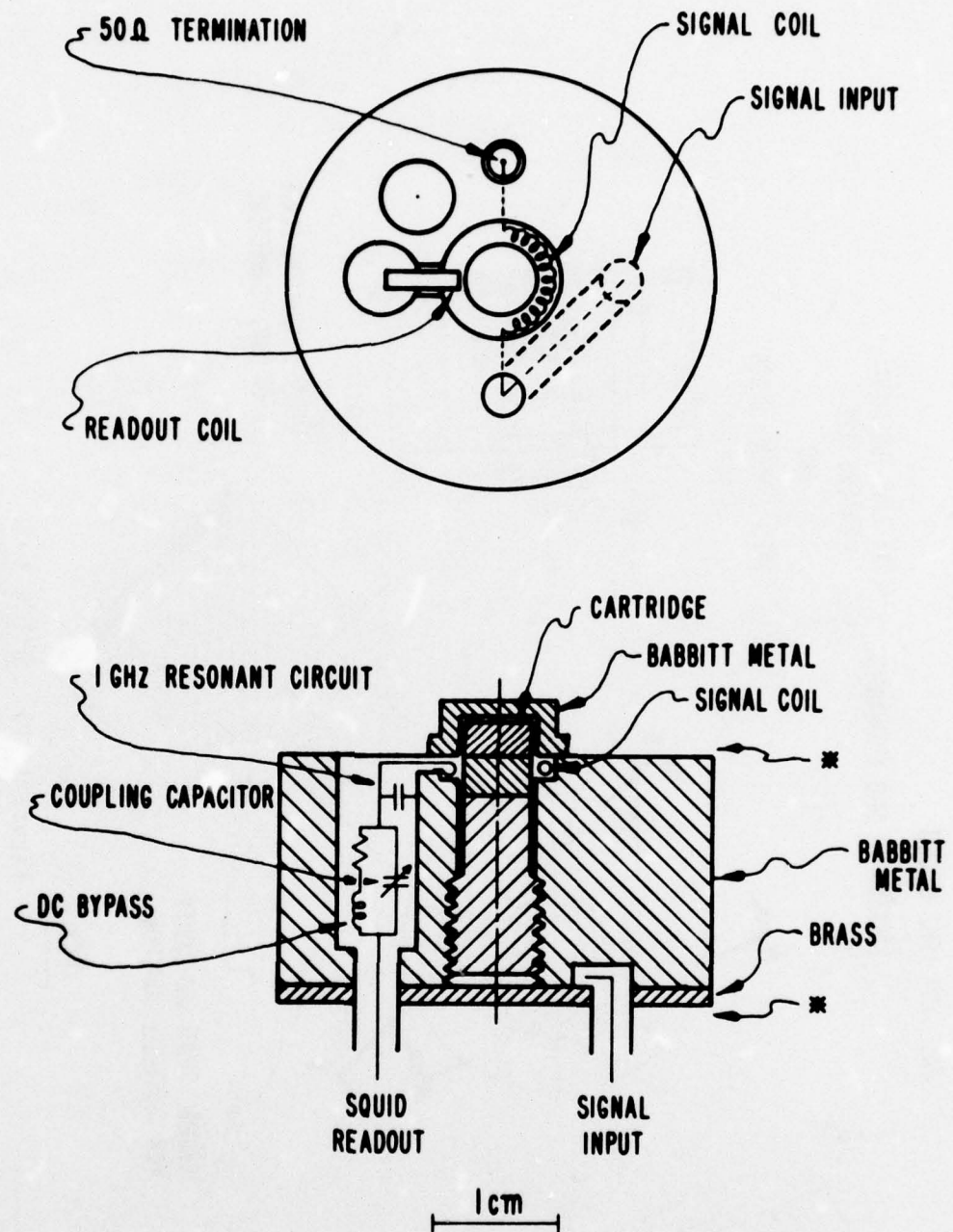
Figure 10(b)

DIAGRAM OF MICROWAVE BIASED SQUID NBS
MODEL CTG-30 WITH PERMANENT POINT CONTACT
CARTRIDGE

✹ NOTE:
NOT SHOWN ARE CAPS OVER BOTH ENDS WHICH SERVE TO SEAL THE SYSTEM
AGAINST MAGNETIC FLUX LEAKAGE

10-3

SPACE FOR 1 GHz CIRCUIT

LOCATION OF 50Ω TERMINATION

COAX LINE FOR SIGNAL
ENTERS HERE
AND
COMES THROUGH BLOCK
HERE

BRASS MOUNTING PLATE
FOR SMA CONNECTORS

TOROIDAL SQUID AND CAVITY
FOR CARTRIDGE JUNCTION

SECTION A–A

SECTION B–B

1 cm
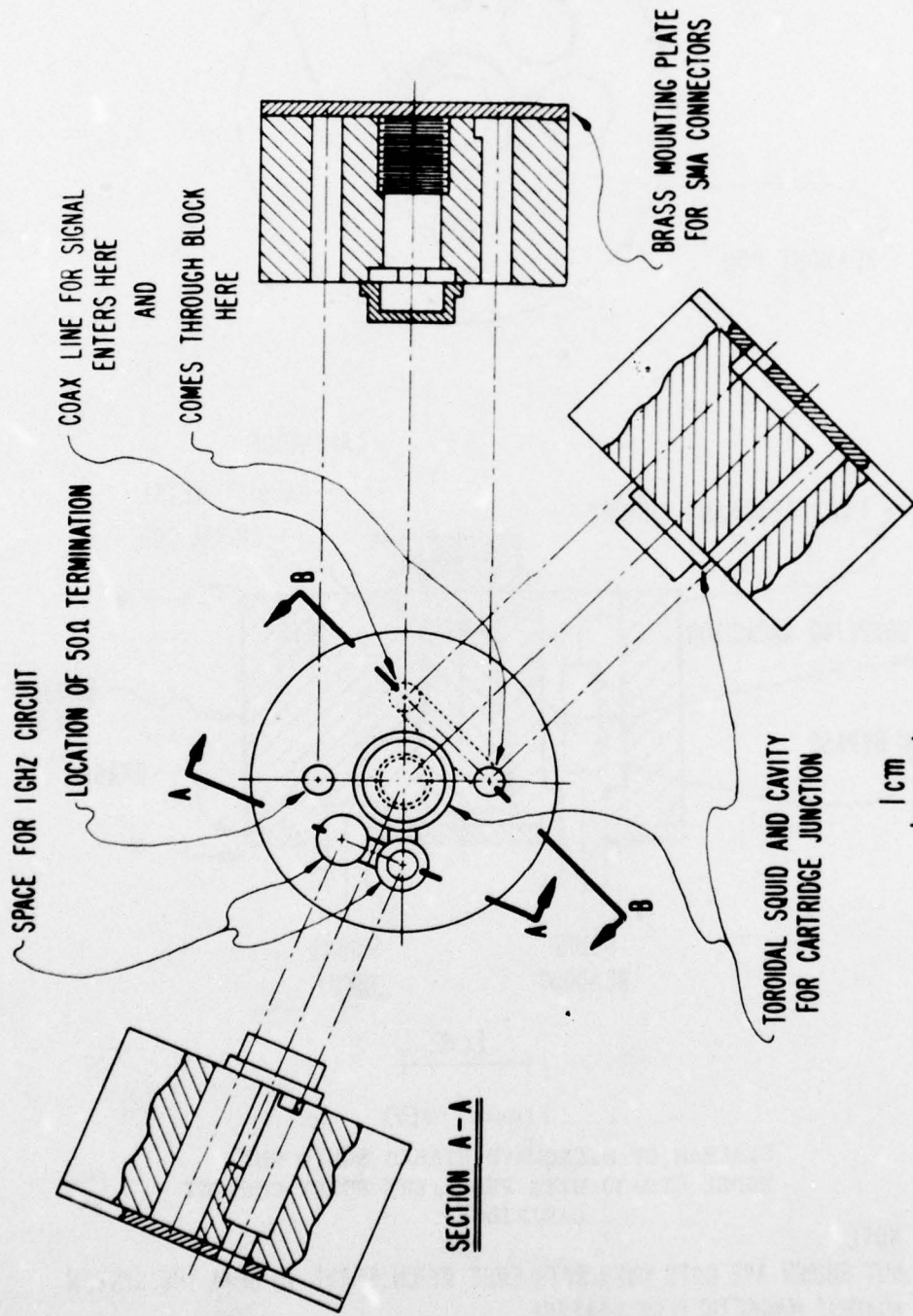
Figure 10(c)

DETAILS OF 1 GHz BIASED SQUID BODY
(CONNECTOR AND COAXIAL COUPLING LINE DETAILS NOT SHOWN)

Cartridge with Permanent Point Contact

Retaining Nut

Niobium Body

Epoxy on Tip

50μm Borosilicate Glass
Spacer - Fused

0.8mm UNM Niobium Screw
(oxidized)

5 mm
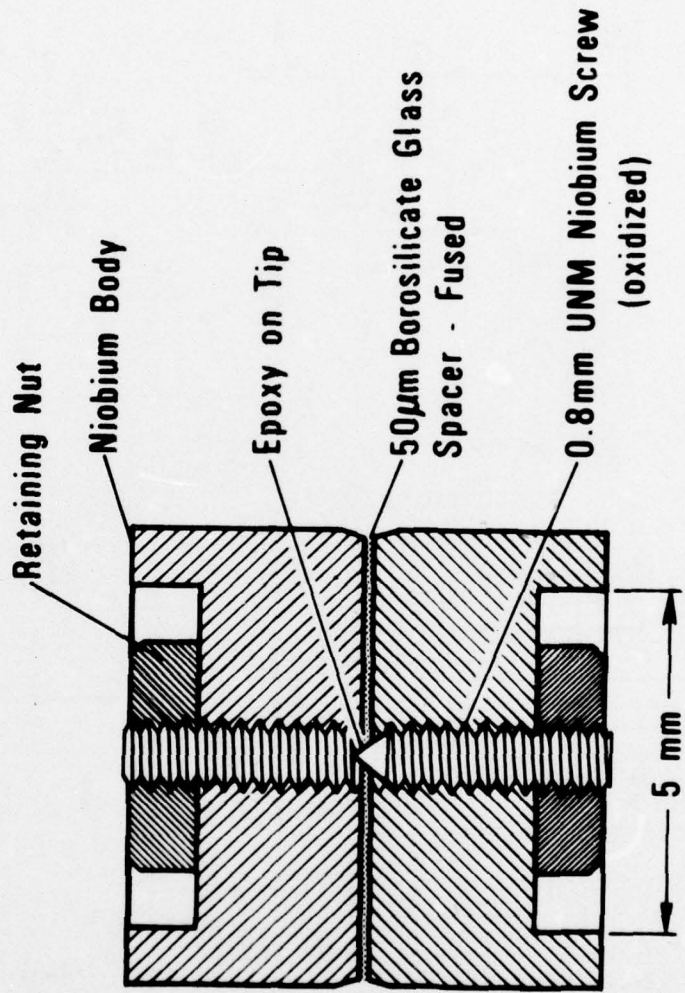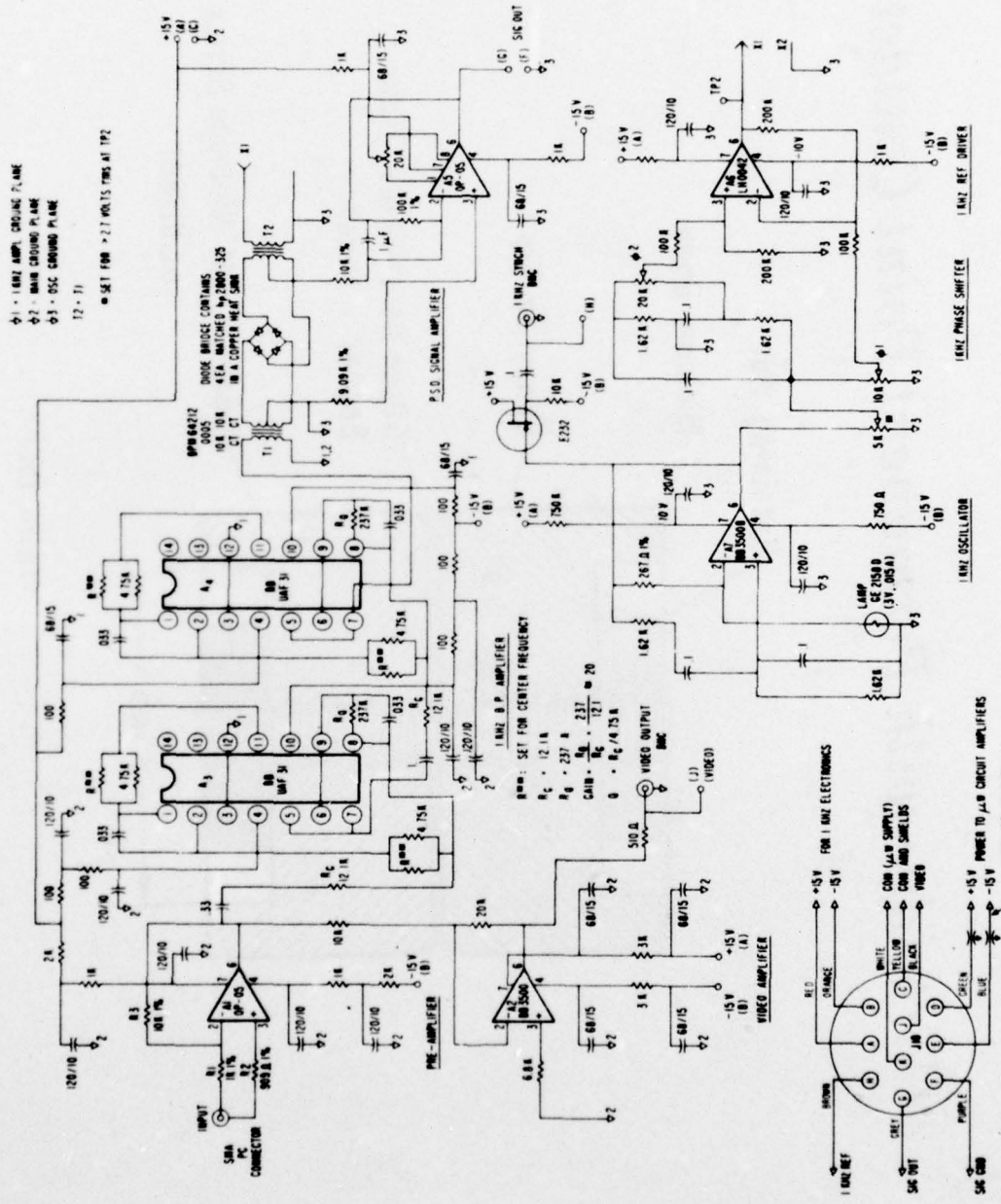
Figure 10(d)

Figure 10(e)

SQUID ATTENUATION MEASUREMENT SYSTEM 1 KHZ CIRCUITS
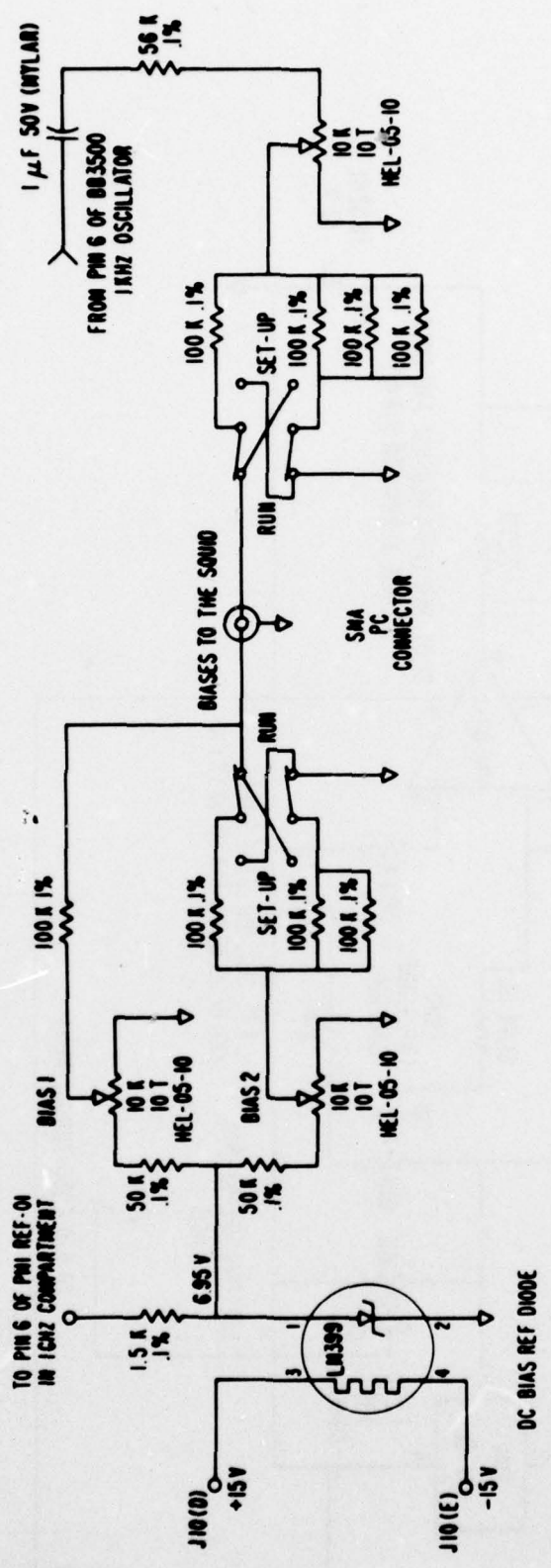
DC AND 1KHz SET-UP CONTROLS
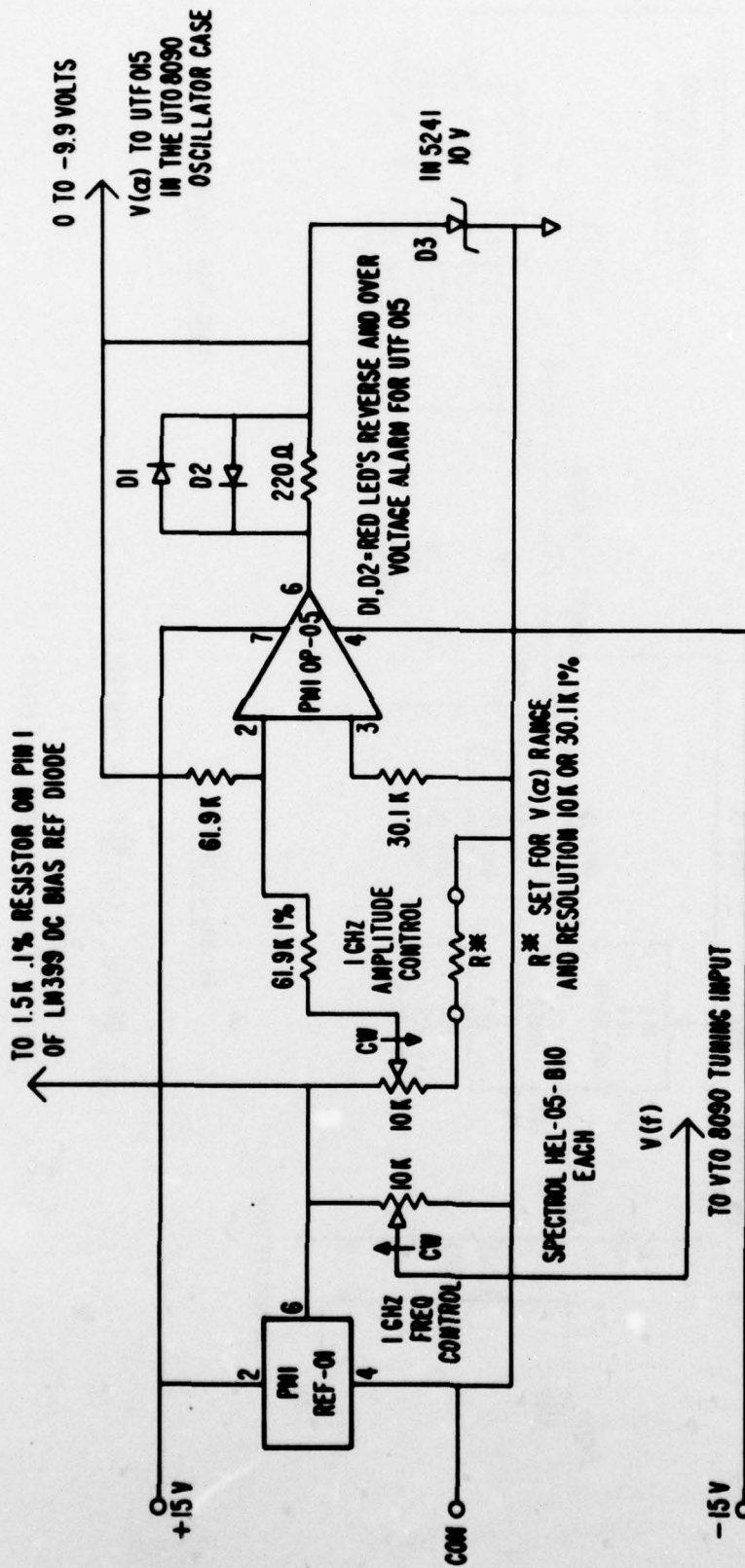
Figure 10(f)

VOLTAGE SOURCE FOR THE VTO 8090 1GHZ OSCILLATOR
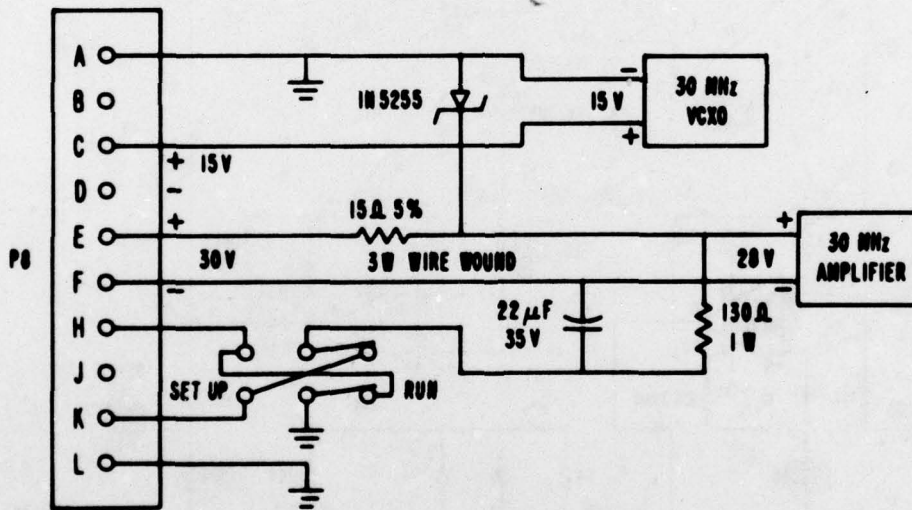AND FOR THE UTF 045 1GHZ ATTENUATOR IN THE VTO 8090 CASE
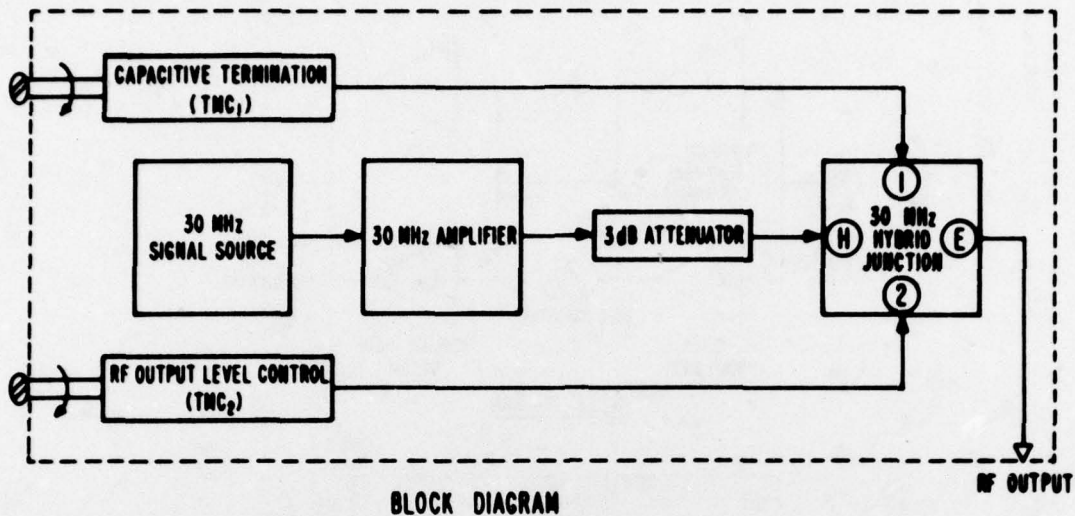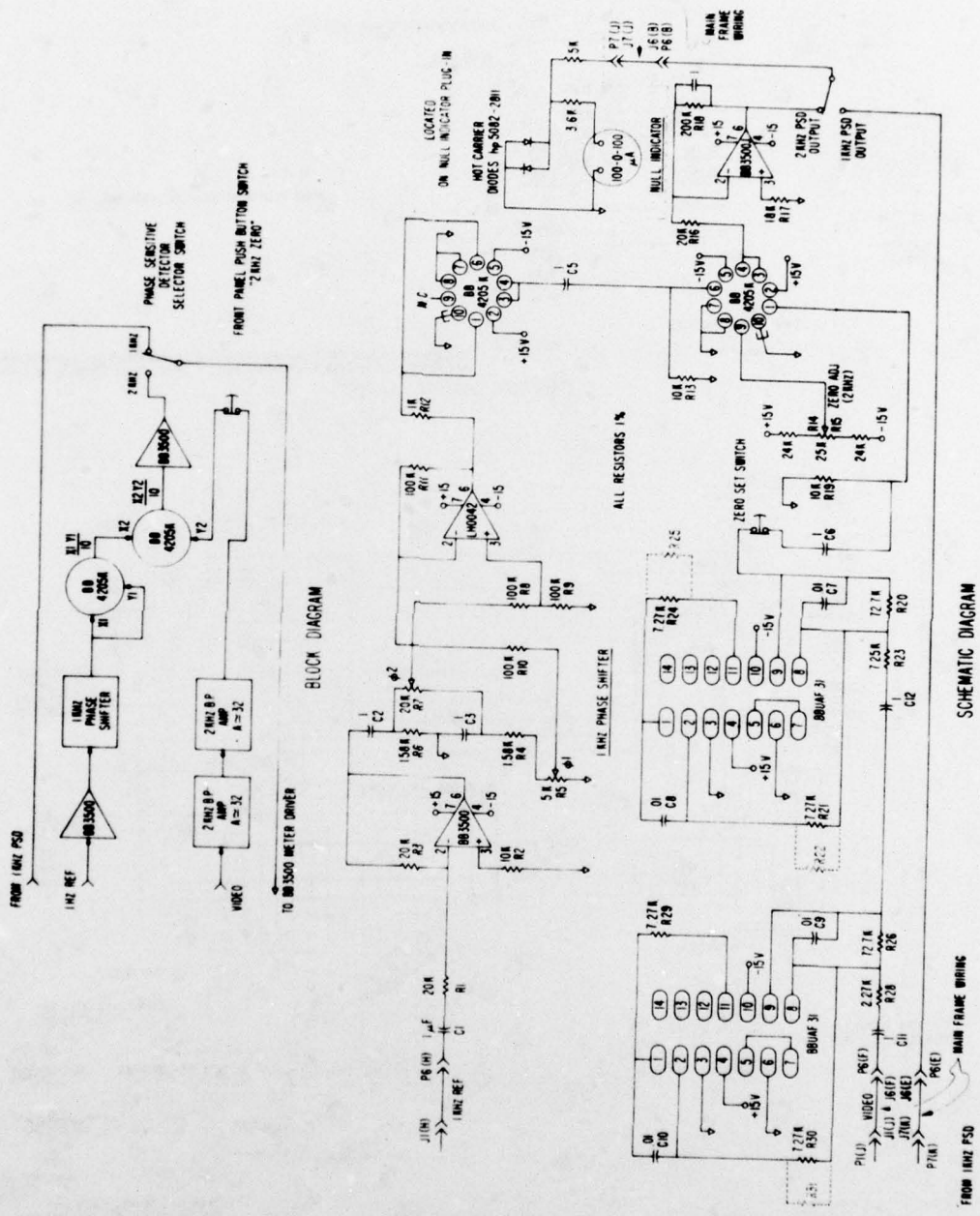
Figure 10(g)

77K2612

10-8
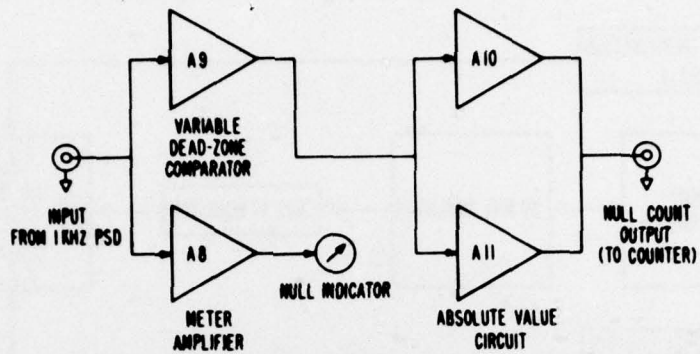
BLOCK DIAGRAM
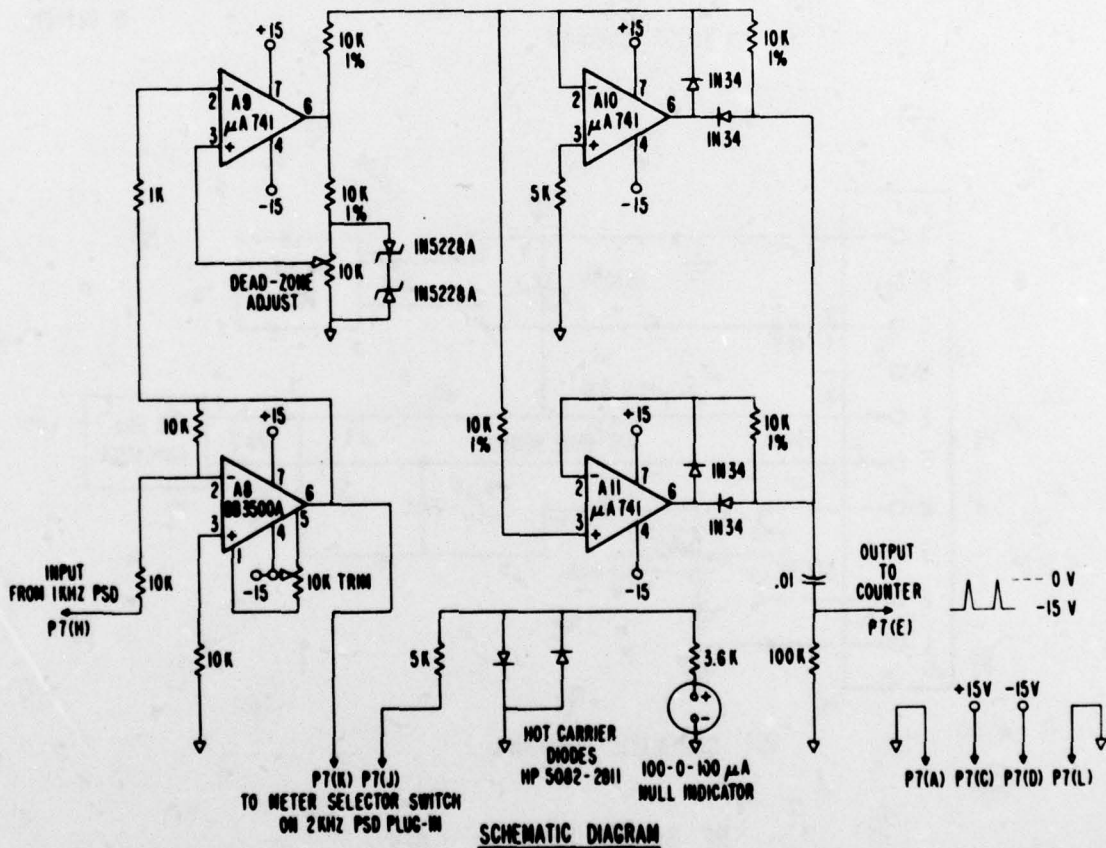
SCHEMATIC DIAGRAM

NULL INDICATOR AND NULL COUNTING TRIGGER CIRCUITS (CONTAINED IN NULL INDICATOR PLUG-IN)

Figure 10(h)

10-9

BLOCK DIAGRAM

SCHEMATIC DIAGRAM

RF SOURCE PLUG-IN

Figure 10(i)

BLOCK DIAGRAM

SCHEMATIC DIAGRAM

2 KHz BAND-PASS AMPLIFIER (BW=200 Hz) AND PHASE SENSITIVE DETECTOR

Figure 10(j)

10-11

AXIS OF SYMMETRY FOR BOTH CABLE ENDS

OUTER BRAID

BENDIX PYGMY CONNECTOR
12-10P
REAR VIEW
(FEMALE)

BENDIX PYGMY CONNECTOR
12-10P
FEMALE TYPE

P1

BENDIX PYGMY 12-10P MALE TYPE CONNECTOR THIS END OF CABLE

DC POWER AND AC SIGNAL CABLE CONTAINS 4(FOUR) RC-174 COAX CABLES AND 6(SIX) #26 STRANDED
HOOK-UP WIRES ALL WITH PVC INSULATION ALL WITHIN A SHIELD. CABLE LENGTH TO BE 5 METERS

DC POWER AND AC SIGNAL CABLE DIAGRAM

SQUID READOUT UNIT MAIN FRAME WIRING DIAGRAM

Figure 10(k)

10-12

SCHEMATIC DIAGRAM

SMA BULKHEAD FEEDTHROUGH CONNECTOR
OSM TYPE 212

VARIABLE PISTON CAPACITOR
JOHANSON .7-30 $\mu\mu$F

3cm LENGTH
OF
No. 22 STRANDED HOOK-UP WIRE

ASSEMBLY OF COMPONENTS

36.69 mm (1.562")

13.72 mm (.540") DIA
12.7 mm (.500") DIA
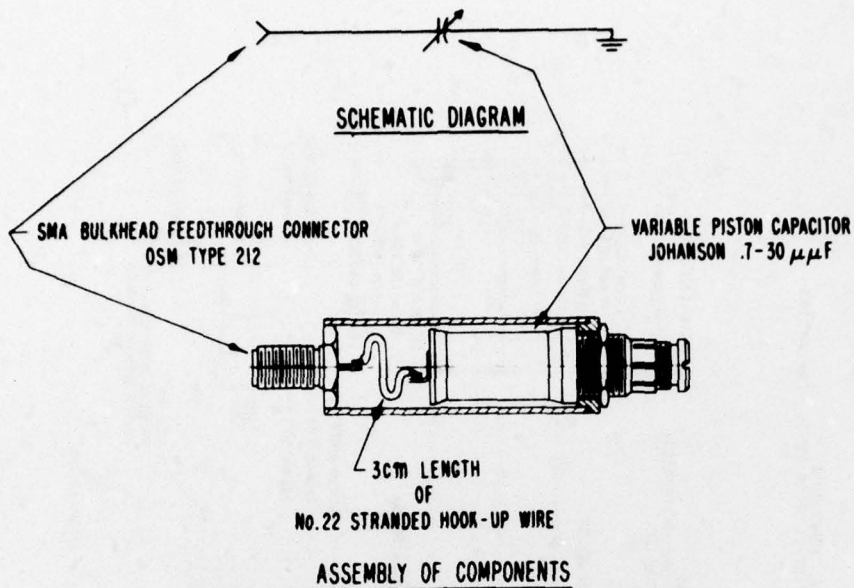
3.17 mm (.125")

1.59 mm (.062")

13.72 mm (.540") DIA
12.7 mm (.500") DIA

9.91 mm (.390") DIA

NOTES

A) ALL DIMENSIONS IN MILLIMETERS - DIMS. IN BRACKETS DENOTE EQUIVALENT VALUES IN INCHES

B) 12.7 mm (.500") D. IN BOTH COMPONENTS IS NOMINAL — ASSURE APPROX. 0.05 mm (.002") CLEARANCE TO ALLOW CAPILLARY FLOW OF SOLDER (USE LOW MELTING POINT SOLDER)

C) FABRICATE COMPONENTS SHOWN IN DETAIL FROM BRASS

D) INSTALL CONNECTOR IN ONE END OF TUBING AS SHOWN ON ASSEMBLY DRAWING AND SOLDER IN PLACE USING LOW MELTING POINT SOLDER — FILL ALSO GAPS BETWEEN INNER SURFACE OF TUBE AND SIDES OF HEXAGONAL NUT OF CONNECTOR

DETAILS OF COMPONENTS TO BE FABRICATED

CAPACITIVE TERMINATION TMC$_1$
FOR USE ON PORT 1 OF 180° HYBRID JUNCTION
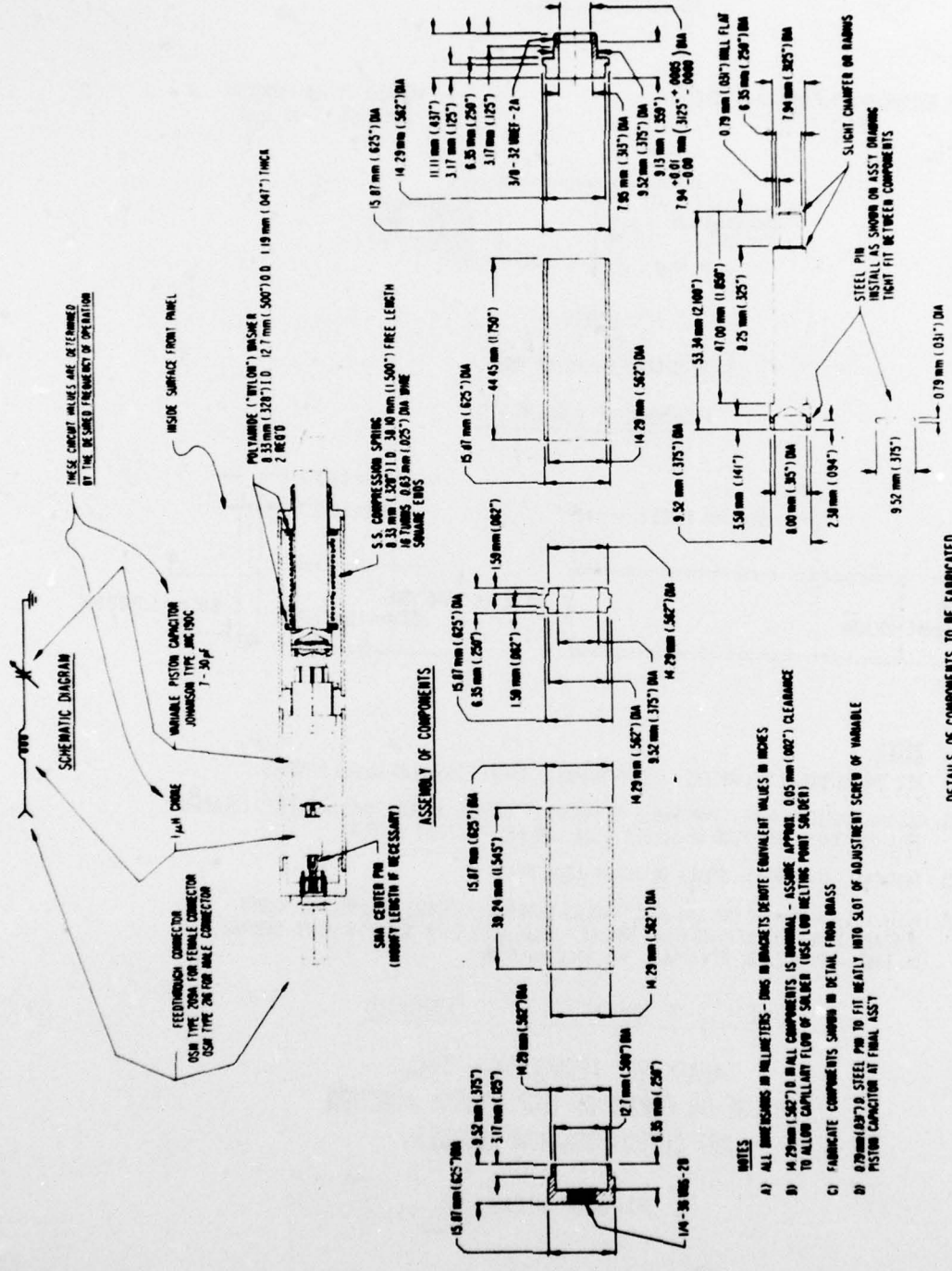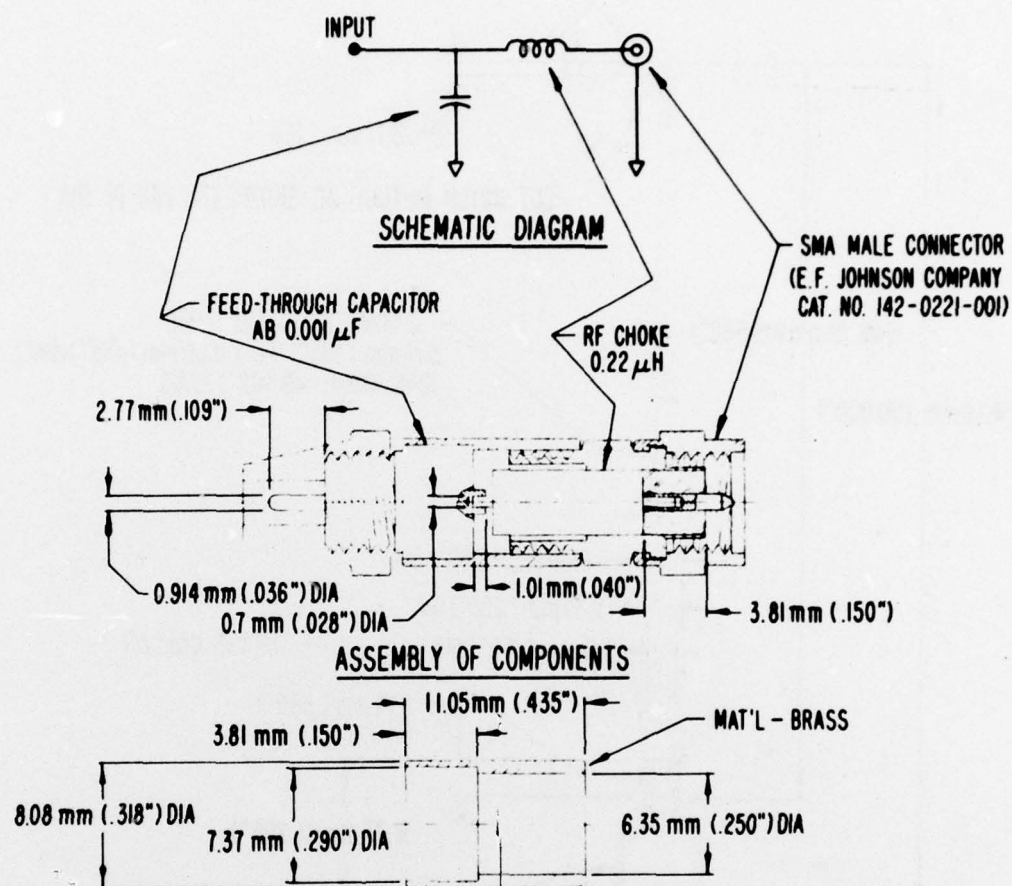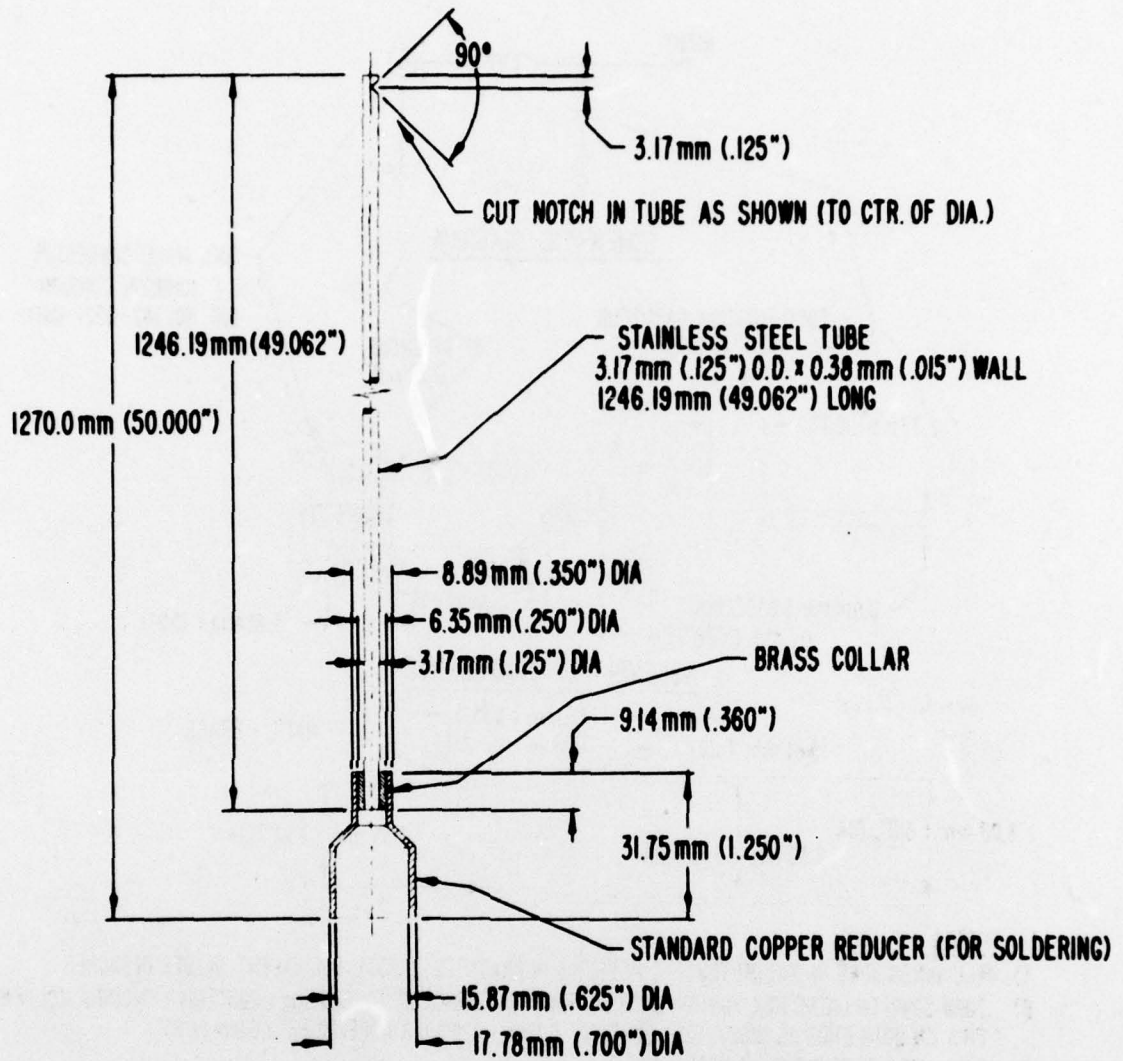(RF OUTPUT MINIMUM ADJUST)

Figure 10(1)

77 E 3079

DETAILS OF COMPONENTS TO BE FABRICATED
SERIES RESONANT CIRCUIT
(RF OUTPUT LEVEL CONTROL TMC$_2$)

Figure 10(m)

INPUT

SCHEMATIC DIAGRAM

FEED-THROUGH CAPACITOR
AB 0.001 μF

RF CHOKE
0.22 μH

SMA MALE CONNECTOR
(E.F. JOHNSON COMPANY
CAT. NO. 142-0221-001)

2.77 mm (.109")

0.914 mm (.036") DIA

0.7 mm (.028") DIA

1.01 mm (.040")

3.81 mm (.150")

ASSEMBLY OF COMPONENTS

11.05mm (.435")

3.81 mm (.150")

MAT'L – BRASS

8.08 mm (.318") DIA

7.37 mm (.290") DIA

6.35 mm (.250") DIA

NOTES

A) ALL DIMENSIONS IN MILLIMETERS – DIMENSIONS IN BRACKETS DENOTE EQUIVALENT VALUES IN INCHES

B) TURN DOWN ON LATHE HEX. PORTION OF FEED-THROUGH CAPACITOR TO 7.25 mm (.285") DIA ; MODIFY SOLDERING
PINS ON BOTH ENDS AS INDICATED – DEPTH OF 0.7 mm (.028") DIA HOLE TO BE 1.6 mm (.063")

C) TRIM WIRES OF RF CHOKE AS NECESSARY

D) MODIFY LENGTH OF DIELECTRIC IN SMA CONNECTOR TO NOTED LENGTH – CUT ALSO LENGTH OF CTR. PIN TO CORRECT
CORRESPONDING LENGTH ; HOLE IN CTR. PIN TO BE 0.7 mm (.028") DIA x 2.5 mm (.098") DEEP

E) SOLDER ALL COMPONENTS USING LOW MELTING POINT SOLDER

LOW PASS FILTER

Figure 10(n)

DIP TUBE

FOR DETERMINATION OF LIQUID HELIUM LEVEL IN STORAGE DEWAR

Figure 10(o)
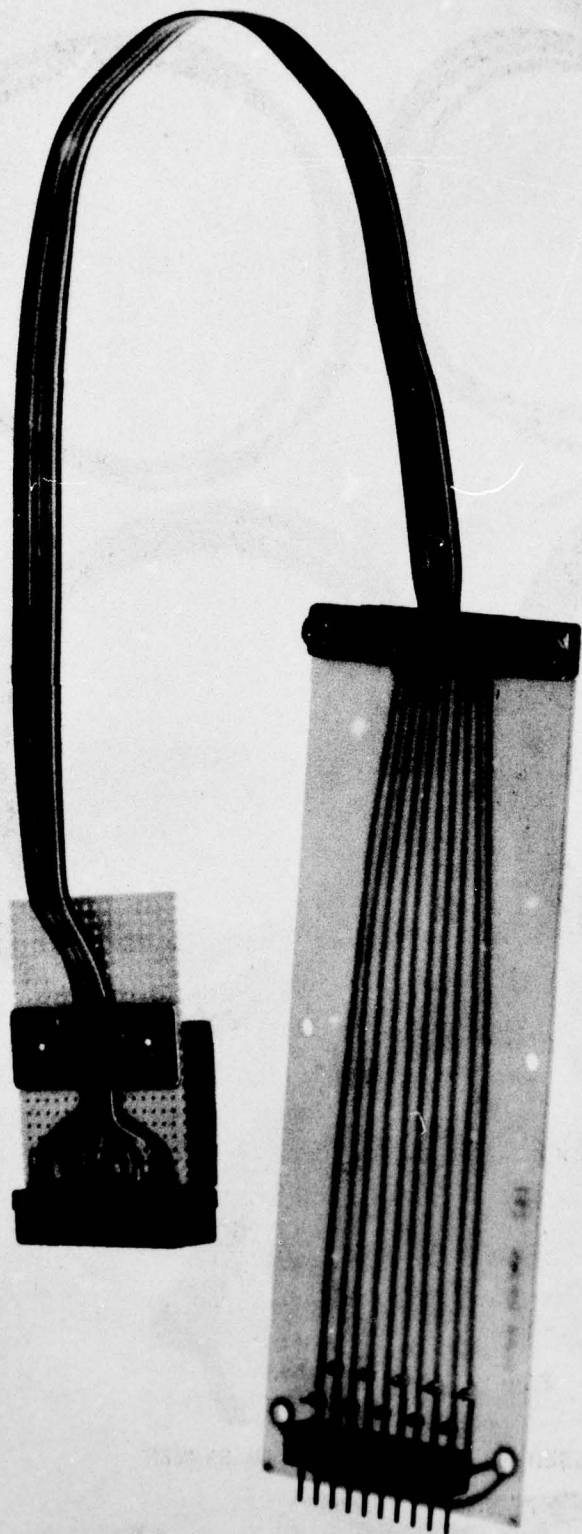
Figure 10(p)

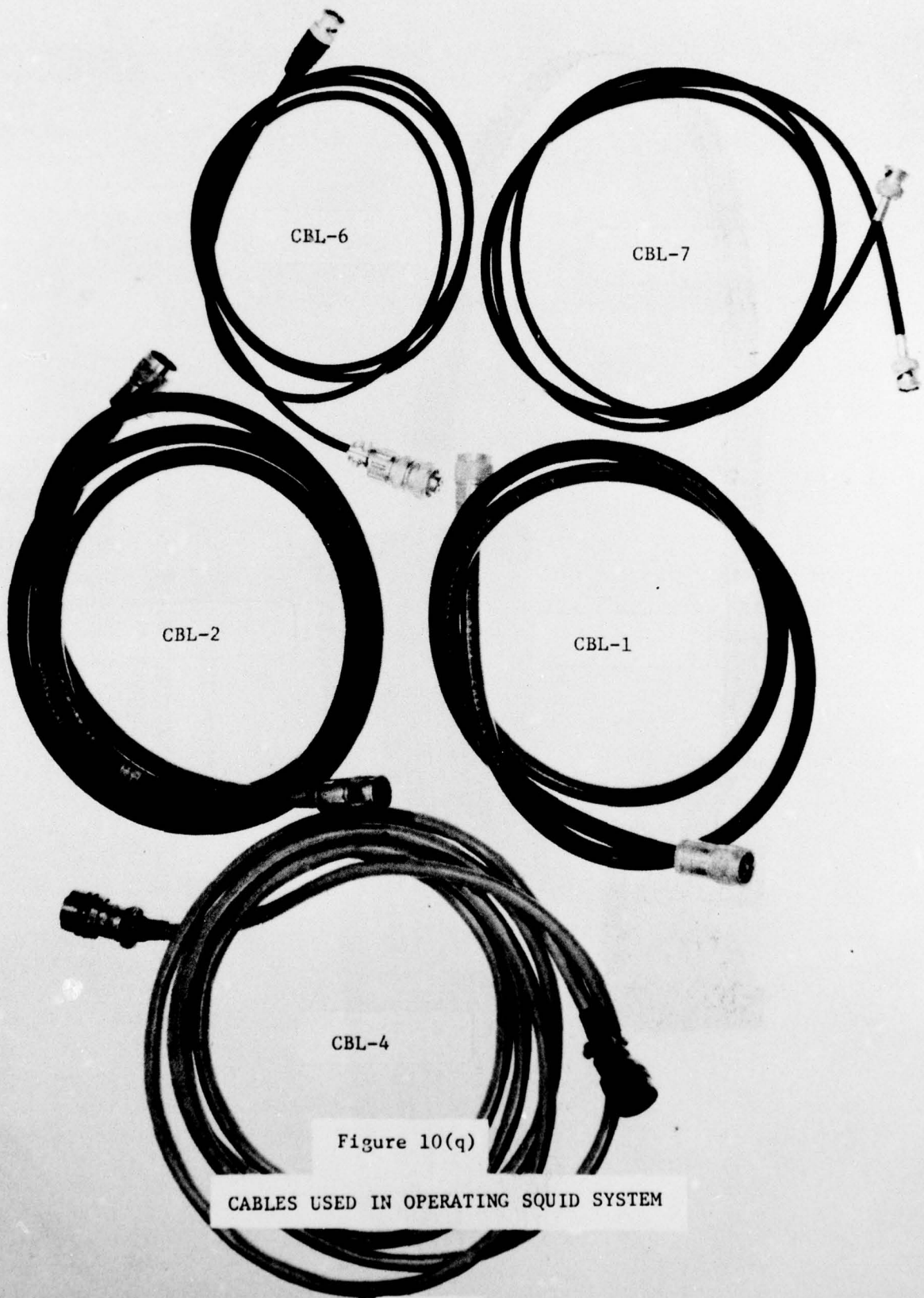PATCH CABLE FOR CONNECTING PLUG-INS TO MAINFRAME
FOR TROUBLESHOOTING

CBL-6

CBL-7

CBL-2

CBL-1

CBL-4

Figure 10(q)

CABLES USED IN OPERATING SQUID SYSTEM

11. APPENDIX C
SYSTEM OPERATION AT OTHER FREQUENCIES

This SQUID Attenuation Measurement System can be used quite satisfactorily at any frequency from 10 KHz to 100 MHz. A good quality signal source must be substituted for the 30 MHz signal source contained in the system. The signal source to be used must have good amplitude stability and must be used with a good quality low pass filter on its output.

Any harmonic of the measuring signal frequency which is allowed to reach the SQUID will cause a SQUID response which is not ideal and this will produce erroneous measurement results. A detailed discussion of these effects appears in Section 2.3.

The total system accuracy and precision should not be significantly affected by operating at other frequencies provided the above procedure is followed.

Procedure for Substitution of an Alternate Frequency Source

1.   Switch the 30 MHz Setup-Run switch to Setup. (This connects a 50 ohm load to the output of the 30 MHz source.)

2.   Disconnect the RG9B/u cable from the "rf output" jack J4.

3.   Perform the system setup procedure as presented in Section 3.5.

4.   Attach the appropriate low pass filter to the alternate frequency signal source output.

5.   Adjust the signal level to 300 milliwatts (nominally) at the filter output.

6.   Connect the RG9B/u cable (removed from J4) to the filter output.

7.   Proceed with the attenuation measurement as outlined for 30 MHz in Section 3.6.

Caution: The rf signal source should not be connected to the SQUID during the setup procedure. Improper setup conditions can result and this will cause incorrect attenuation measurement results.

NBS-114A (REV. 7-73)

U.S. DEPT. OF COMM. BIBLIOGRAPHIC DATA SHEET	1. PUBLICATION OR REPORT NO. NBSIR 77-863	2. Gov't Accession No.	3. Recipient's Accession No.

4. TITLE AND SUBTITLE RF Attenuation Measurement System Using a SQUID	5. Publication Date September 1977
	6. Performing Organization Code 276 and 275

7. AUTHOR(S) Robert T. Adair, Nolan V. Frederick, and Donald B. Sullivan	8. Performing Organ. Report No.

9. PERFORMING ORGANIZATION NAME AND ADDRESS NATIONAL BUREAU OF STANDARDS DEPARTMENT OF COMMERCE WASHINGTON, D.C. 20234	10. Project/Task/Work Unit No. 2761446
	11. Contract/Grant No. CCG Project No.72-72C

12. Sponsoring Organization Name and Complete Address (Street, City, State, ZIP) Army/Navy/Air Force Calibration Coordination Group	13. Type of Report & Period Covered
	14. Sponsoring Agency Code

15. SUPPLEMENTARY NOTES

16. ABSTRACT (A 200-word or less factual summary of most significant information. If document includes a significant bibliography or literature survey, mention it here.)

This report describes a unique portable system for measuring attenuation at 30 MHz over a range of 50 dB to an accuracy of 0.005 dB per 20 dB. This system does not require any reference standard. A SQUID (Superconducting QUantum Interference Device) with its associated instrumentation is used to determine attenuation in terms of Bessel Function Zeros. A SQUID is a loop of super-conducting metal closed by a weak point contact called a Josephson junction, operating in liquid helium.

The system specifications, description, and theory of operation are presented. A complete system operating procedure including data reduction techniques is given along with a discussion of sources of errors.

Considerable additional information and diagrams are presented as an aid to the user in understanding and operating the system.

17. KEY WORDS (six to twelve entries; alphabetical order; capitalize only the first letter of the first key word unless a proper name; separated by semicolons)

Josephson junction; quantum interference; rf attenuation; superconductivity.

18. AVAILABILITY ☒ Unlimited	19. SECURITY CLASS (THIS REPORT)	21. NO. OF PAGES
☐ For Official Distribution. Do Not Release to NTIS	UNCLASSIFIED	160
☐ Order From Sup. of Doc., U.S. Government Printing Office Washington, D.C. 20402, SD Cat. No. C13	20. SECURITY CLASS (THIS PAGE)	22. Price
☒ Order From National Technical Information Service (NTIS) Springfield, Virginia 22151	UNCLASSIFIED	$8.00

ABSTRACT

USCOMM-DC 29042-P74

INSTRUCTIONS

FORM NBS-114A: BIBLIOGRAPHIC DATA SHEET (REVERSE SIDE). This Bibliographic Data Sheet is an NBS adaptation of the form prescribed by COSATI guidelines (Appendix F. NBS Manual for Scientific and Technical Communications). Please complete with extreme care. This sheet will provide the basis for the literature citation of the publication, and in most cases it will become an integral part of the final publication itself.

A. Complete item 1 if information is available; otherwise, OTP will complete later. If non-NBS publication, state:"see item 15". (Additional instructions under K below.)

B. Ignore items 2, 3, 6, and 14; these are reserved for possible future use.

C. Complete items 4 and 7. When NBS-114A is resubmitted these items must be as they will actually appear on the published paper.

D. Leave items 5, 21, and 22 blank; OTP will complete.

E. Items 9, 19, and 20 are preprinted; you need add nothing.

F. Complete items 10, 11, and/or 12 when applicable. If no sponsor is involved, in item 12 state: same as item 9.

G. For item 13, enter "Final" or "Interim" and calendar period covered, as appropriate.

H. For item 15, enter other relevant information. (For example, upon receipt of completed Form NBS-266 from author, OTP will enter the complete citation for NBS-authorized papers published in non-NBS media.)

I. Complete items 16 and 17. Guidance is given in Section 4 and Appendix B of the NBS Manual for Scientific and Technical Communications. The abstract must agree with the one of the published paper.

J. For item 18, indicate one of the following: "Unlimited" - for open-literature documents cleared under NBS editorial procedures, or "For official distribution. Do not release to NTIS" - for limited, restricted, or need-to-know material. (See 5.1.4.2.1 of Brady memo dated January 16, 1973 "Reports to Sponsors.")

K. In completing item 1, use the brief designators shown in the right-hand column below. Each designator will be followed by the specific publication number for that item. This number will be the same in both the longer and briefer designators for the same document. For example: NBS Technical Note 548 will be equivalent to NBS TN-548. You would enter NBS TN-548 in item 1 of Form NBS-114A.

NBS Identification

NBS Technical Note	NBS TN-
NBS Monograph	NBS MN-
NBS Handbook	NBS HB-
NBS Special Publication	NBS SP-
NBS Applied Mathematics Series	NBS AMS-
NBS National Standard Reference Data Series	NBS NSRDS-
NBS Building Science Series	NBS BSS-
NBS Federal Information Processing Standards Publication	NBS FIPS-
NBS Voluntary Product Standards	NBS PS-
NBS Consumer Information Series	NBS CIS-
NBS Journal of Research Section A	NBS JRA-
NBS Journal of Research Section B	NBS JRB-
NBS Dimensions	NBS D-
NBS Interagency or Internal Report •	NBS IR-

Since each paper in the two volume NBS Journal of Research is assigned a specific designator, OTP will add appropriate Journal designator for item 1.

•If the outside sponsor assigned his own number, enter his number in item 1, and the NBSIR number in item 8.